OAK RIDGE
NATIONAL LABORATORY
MANAGED BY UT-BATTELLE
FOR THE DEPARTMENT OF ENERGY

ORNL/SUB/99-B99398V-4

Design Studies of "100% Pu" MOX Lead Test Assembly

A. M. Pavlovichev
S. S. Alioshin
S. N. Bolshagin
A. Kalashnikov
E. Kapranova
V. Korobitsyn
Y. A. Styrin

Fissile Materials Disposition Program

UT-BATTELLE
ORNL-27 (4-00)

ORNL/SUB/99-B99398V-4

DESIGN STUDIES OF "100% Pu" MOX LEAD TEST ASSEMBLY

A. M. Pavlovitchev
S. S. Alioshin
S. N. Bolshagin
A. Kalashnikov
E. Kapranova
V. Korobitsyn
Y. A. Styrin

Date Published: May 2000

Prepared by
Russian Research Center "Kurchatov Institute"
Institute of Nuclear Reactors
Under subcontract 85B-99398V

Funded by
Office of Fissile Materials Disposition
U.S. Department of Energy

Prepared for
Computational Physics and Engineering Division
OAK RIDGE NATIONAL LABORATORY
Oak Ridge, Tennessee 37831
managed by
UT-BATTELLE, LLC
for the
U.S. DEPARTMENT OF ENERGY
under contract DE-AC05-00OR22725

Russian Research Center "Kurchatov Institute"
Institute of Nuclear Reactors
VVER Division

Joint U.S. / Russian Project to Update, Verify and Validate Reactor Design/Safety Computer Codes Associated with Weapons-Grade Plutonium Disposition in VVER Reactors

Design Studies of «100% Pu» MOX Lead Test Assembly

(Final Report for FY99)

General Order 85B-99398V. Work Release 02. P. 99-1b

Project Manager

A.M.Pavlovichev

Executed by

S.S.Alioshin
S.N.Bolshagin
A.Kalashnikov
E. Kapranova
V. Korobitsyn
Y.A.Styrin

Moscow 1999

ACRONYMS

Russian		American Equivalent
AZ	emergency (accident) protection	AP
AZ-1	state with all the control rods fully inserted except of one the most effective stuck in upper position	AP-1
BOC	Beginning Of fuel Cycle	BOC
BPR	Burnable Poison Rod	BPR
DNBR	Departure from Nucleate Boiling Ratio	DNBR
DTC	Doppler Temperature Coefficient	DTC
EFPD	Effective Full Power Day	EFPD
EOC	End Of fuel Cycle	EOC
FP	Fission Products	FP
IPPE	Institute of Physics and Power Engineering (Obninsk)	IPPE
KI	Kurchatov Institute	KI
LTA	Lead Test Assembly	LTA
LWR	Light Water Reactor	LWR
MCL	Minimum Controllable reactor power Level	MCL
MDC	Moderator Density Coefficient	MDC
MOX	Mixed Oxide (uranium-plutonium fuel)	MOX
MTC	Moderator Temperature Coefficient	MTC
NPP	Nuclear Power Plant	NPP
OR	Regulatory Body (Control Rod)	CR
PWR	Pressurized-Water Reactor	PWR
RCT	Repeat Criticality Temperature	RCT
SUZ	Reactor Control and Protection System	RPS
TVS, FA	Fuel Assembly	FA
UOX	Uranium Oxide Fuel	UOX
VVER	Russian water-water reactor	VVER

EXECUTIVE SUMMARY

In this document the results of neutronics studies of «100%Pu» MOX LTA design are presented. The parametric studies of infinite MOX-UOX grids, MOX-UOX core fragments and of VVER-1000 core with 3 MOX LTAs are performed. The neutronics parameters of MOX fuelled core have been performed for the chosen design MOX LTA using the Russian 3D code BIPR-7A and 2D code PERMAK-A with the constants prepared by the cell spectrum code TVS-M.

ADD:
1. NEW LIMITATIONS (FROM GOROKHOV)

2. AXIAL REFLECTOR DESCRIPTION

CONTENTS

INTRODUCTION

This work is a part of Joint U.S. / Russian Project with Weapons-Grade Plutonium Disposition in VVER Reactor and presents the results of studies of full scale MOX LTA named also «100%Pu» MOX LTA.

It is like to the worldwide type of MOX assembly with 3 types of fissile plutonium enrichment and its simplified design is presented in Fig.2.5.

The presented studies include the following stages:

- **"Assembly",**
- **"Core fragments",**
- **"Core".**

This report completes the studies partially executed in [3] and [6] and can be considered as a one compiled the previous parametric studies of LTAs of «100%Pu» type and VVER-1000 core configurations with 3 MOX LTAs of this type.

At the **stage "Assembly"** in the process of parametric studies the infinite grid is considered with the following periodical element:

- a central MOX LTA surrounded by typical uranium assemblies.

Parametric studies must be resulted in the following features of MOX LTA design:

- Proximity of power generation in MOX LTA and in some replaced uranium assembly that was used as a base or reference FA (Fig.2.1);
- MOX LTA zoning that ensures an acceptable power peaking factor in calculational system.

The Russian cell code TVS-M [4] is used as a calculational instrument at the stage "Assembly".

At the **stage " Core fragments "** in the process of parametric studies the infinite grid is considered with the periodical element that simulates a typical core fragment. It is shown in Fig. 2.8.

The object of calculations was to make an estimate of the optimal ratio between fissile nuclides in UOX and MOX FAs and optimal MOX FA zoning.

The codes of IPPE are used in these calculations.

In comparison with [6] the present paper describes the refined variant of this model, which takes into account burnup non-uniformity in various FA regions and FAs reloading simulation. In addition, the version of the TRIANG-PWR code was made to apply periodic boundary conditions instead of reflection conditions used previously. The reflection conditions are incorrect as applied to this model and they being used introduced essential error into power distribution calculations.

The **stage "Core"** comprises studies of characteristics of some base Uranium core (Fig.A.1) with 3 MOX LTAs introduced.

The code TVS-M is used here for generation of neutronics constants to be used in:

- coarse-mesh (assembly-by-assembly) core calculations by the Russian code BIPR-7A [7];
- fine-mesh (pin-by-pin) calculations by the Russian code PERMAK-A [7].

The stages "Assembly", "Core fragments" and "Core" are described correspondingly in Chapters 2, 3 and 4.

In Annex the used codes are briefly described and the detailed reflector description is presented.

1. Definitions

Table 1.1. Definitions

Parameter	Abbreviation	Units	Remarks
Calculational system	CS		Infinite grid of multi-assemblies/single assemblies or core
CS symmetry sector	Sim		30 for 30°, 60 for 60°, 120 for 120°, 360 for full CS.
Reactivity of CS	RO	pcm	RO = (Keff-1)/Keff*1.E5
Calculational volume	Vij		Axial fraction j of assembly number i. In VVER-1000 calculations, 10-30 axial fractions of equal volume are usually used.
Effective multiplication factor of CS	Keff		
Multiplication factor of CS	Ko		Relation of neutron generation to neutron absorption. For core calculations Ko values are attributed to Vij
3-D power distribution in core	q_{ij}		Power in Vij normalised by average Vij power
Volume power peaking factor	Kv		Maximum in q_{ij} values
Radial position of volume power peaking factor	N (Kv) or N_K		Number of assembly in calculational core sector where Kv is realised
Axial position of volume power peaking factor	M (Kv) or N_Z		Number of axial level where Kv is realised
3-D burnup distribution in core	BUij	MWd/kg	Burnup in Vij.

		or GWd/t	
2-D power distribution in core	q_i		Assembly powers normalised by average assembly power in core.
Radial power peaking factor	Kq		Maximum in qi values
Radial position of radial power peaking factor	N (Kq) or N_K		Number of assembly in calculational core sector where Kq is realised
Pin linear power	Ql	W/cm	Pin power for 1 cm of an axial calculational fraction
Moment during fuel irradiation	T	EFPD	
2-D burnup distribution in core	BUi	MWd/kg	Average-assembly burnup distribution in core.
Average burnup in Uranium assemblies	$\bar{B}_U$	MWd/kg or GWd/t	
Average burnup in MOX assemblies	$\bar{B}_{MOX}$	MWd/kg or GWd/t	
Average Boron acid (H_3BO_3) concentration[a] in coolant	Cb or C_{H3BO3}	ppm or g/kg	H_3BO_3 fraction in coolant (unit "ppm" means mg of boron acid in 1 Kg of H_2O)
Critical boron acid concentration in coolant	Cb^{crit}	ppm or g/kg	Cb (C_{H3BO3}) value ensuring Keff=1
2-D power distribution in CS	q_k-CS		Power of fuel pins normalised by average fuel pin power in CS.
Peaking factor of 2-D power distribution in CS	K_{FA}–CS		Maximum in q_k-CS values
2-D power distribution in assembly	q_k		Power of fuel pins normalised by average fuel pin power in assembly (in some axial fraction).
3-D power distribution in axial volumes	q_{ijk}		Power of axial volumes of fuel pins normalised

[a] Boron acid concentration divided by the coefficient 5.72 means natural boron (nat B) concentration. In VVER-1000 calculations the term of boron acid concentration is widely used. Below, Cb means boron acid concentration if there is no special indication.

of fuel pins in core			by average power in such volumes over a whole core
Pin power peaking factor in assembly	Kki		Among q_k values for an assembly number i for a fraction number j where maximum q_{ij} for this assembly is realised.
Radial pin power peaking factor	Kr		max (qi * Kki)
Radial position of radial pin power peaking factor	N (Kr) or N_K		Number of assembly in calculational core sector where Kr is realised
2-D power peaking factor in assembly	K_{FA} (in Russian exploitation calculations the notation Kk or Kk_{max} is also used)		Maximum relative power of fuel pins (maximum in q_k values)
Axial power peaking factor in assembly or in fuel pin	Kz		Maximum relative power of axial volume in assembly or in fuel pin normalised by average power in such volumes (in assembly or in fuel pin)
Total power peaking factor	Ko or $K_{o\text{-}total}$		$\max_{ij} (q_{ij} * Kki) = Kr*Kz$
Radial position of total power peaking factor	N ($K_{o\text{-}total}$) or N_K		Number of assembly in calculational core sector where $K_{o\text{-}total}$ is realised
Axial position of total power peaking factor	M ($K_{o\text{-}total}$) or N_Z		Number of axial level where $K_{o\text{-}total}$ is realised
Engineering factor	K_{eng}		Coefficient taking account of uncertainty of a hot point (maximum fuel pin local power) calculations
2-D burnup distribution in assembly	BUk	MWd/kg or GWd/t	Average-pin burnup distribution in CS.

1-D burnup distribution in fuel pin	BUpin		Burnup distribution in concentric zones of equal volume in fuel pin, normalised by average zone burnup.
1-D power distribution in fuel pin	q_{pin}		Power distribution in concentric zones of equal volume in fuel pin, normalised by average zone power.
Regulation bank position	H_{reg}	cm	Distance from core bottom till rods lower edge
Control rods worth (in core)	$(RO)_{AP-1}$	ppm	Effect of control rods insertion in core supposing the most effective single CR stuck in upper position. It is defined as a reactivity difference in two states: $(RO)_{AP-1}$= RO1-RO2. The second state differs from the first one only by additional CRs inserted in core. All the other parameters correspond to the first state: Cb (that is equal to Cb crit for the first state), temperature and FP distribution in core.
Repeat Criticality Temperature	RCT	°C	Temperature that ensures a secondary critical state during core cooling in EOC in such conditions: all control rods inserted in core except one the most effective, zero boron concentration, equilibrium xenon concentration corresponding to reactor power before its shut-down.
Moderator temperature coefficient (in core)	MTC	pcm/°C	
Moderator density coefficient (in core)	MDC	pcm/g/cc	
Doppler temperature coefficient (in core)	DTC	pcm/°C	Calculated supposing average fuel temperature changing of 1°C
Doppler isotermic temperature coefficient (in core)	DTC*	pcm/°C	Calculated supposing local fuel temperature changing of 1°C

Doppler power coefficient (in core)	DPC	pcm/MW	
Boron reactivity coefficient (in core)	DRO/DCB	pcm/ppm	
Effective fraction of delayed neutrons	βeff or $\beta_{ef.}$	ppm	General characteristic of infinite grid or core
Lifetime of prompt neutrons	λ_m or λ_{im}	s	General characteristic of infinite grid or core
Reactor thermal power	W	MW	
Specific reactor thermal power in CS	Wv	KW/litre	Reactor thermal power in CS volume unit
Nominal reactor thermal power	Wnom	MW	Equal to 3000 MW for VVER-1000
Minimum controllable level of reactor power	MCL	MW	In calculations corresponds to Zero Power and uniform temperature 280°C in core.
Core coolant flow rate	G	m^3/h	
Average entry core temperature	t_{entry}	°C or K	
Average outer core temperature	t_{out}	°C or K	
Average coolant-moderator temperature in CS	t_{mod}	°C or K	
Average coolant-moderator density in CS	γ_{mod}	g/cm^3	
Fuel temperature	t_{fuel}	K	
Average temperature of other CS components	t_{con}	°C or K	
Fuel pin cladding temperature	t_{clad}	°C or K	
Xenon-135 concentration distribution in core	Xe	10^{24} /cc	For 1 cc in fuel. Xe = 0 → xenon is absent; Xe = 1 → Xe=Xe eq (W).
Equilibrium Xenon-135 concentration distribution in core	Xe eq (W)	10^{24} /cc	Concentration formed during long working with W power, regulating bank in nominal position[b]
Sm-149 concentration distribution in core	Sm	10^{24} /cc	For 1 cc in fuel. Sm = 0 → samarium is absent, Sm = 1 → Sm=Sm eq, Sm = 3 → full decay of Pm-149 into Sm-149 is

[b] In VVER-1000 calculations Hreg in nominal position is equal to 80% if there is no special indication

			simulated in BOC.
Equilibrium Sm-149 concentration distribution in core	Sm eq	10^{24} /cc	Concentration formed during long working, regulating bank in nominal position
Samarium-149 concentration distribution, all Prometium-149 decayed in Sm	Smh	10^{24} /cc	
Core reactivity while reactor shut-down	RO_{STOP}	pcm	Under conditions: W=0, Xe=0,Sm=Smh, t_{mod}= t_{fuel}= t_{con}=20°C, Cb= 16000 ppm

2. Parametric Studies of MOX LTA design (Stage "Assembly")

2.1. Calculational Model

Calculational system (CS) for MOX LTA design parametric studies is presented by the infinite grid with the following periodical element:

- central plutonium assembly surrounded by uranium assemblies of 3.7 %Wt. U-235. The 60° sector of CS is shown in Figure 2.6.

Composition of weapons grade plutonium, adopted for calculations, is presented in Table 2.1. The design parameters of plutonium and uranium assemblies are described in Tables 2.2-2.6.

Two ***limitations*** has been adopted while defining an acceptable MOX FA zoning (fissile plutonium distribution in a fresh MOX FA):

- power peaking factor in CS is conventionally limited by the value of 1.1. It is supposed that under such condition the global power peaking factors in core calculations could be rested in acceptable range described in Chapter 4.
- minimum allowable fissile plutonium enrichment (Pu-239 and Pu-241) is equal to 2% according to technological considerations.

2.1.1 Fuel Irradiation Simulation

This regime is used for MOX LTA zoning studies under the conditions described in [2]. They comprise irradiation simulation in CS as a rule on the interval [0-40 MWd/kg] with the step 2 MWd/kg.

In the process of irradiation:

- Axial buckling is 1.E-4cm^{-2};
- Cb (nat B)= 600 ppm. A set of calculations for zero irradiation has been executed with Cb=0 and Cb (nat.B)=1200ppm;
- Wv = 108 KW/litre;
- t_{mod} = 302°C;
- t_{con} = 302°C;
- t_{fuel} = 1027 K;
- Xe=Xe eq;
- Sm=Sm eq.

2.1.2. Zero Power Calculations

This regime is aimed to define reactivity effects due to temperature and Cb variations and to compare Keff with eventual verification calculations to be carried out by other codes.

Calculations are executed in five irradiation points:
0, 10, 20, 30, 40 GWd/t
where states are to be formed by different combinations of the following values:
Cb (nat.B): 0, 600,1200 ppm;
$t_{mod}=t_{con}=t_{fuel}$: 20, 280 °C.

2.2. Results

2.2.1. Zoning Parametric Studies

Zoning parametric studies consisted in variation of fissile plutonium content in 3-zones MOX LTA (Figures 2.5 and 2.6).

The results of calculations simulating fuel irradiation in plutonium and uranium assemblies are presented in Tables 2.8-2.13. Two options of Uranium reference assembly are considered:

- without BPR i.d. with guide tubes filled by water in 18 positions in assembly (see for example Fig.2.1);
- with BPRs of properties presented in Table 2.6.

It can be seen that 2% fissile plutonium content in periphery entails significantly lower values of power peaking factor "Kkmax-CS" than 2.4% content (compare Tables 2.10 and 2.11). That is why 2% content in periphery has been adopted. Plutonium content in the central and intermediate zones was variable to obtain Ko value similar to reference uranium CS.

Finally the plutonium content of 4.2/3.0/2.0 has been chosen as acceptable. The Ko evolution in the process of fuel irradiation for the reference uranium and different plutonium assemblies is shown in Figure 2.8*.

Fig.2.9 shows "Kkmax-CS" evolution in the process of irradiation. The increase of "Kkmax-CS" for 3-zones MOX LTAs is observed from a certain moment. As it is seen from the Table 2.13 and Figure 2.6, during irradiation maximum CS power passes from uranium pins out of MOX LTA to the interior of MOX LTA. This effect should be studied in future more attentively taking into account that in real conditions a fresh MOX LTA will be surrounded by both fresh and irradiated uranium assemblies that can lead to mitigating of the mentioned effect. It will be seen in Chapter3.

* The results for "Island" type MOX LTA [10] are also presented in Figures 2.8 and 2.9.

2.2.2. Zero Power Calculations

The results of calculations are presented in Table 2.7. It may be seen that the positive temperature reactivity effect appears for the great boron concentrations of 1200 ppm. In MOX LTA this effect is lower owing to more absorbable properties of MOX fuel as compared with uranium one.

3. Parametric Studies of MOX LTA design (Stage "Core Fragments")

In these calculations the simplest core design was considered (without BPRs in FAs).

3.1. Description of calculational model

The pattern for the core of VVER-1000 with FA lifetime of three years and partial (1/3 of FAs) MOX loading, under steady-state operation at the beginning of cycle, is as follows: 1 fresh MOX assembly - 1 MOX FA having operated for 1 year - 1 MOX FA having operated for 2 years - 2 fresh UO_2 FAs, and UO_2 FAs taken two at a time having operated for 1 and 2 years, respectively. Thus, the symmetric element of the core contains 9 FAs. This symmetric element is shown in Fig.3.1. The use of this symmetric element makes it possible to study various ways for arrangement of positions of MOX and uranium FAs with different burnups. In this case, a correct normalization of power distribution is achieved.

It should be noted that Fig.3.1 shows only one of possible variants of symmetric element configuration. The model allows us to consider any one of other regular core configurations.

The zonned uranium FA shown in Fig.2.1 (so-called reference uranium FA) was used as UO_2 FA.

The three-zones FA with MOX fuel was used as MOX FA. The map of this FA is shown in Fig.2.5.

At the first stage of calculations the core parameters during burnup were taken the same as those at the stage "Assembly" (Chapter 2):

C_B (nat. B) = 600 ppm,
W_V = 108 KWt/l,
t_{mod} = 302 °C,
t_{fuel} = 1027 K.
The axial buckling was taken to be zero.

At the second stage of calculations the axial buckling was determined on condition that the K_{eff} value of system is equal to one at the end of cycle and with zeroth boron concentration in water. The initial boron concentration is equal to 1200 ppm and this value approximately corresponds to initial boron concentration in VVER-1000 core with partial (1/3) MOX fuel loading (in terms of boron acid concentration it corresponds to 6864 ppm – compare with the values in Tables 4.7, 4.9 and 4.11)

Power distribution calculation during burnup and reloading simulation were made with the use of IPPE code complex TRIANG-PWR in two-group diffusion approximation. Macroconstant calculations were performed by the WIMS-ABBN code which is the updating version of the well-known English WIMS-D4 code.

When constructing the calculational model , it was assumed that fuel rods in FA are divisible into several groups (inner fuel rods, corner rods, periphery ones of 1-st row and so on) with the aim to describe the differences in regions surrounding fuel rods (water holes, inter-assembly water). Cell burnup calculations for macroconstant preparation were carried out with the use of these groups. Assessment of calculational error in pin-by-pin power distribution with the use of TRIANG code and indicated procedure of macroconstant preparation was made in [9] by comparison with calculations performed using the benchmark multigroup CONKEMO code based on the Monte Carlo method for neutron flux calculation. Burnups were studied for models with graded and non-graded MOX FAs surrounded by UO_2 FAs. Maximum discrepancy in pin-by-pin power distribution in both cases was demonstrated to do not exceed 5 % for all burnup steps.

3.2. Results of the first stage study

3.2.1. Boundary condition effect

As noted above, periodic boundary conditions was realized in TRIANG code with the aim to describe the given models properly in the case that the outer system boundary is regular hexagon. Table 3.1 gives the calculational results of power peaking factors for six FA arrangements (see Fig.3.2) with graded MOX FAs shown in Fig.2.5.

For each variant the first two lines are related to uranium core model, the second two lines apply to 1/3 MOX FAs core model. The first line gives the values for reflection boundary conditions, the second one gives the data for periodic boundary conditions. As evident from the Table 3.1, the error in power peaking factor due to incorrect boundary conditions may be as much as 18 %. In what follows that the calculation results should be obtained with the use of periodic boundary conditions.

3.2.2. Effect of plutonium content in MOX FAs on power non-uniformity

The calculations have shown that for all FA arrangement variants given in Table 3.1 with MOX fuel zoning from Chapter 2 (4.2/3.0/2.0) the fuel elements with maximum power are positioned in FAs with UO_2 fuel, and power peaking factors in 1/3 MOX FA core model are higher than these values in core model with UO_2 fuel.

In this connection in addition to 4.2/3.0/2.0 (average content of fissile Pu is 3.34 %) six supplemental variants of fuel zoning have been considered: 4.4/3.2/2.0; 4.5/3.3/2.1; 4.6/3.4/2.2; 4.7/3.5/2.3; 4.8/3.6/2.4; 4.9/3.7/2.5. The average contents of fissile Pu are 3.5; 3.6; 3.7; 3.8; 3.9; 4.0 respectively. For these cases Fig. 3.3 demonstrates dependence of K_K *–CS (or* K_{Kmax}*-CS)* and K_K *–CA (or* K_{Kmax}*-CA)* on Pu content, here

K_{Kmax} - *CA (CA* - central assembly) is the maximum fuel element power in the central FA with normalization to the average value over the system.

As is seen from the figure in variants V1-V3, the K_{Kmax} - *CS*, already having rather low values, with a rise of Pu content is reduced and the K_{Kmax} - *CA* increases, i.e. power distribution is flattening. In this case the maximum values of fuel element power in uranium and MOX FAs come close together as fissile Pu content becomes equal to about 4.3 %.

In varians V4-V5 the K_{Kmax} - *CS* and K_{Kmax} - *CA* come closer together rather rapidly and even at Pu contents of 3.9 % and 3.8 % respectively they level off, i.e. maximum power peaking factor moves to the MOX FA and remains there with further Pu content increasing. Variant V6 is identical to the variant V5.

It is seen that in the variant V5, having the worst K_{Kmax} - *CS* curve, the minimum value of K_{Kmax} - *CS* is achieved at Pu content of about 3.7 %. Therefore, the further study was done using MOX FAs with average fissile Pu content of 3.7 %.

3.2.3. Effect of plutonium zoning in MOX FAs on power non-uniformity

Table 3.2 gives the power peaking factors for non-zonned MOX FAs. It is clear that in this case maximum power peaking factors are very high even for the variants with relatively flat power distribution. To choice optimal Pu zonning the calculations of each of six arrangements with four various zonning variations (4.4/3.4/2.6; 4.5/3.4/2.4; 4.6/3.4/2.2; 4.7/3.4/2.0) were carried out. All four variations give average fissile Pu content equal to 3.7 %. In Tables 3.3-3.6 the power peaking factors over the whole system, over the central FA and average power peaking factors in central FA are listed. The FA burnup non-uniformity was neglected in these calculations. As is seen from Tables 3.3-3.6, the least maximum peaking factors over the whole system are achieved at zonning of 4.6/3.4/2.2.

3.2.4. Refinement of the results with consideration for FA burnup non-uniformity and fuel reloadings

Generally speaking, one should take account of the individual burnup in each fuel element. However with the aim of saving the computation time it was decided to separate the central part of FA, and periphery was divided into 6 sectors (of four regions each) simulating FA zonning, among them corner fuel elements taking individually. Altogether there are 25 burning regions per FA. A choice of such model follows from analysis of power distributions at initial state showing that maximum discrepancies from average values are equal to 2 % in each region separated. In doing so, it should be remembered that power distribution is flattening during burnup.

Figure 3.4 shows FA arrangements considered and the conventional three-digit numbers used by TRIANG code complex for simulation of FA reloadings. The first digit shows FA operating years, the next two digits are used for numbers of FAs of each operating year. In this case uranium FAs have numbers 1 and 2, and MOX FA has number 3.

Table 3.7 represents FA reloading schemes possible within the limits of a given symmetry element. Table 3.8 gives power peaking factors for equilibrium fuel cycle for all four possible reloading schemes. MOX FA with x_{Pu^f} = 4.6 %/3.4 %/2.2 % is used in all cases.

The data given in Table 3.8 allow us to make following conclusions. Firstly, the largest values of power peaking factors in equilibrium fuel cycle occur at the cycle beginning. Secondly, variations in fuel reloading scheme do not markedly affect the run of power peaking factor during burnup. Comparing the data of Tables 3.5 and 3.8, one can see that the maximum increase of power peaking factor K_{Kmax}-*CS* due to burnup non-uniformity and fuel reloading simulation is about 2 %.

3.3. Results of the second stage study

On the second stage of calculations the boron concentration during burnup was taken as linearly decreasing from 1200 ppm at the cycle beginning to zero at the cycle end. Axial buckling was defined when K_{eff} =1 at the cycle end and with zeroth boron concentration.

The graded MOX FA with $\bar{x}_{Pu^f}$=3.34 % was taken as a basis for calculations. In the new set of calculational variants the fissile Pu content were either reduced or increased by 0.1 % in all zonning regions simultaneously. A set of average Pu content was as follows: $\bar{x}_{Pu^f}$=3.04 %, 3.14 %, 3.24 %, 3.34 %, 3.44 %, 3.54 %.

For three FA arrangements, namely, V1, V4 and V6 the calculations were carried out with regard to fuel reloadings. Six burnup cycles were simulated. Fig. 3.5 shows the K_{Kmax} - *CS* and K_{Kmax} - *CA* values for the initial zeroth and the last fifth cycles. It is seen from Fig. 3.5 that maximum in power peaking factor in V1 and V4 moves to uranium FAs at $\bar{x}_{Pu^f} \leq$ 3.44 %. In V6 variant the maximum value remains in MOX FA even with $\bar{x}_{Pu^f}$ reducing to 3.14 %. It is also seen that dependence of K_{Kmax} - *CS* and K_{Kmax} - *CA* on $\bar{x}_{Pu^f}$ and position of optimum in zeroth and last cycles are practically the same. A consideration of fuel reloadings and burnup non-uniformity causes power peaking factors to increase by 2-3 %. It allows us to make an estimate of Pu content using only one burnup cycle.

In the mentioned above set of calculations the optimum Pu content distribution over the zoning regions in MOX FA was not under control. In the next set of calculations Pu content distribution over the zoning regions was corrected for each $\bar{x}_{Pu^f}$ to meet conditions of maximum power equivalence in fuel elements in these regions. Calculations were carried out for zeroth fuel reloading.

Fig. 3.6 gives dependence of power peaking factors on Pu content for the last set of calculations (continuous lines) and for previous one (dotted lines). Refined values of K_{Kmax} - *CS* computed for fifth reloading at x_{Pu^f}=3.51 % are shown for each variant with separate points.

From Fig. 3.3 and Fig. 3.6 it follows that the use in calculations of actual boron content in water caused the optimum Pu concentration in MOX FA to reduce. This is because an increase of boron content tends to reduced power of uranium FA as compared with MOX FA on account of significantly larger thermal neutron capture in MOX FAs. This effect is most pronounced in fresh FAs.

From Fig. 3.6 it also follows that an optimum content of fissile Pu in MOX FAs with weapons-grade plutonium at which maximum fuel element powers in MOX and uranium ($\bar{x}_5$=3.6 %) FAs are equal is about 3.5 %. In this case optimum Pu content distribution in zonning regions is as follows: x_{Pu^f} = 4.3 % / 3.3 % / 2.1 (for fuel element positions in MOX zonned FA shown in Fig. 2.5). The K_{Kmax} - *CS* values are equal about to 1.30 and 1.40 in V1-V3 and V4-V6 variants, respectively. Fig. 3.7 shows power distributions for six studied fuel arrangements in anoptimum case.

It should be noted that in the case of the use of boron burnable rods or fuel elements with gadolinium the relative reduction of power in uranium FA takes place. It tends to further reduction of optimum Pu content in MOX FA as compared with U-235 content in uranium FAs.

On the other hand, calculational estimates of Pu content in MOX FA that is equivalent in cycle duration to uranium FA with $\bar{x}_5$=3.6 % give the $\bar{x}_{Pu^f}$ value equal to 3.9 %.

Conclusion on Chapter 3

1. The refinements of the model for symmetric element calculations have been introduced. They involve
   - periodic boundary conditions instead of reflection conditions on outer boundaries,
   - taking into account burnup non-uniformity and FA reloadings.
2. The error in power peaking factor due to incorrect boundary conditions was demonstrated to be as much as 18 %. Taking into account fuel reloadings and burnup non-uniformity causes power peaking factor to increase by 2-3 %.
3. Taking account of actual instead of average boron content in water tends to reduction of optimum Pu concentration in MOX FA, at which maximum fuel element powers in MOX and uranium FAs are equal. This is because an increase of boron content tends to reduced power of uranium FA as compared with MOX FA on account of significantly larger thermal neutron capture in MOX FA. This effect is most pronounced in fresh FAs.
4. Optimum Pu content in MOX FA from the standpoint of power distribution flattening is about 3.5 % with U-235 content in uranium FAs of 3.6 %. In this case optimum Pu content distribution on zonning regions is as follows: x_{Pu^f} = 4.3 % / 3.3 % / 2.1 % (for fuel element positions in MOX zonned FA shown in Fig. 2.5).

   Pin-by-pin power peaking factor varies between 1.3 and 1.4 depending on FA arrangements.
5. Results given above apply to the simplest design of core, in which boron burnable rods and fuel elements with gadolinium are unused. The use of boron burnable rods or fuel elements with gadolinium in FAs will result in further reduction of optimum Pu content in MOX FAs as compared with U-235 content in FAs with uranium fuel. Hence, given model considerations couldn't be proposed as final recommendation on zonning choice. Just the same, they are useful for establishing regular trends,

comparing different computer codes and choosing preliminary zonning. The final choice of fuel zonning can be only done by means of pin-by-pin power distribution calculations in reactor having regard to actual FA composition of fuel and burnable poison.

6. The Pu content in MOX FA that is equivalent to uranium FA with $\bar{x}_5 = 3.6\ \%$ in cycle duration is equal to $\bar{x}_{Pu^f} = 3.9\ \%$.

4. CALCULATIONS OF VVER-1000 CORE WITH 3 MOX LTAs (Stage "Core")

These studies comprise:

- ***"Uranium Core"***. Calculation of the so-called Advanced VVER-1000 core with boron BPRs for the equilibrium fuel cycle [2] that was defined as basic for 3 MOX LTAs introduction.

- ***"MOX Core"***. Studies of VVER-1000 core with introduction of 3 LTAs of "100%Pu" design with the zoning chosen in Chapter 2. Three cycles till MOX LTAs discharge have been studied. Corresponding loading patterns for every cycle have been chosen to minimize power peaking factors.

"Uranium core" loading pattern is shown in Fig.4.1. This figure includes particularly the reloading scheme (the FA locations in previous fuel cycle are indicated), the FA locations in current equilibrium cycle with the indication of its type (according to Figures 2.1, 2.3 and 2.4) and initial average assembly burnups.

The core, FA, fuel pins, CR and Boron BPR geometric and material parameters are indicated in Tables 2.1-2.6.

The reflectors are described in Annex.

4.1. Limitations

Safety limitations

Composed core loading patterns must meet a number of safety requirements.

Tables 4.1 and 4.2 present the requirements that are officially adopted nowadays for VVER-1000 Uranium cores.

For MOX fueled cores the limitations, not yet officially established, have been conventionally strengthened for power peaking factors and RCT. They are presented in Tables 4.3 and 4.4. It was tried to meet these conventional requirements either for MOX LTAs only (it concerns power peaking factors) or for the core (it concerns RCT).

Other limitations

3 MOX LTA are placed in the core under the following conditions:

- respect 120° symmetry;
- not to occupy the positions without in-core measurement system (the self-powered detectors are shown in Fig. 4.6);
- it is desirable to place MOX assemblies symmetrically to the uranium ones that are equipped by detectors.

4.2. Fuel Irradiation Simulation

Irradiation of the fuel loading is simulated with the step 20 EFPD. Cb crit is found in sequence (below these values are named "Cb burnup") until reactivity margin reaches 0, i.e. Cb crit becomes 0. This moment defines T cycle - a value of cycle length usually presented in EFPD unit.

In the process of irradiation:

- Regulating Bank N 10 (Figure 4.6) is 20% inserted in core; other banks are out of core;
- W=Wnom (3000 MW);
- t_{entry} = 287°C;
- Xe=Xe eq;
- At the beginning of irradiation Sm = Smh.

At the stage "MOX core", while studying of acceptable MOX location in the Uranium loading pattern (Fig.4.1), calculations of three successive cycles are carried out with corresponding description of reloading scheme.

4.3. Calculational States

The states that are considered at the stage "Core" are characterized by:

- CRs positions in core (X% N↓ means that the Bank N is X% inserted in core). No indication means that all the CRs are out of the core;
- Cb;
- Average FP concentration in core (Xe-135 and Sm-149 poisoning are considered separately);
- Xe;
- Sm;
- W (in these studies two power levels are considered - W_{nom} и MCL);
- t_{mod};
- t_{fuel};
- t_{con}.

It is necessary to remark that three last parameters are not generally independent.

All the states considered in the process of irradiation will be named "Burn-up".

The specific moments are introduced: the beginning of cycle (BOC) and the end of cycle (EOC). They characterize FP concentration (average in core) in these moments. It should be noted that the other above-mentioned parameters are not

always connected directly with irradiation conditions in these moments; their values may depend on reactor start-up conditions before irradiation or cooling conditions in the end of irradiation.

4.4. Information Release

The table below presents the states considered and the parameters calculated. The second column indicates the list of results presented in this report. The rest of calculated parameters and additional information can be received by addressing to Youri Styrine (email: Youri.Styrine@vver.kiae.ru).

Parameter	Presented in the Report	States							
qi	+		Burn-up						
qij			Burn-up						
qk	+		Burn-up[c]						
Kr	+		Burn-up[c]						
$K_{o\text{-}total}$	+		Burn-up[c]						
Kk i	+		Burn-up[c]						
Ql	+		Burn-up						
BUi	+		Burn-up						
BUij			Burn-up						
BUк			Burn-up						
MTC	+		Burn-up	BOC, MCL, Xe=0, t_{mod}= t_{fuel}= t_{con}= 280°C, Cb crit	EOC, MCL, Xe=Xe eq, t_{mod}= t_{fuel}= t_{con}= 280°C, Cb crit				
MDC	+		Burn-up	BOC, MCL, Xe=0, t_{mod}= t_{fuel}= t_{con}= 280°C, Cb crit	EOC, MCL, Xe=Xe eq, t_{mod}= t_{fuel}= t_{con}= 280°C, Cb crit				

[c] For MOX assemblies and for an assembly with maximum qi.
[c] For MOX assemblies and for an assembly with maximum qi.
[c] For MOX assemblies and for an assembly with maximum qi.
[c] For MOX assemblies and for an assembly with maximum qi.

DTC	+		Burn-up	BOC, MCL, Xe=0, t_{mod}= t_{fuel}= t_{con}= 280°C, Cb crit	EOC, MCL, Xe=Xe eq, t_{mod}= t_{fuel}= t_{con}= 280°C, Cb crit				
DRO/DCB	+		Burn-up	BOC, MCL, Xe=0, t_{mod}= t_{fuel}= t_{con}= 280°C, Cb crit	EOC, MCL, Xe=Xe eq, t_{mod}= t_{fuel}= t_{con}= 280°C, Cb crit				
βeff and λm	+		Burn-up	BOC, MCL, Xe=0, t_{mod}= t_{fuel}= t_{con}= 280°C, Cb crit	EOC, MCL, Xe=Xe eq, t_{mod}= t_{fuel}= t_{con}= 280°C, Cb crit				
Cb crit	+		Burn-up	BOC, MCL, Xe=0, t_{mod}= t_{fuel}= t_{con}= 280°C, Cb crit	EOC, MCL, Xe=Xe eq, t_{mod}= t_{fuel}= t_{con}= 280°C, Cb crit				
RO stop	+	W=0, Xe=0, Sm=Smh t_{mod}= t_{fuel}= t_{con}= 20°C , Cb = 16000 ppm							

RCT	+	EOC, MCL, Xe=Xe eq, t_{mod}= t_{fuel}= t_{con}= 280°C, Cb = 0, 100% 1-10↓ (except of the most effective single CR)							
$(RO)_{AP-1}$	+	**S1**:BOC, Wnom, Xe=Xe eq, t_{entry}=287°C, Cb burnup 100 % 5↓ 30 % 10↓ **S2**[b]: the same but 100% 1-10↓	**S1**:BOC, MCL, Xe=0, t_{entry}=280°C Cb crit 30% 10↓ **S2**: the same but 100% 1-10↓	**S1**:BOC, MCL, Xe=Xe eq, t_{entry}=280°C Cb crit 30% 10↓ **S2**: the same but 100% 1-10↓	**S1**:EOC, Wnom, Xe=Xe eq, t_{entry}=287°C Cb burnup 100 % 5↓ 30% 10↓ **S2**: the same but 100% 1-10↓	**S1**:EOC, MCL, Xe=Xe eq, t_{entry}=280°C Cb crit 100 % 5↓ 30 % 10↓ **S2**: the same but 100% 1-10↓	**S1**:EOC, MCL, Xe=0, t_{entry}=280°C Cb crit 100 % 5↓ 30 % 10↓ **S2**: the same but 100% 1-10↓	**S1**:BOC, Wnom, Xe=Xe eq, t_{entry}=287°C, Cb burnup 20 % 10↓ **S2**: the same but with successive introduction of the Banks 1-9 (0%↓, 10%↓, 20%↓… 100%↓)	**S1**:EOC, Wnom, Xe=Xe eq, t_{entry}=287°C Cb burnup 20 % 10↓ **S2**: the same but with successive introduction of the Banks 1-9 (0%↓, 10%↓, 20%↓… 100%↓)

[b] For all the states S2 : the most effective single CR is supposed stuck in upper position.

4.5. Calculational Results

4.5.1 Uranium Core

The Table 4.5 and Fig. 4.1 show the results of kinetics parameters calculations for the equilibrium fuel cycle in the Uranium base core that have been performed by the code BIPR-7A[a].

The attained power peaking factors obtained by pin-by-pin code PERMAK-A are presented in Table 4.13. The linear pin powers for BOC and EOC are presented correspondingly in Figures 4.2 and 4.3. It is seen from combination of BIPR-7A and PERMAK-A calculations that maximum linear pin power in BOC is attained on level 4[b], in EOC – on level 2. It justifies PERMAK-A calculations to be performed as usual on level 4 (more details about PERMAK-A calculational scheme are described in Annex).

Pin-by-pin power distributions in the most powered assembly for BOC and EOC are presented correspondingly in Figures 4.4 and 4.5.

Table 4.6 shows the parameters values in zero power states calculated by the code BIPR-7A.

It is seen that Uranium core meets the safety requirements presented in Tables 4.1 and 4.2 for power peaking factors and reactivity coefficients.

Table 4.15a and 4.15b show the CRs worth calculated with certain conservatism (the lowest possible position of Bank 5 that serves for offset regulation and of regulating Bank 10). It is seen that the limiting value of 5500 pcm is respected.

Table 4.16 shows core reactivity evolution in the process of control rods simultaneous movement (when AP is actuated) from top to the bottom of core. BOC and EOC moments are considered including the situations when the most effective single control rod is stuck in upper position. In initial position all the banks except of Regulating bank 10 were in the upper position.

Table 4.17 shows the RCT value that is essentially lower than the allowable one in Table 4.1.

Table 4.14 describes the scheme of conservative evaluation of core subcriticality (scram margin) after scram actuation and reactor state transformation from nominal power to MCL. The effects and uncertainties involved in this scheme (vapor effect, absorbent irradiation, uncertainty of CRs worth calculation etc.) correspond to ones adopted in the West, particularly, in the US and France.

---

[a] Temperature drop in Fig.4.1 is the difference between output and input coolant temperatures for an assembly considered as a channel.

[b] It should be reminded that the level numeration begins from the core bottom and the number of calculational levels in BIPR-7A was 10.

4.5.2. MOX Core

3 MOX assemblies have been located in uranium reference core according to the principals mentioned in p.4.1.

The positions 8, 88 and 150 for the first MOX loading (Fig.4.7) have been chosen because they possess self-powered detectors (see Fig.4.6). Other assemblies have been replaced to ensure a minimum value of Kq calculated by BIPR-7A. Besides, several fresh assemblies of "Ba" type (it is described in Fig.2.3) have been added to the first MOX loading. Reloading schemes for second and third cycles with 3 MOX LTAs are presented correspondingly in Figures 4.17 and 4.27.

The values of average assembly parameters calculated by the code BIPR-7A are presented for 3 successive fuel cycles in Figures 4.8-4.10 and Tables 4.7 (first cycle), Figures 4.18-4.20 and Tables 4.9 (second cycle), Figures 4.28-4.30 and Tables 4.11 (third cycle).

The attained power peaking factors obtained by pin-by-pin code PERMAK-A are presented in Table 4.13. The linear pin powers for BOC and EOC are presented correspondingly in Figures 4.11 and 4.12 (first cycle), Figures 4.21 and 4.22 (second cycle), Figures 4.31 and 4.32 (third cycle). Pin-by-pin power distributions in BOC and EOC both for the most powered assemblies and for MOX LTAs are presented in Figures 4.13-4.16 (first cycle), 4.23-4.26 (second cycle), 4.33-4.36 (third cycle).

Table 4.8, 4.10 and 4.12 show correspondingly the parameters values in zero power states for the first, the second and the third fuel MOX cycles calculated by the code BIPR-7A.

It is seen that MOX cores meet the safety requirements presented in Tables 4.1-4.4 for power peaking factors and reactivity coefficients.

Table 4.15a and 4.15b show the CRs worth. It is seen that the conventional limiting value of 5500 pcm (Table 4.3) is respected.

Table 4.16 shows core reactivity evolution in the process of AP actuation.

Table 4.17 shows the RCT values that are strongly lower than the conventional allowable value of 210°C.

Table 4.14 describes the scheme of conservative evaluation of core subcriticality (scram margin).

It can be seen that the presence of 3 MOX LTAs does not influence $(RO)_{AP}$ in clear manner. Its value is determined first of all by core loading pattern. It may be supposed that only significant value of MOX assemblies in core could lead to lowering of control rods worth because of strong absorbing capacity of MOX fuel.

CONCLUSION

The report presents the results of design studies of full scale ("100%Pu") MOX LTA:

- Parametric studies of multi-assemblies to define MOX LTA structure primarily to choose plutonium content in assembly zones that ensures reasonable power peaking factors and power generation equivalence in MOX and UOX assemblies.
- Parametric studies of "core fragments" in order to understand an influence of UOX environment (varying its properties distribution) on MOX assemblies optimal characteristics.
- Studies of VVER-1000 core characteristics with 3 MOX LTAs introduced for three successive fuel cycles.

The parametric studies have been executed by the code TVS-M that is at the final stage of licensing and it is to be used in the nearest future as a base instrument for VVER core calculations while using both uranium and MOX fuel.

For core investigation the fissile plutonium content composition 4.2%/3.0%/2.0% in MOX assembly has been chosen.

Parametric studies allow to find more or less acceptable plutonium grading in MOX assembly on the base of existing safety limitations. Final choice of a chosen MOX assembly structure must be confirmed in the process of MOX core calculations.

VVER-1000 core with boron burnable control rods has been chosen as a base for 3 MOX LTAs introduction.

Fuel loadings with 3 MOX LTAs have been optimized to ensure a minimum value of power peaking factor Kq.

Evolution of main neutronics parameters during 3 successive cycles with MOX LTAs is presented. It is shown that MOX loaded cores meet the safety requirements preliminary adopted for MOX fuel concerning power peaking factors, reactivity coefficients and control rods worth.

REFERENCES

1. Y.A. Styrin. Fuel Assembly and Core Model for Neutronics Calculations of VVER-1000. Draft.
Moscow, Kurchatov Institute 1998.

2. Y.A. Styrin, I.K.Levina. Design of Lead Test MOX Assemblies for Pilot Irradiation in VVER-1000 and Related Parametric Studies. Draft.
Moscow, Kurchatov Institute 1998.

3. S.A. Bichkov, A.P.Lazarenko, V.D.Sidorenko, Y.A. Styrin. Results of Parametric Design Studies of MOX Lead Test Assembly (Final Report).
Moscow, Kurchatov Institute 1998.

4. V.D.Sidorenko et al. Spectral Code TBC-M for calculation of Characteristics of Cells, Super-cells and Fuel Assemblies of VVER-Type Reactors. 5-th Symposium of the AER.

5. Neutronics Benchmarks for the Utilisation of Mixed-Oxide Fuel: Joint U.S./Russian Progress Report for Fiscal Year 1997. Volume 3 – Calculations Performed in the Russian Federation. ORNL/TM-13603/V3.

6. Y.A. Styrin. Calculations of MOX LTA Performance in VVER-1000 Core. Moscow, Kurchatov Institute 1998.

7. In-core fuel management code package validation for WWERs. IAEA-TECDOC-847. November 1995.

8. Kaloinen E., Siltanen P., Terasvirta R. Two-group nodal calculations in hexagonal fuel assembly geometry. – In: Proc. of NFACRP Specialists' Meeting on Calculation of 3-D Rating Distributions in Operating Reactors. Paris, 1979.

9. Z.N. Chizhikova, A.G. Kalashnikov et al.Verification Calculation Results to Validate the Procedures and Codes for Pin-by-Pin Power Computation in VVER Type Reactors with MOX Fuel Loading. Fifth Technical Specialists Meeting. Water Reactors-1. Oak Ridge. November, 11-13, 1998.

10. S.S.Alioshin, S.A. Bichkov, S.N.Bolshagin, A.P.Lazarenko, V.D.Sidorenko, Y.A. Styrin. Design Studies of «Island» Type MOX Lead Test Assembly. Moscow, Kurchatov Institute 1999.

Table 2.1. Composition of weapons grade plutonium

Isotope / content (Wt. %)				
Pu-238	Pu-239	Pu-240	Pu-241	Pu-242
0.0	93.0	6.0	1.0	0.0

Table 2.2. Main Core Parameters

Parameter	Units	Value
Thermal Power	MW thermal	3000
Electrical Power	MW	1000
Number of Coolant Loops		4
Number of Fuel Assemblies		163
Core Equivalent Diameter	m	3.164
Core Fuel Height	m	3.53
Core Volume	m^3	27.8
Core Power Density	W/cm^3	108
Control / Shut off Rod Banks		10
Position of Regulating Rod Bank	%	80
Core Coolant Flow Rate	m^3/hr	84000
Pressure at Core Inlet	MPa	15.7
Core Inlet Temperature	°C	287

Table 2.3. Fuel Assembly Design Parameters

Parameter	Units	Value
Shape of Fuel Assembly		Hexagonal
Distance Across Assembly (between flats)	cm	23.4
Distance Between Fuel Assembly Centres	cm	23.6
Fuel Pin Lattice Pitch	cm	1.275
Number of Fuel Pins in Fuel Assembly		312
Number of Guide Tubes for Control Rods / Burnable Absorber Pins		18
Inner Diameter of Guide Thimbles	cm	1.1
Thickness of Guide Thimbles	cm	0.1
Material of Guide Thimbles		Zirconium Alloy*
Central Instrumentation Tube Inner Diameter	cm	1.1
Thickness of Central Instrumentation Tube	cm	0.1
Material of Central Guide Tube		Zirconium Alloy *
Number of Spacer Grids in Fuel Assembly		13
Material of Spacer Grids		Zirconium Alloy*
Spacer Grid Weight (each)	Kg	0.55

Compositions Weight percent:
*

Zr	Nb	Hf
98.97	1.0	0.03

Table 2.4. Uranium Fuel Pin Design Parameters

Parameter	Units	Value
		Advanced Core Design
Inner Clad Diameter	cm	0.772
Clad Thickness	cm	0.069
Clad Material		Zirconium Alloy*
Clad Density	g / cc	6.5153
Fuel Pellet Diameter	cm	0.755
Central Hole Diameter	cm	0.15
Fuel Pellet Material		L.E. UO2
Height of Fuel Column	cm	353 (cold) 355 (hot)
Mass of UO2 in Fuel Pin	kg	1.575

Compositions Weight percent:

*

Zr	Nb	Hf
98.97	1.0	0.03

Table 2.5. MOX fuel Pin Design Parameters

Parameter	Units	Value
Inner Clad Diameter	cm	0.772
Clad Thickness	cm	0.069
Clad Material		Zirconium Alloy*
Clad Density	g / cc	6.5153
Fuel Pellet Diameter	cm	0.755
Central Hole Diameter	cm	0.15
U-235 content in MOX fuel	%	0.2
Fuel Pellet Material		PuO2-UO2
Height of Fuel Column	cm	353 (cold) 355 (hot)
Mass of MOX fuel in Fuel Pin	kg	1.600

Compositions Weight percent:

*

Zr	Nb	Hf
98.97	1.0	0.03

Table 2.6. Discrete Burnable Poison Pin Design Parameters

Parameter	Units	Value	
Clad Inner Diameter	cm	0.772	
Clad Thickness	cm	0.069	
Clad Material		Zirconium Alloy*	
Clad Density	g / cc	6.5153	
Absorber Diameter	cm	0.758	
Absorber Density	g./ cc	2.945	
Absorber Composition		Boron g / cc	
		0.036	0.065
B10	Wt%	0.2279	0.4046
B11		1.0153	1.8028
Al		91.7424	88.5951
Fe		0.1915	0.1850
Ni		1.9153	1.8496
Cr		2.9923	5.3133
Zr		1.9153	1.8496

Compositions Weight percent:
*

Zr	Nb	Hf
98.97	1.0	0.03

Table 2.6a. Control Rod Design Parameters

Parameter	Units	Value
Clad Inner Diameter	cm	0.700
Clad Thickness	cm	0.06
Clad Material		Stainless Steel*
Absorber Diameter	cm	0.700
Absorber Material		Natural B4C**
Absorber Density	g / cc	1.80

*Compositions Weight percent:

C	Cr	Ni	Ti	Fe
0.12	18.5	10.5	1.0	69.88

** Content of ^{10}B is 19.8% atoms.

Remark. The lower part (30 cm) of control rods consists of Dy2O3 TiO2 of density 4.9 g / cc.

Table 2.7. Keff in Zero Power States

Irradiation Point →	0				10, GWd/t				20, GWd/t				30, GWd/t				40, GWd/t			
	Tmod=Tfuel =Tcon =20°C		Tmod=Tfuel =Tcon =280°C		Tmod=Tfuel =Tcon =20°C		Tmod=Tfuel =Tcon =280°C		Tmod=Tfuel =Tcon =20°C		Tmod=Tfuel =Tcon =280°C		Tmod=Tfuel =Tcon =20°C		Tmod=Tfuel =Tcon =280°C		Tmod=Tfuel =Tcon =20°C		Tmod=Tfuel =Tcon =280°C	
Cb (nat.B) → Pu/U Content, % ↓	0	1200	0	1200	0	1200	0	1200	0	1200	0	1200	0	1200	0	0	1200	0	1200	1200
U: 3.7/3.3 no BPR	1.4390	1.2266	1.3965	1.2370	1.2731	1.0952	1.2295	1.1028	1.1815	1.0134	1.1397	1.0221	1.0982	0.9374	1.0620	0.9501	1.0170	0.8637	0.9869	0.8802
U: 3.7/3.3 with BPR	1.4010	1.1991	1.3513	1.2015	1.2484	1,0786	1.2019	1.0817	1.1683	1.0061	1.1244	1.0113	1.0905	0.9345	1.0517	0.9436	1.0155	0.8660	0.9839	0.8802
PU: 4.4/3.0/2.4	1.4242	1.2341	1.3725	1.2342	1.2576	1.0967	1.2102	1.0979	1.1689	1.0152	1.1245	1.0188	1.0896	0.9414	1.0510	0.9492	1.0174	0.8742	0.9858	0.8872
PU: 4.4/3.0/2.0	1.4233	1.2322	1.3720	1.2331	1.2563	1.0945	1.2093	1.0963	1.1674	1.0130	1.1234	1.0171	1.0880	0.9392	1.0498	0.9476	1.0157	0.8720	0.9846	0.8855
PU: 4.4/3.2/2.0	1.4237	1.2331	1.3724	1.2337	1.2572	1.0958	1.2100	1.0974	1.1685	1.0144	1.1243	1.0183	1.0891	0.9407	1.0508	0.9488	1.0169	0.8735	0.9856	0.8868
PU: 4.2/3.0/2.0	1.42291	1.2315	1.3717	1.2325	1.2536	10920	1.2066	1.0940	1.1636	1.0096	1.1197	1.0138	1.0837	0.9354	1.0457	0.9440	1.0114	0.8683	0.9805	0.8820

Table 2.8. Parameters Evolution in the Process of Fuel Irradiation. Reference Uranium Assemblage. No BPR

Irradiation Point →	Burnup, GWd/t																			
Parameters ↓	0	2	4	6	8	10	12	14	16	18	20	22	24	26	28	30	32	34	36	38	40
Keff	1.2358	1.2168	1.1971	1.1768	1.1569	1.1378	1.1194	1.1018	1.0848	1.0684	1.0525	1.0370	1.0219	1.0071	0.9927	0.9786	0.9648	0.9513	0.9381	0.9252	0.9126
Ko	1.2402	1.2212	1.2014	1.1809	1.1608	1.1415	1.1230	1.1052	1.0881	1.0715	1.0555	1.0398	1.0246	1.0097	0.9951	0.9809	0.9669	0.9534	0.9401	0.9271	0.9145
Kkmax-CS	1.0740 (46)	1.0726 (46)	1.0708 (46)	1.0688 (46)	1.0664 (46)	1.0642 (46)	1.0619 (46)	1.0594 (46)	1.0565 (46)	1.0539 (46)	1.0514 (46)	1.0486 (46)	1.0460 (46)	1.0431 (46)	1.0407 (46)	1.0378 (46)	1.0353 (46)	1.0329 (46)	1.0305 (46)	1.0284 (46)	1.0262 (46)
βeff	0.007197	0.006915	0.006668	0.006463	0.006287	0.006133	0.005996	0.005873	0.005762	0.005660	0.005567	0.005480	0.005399	0.005323	0.005252	0.005184	0.005121	0.005061	0.005003	0.004949	0.004897

Table 2.9. Parameters Evolution in the Process of Fuel Irradiation. Reference Uranium Assemblage with Boron BPRs

Irradiation Point →	Burnup, GWd/t																			
Parameters ↓	0	2	4	6	8	10	12	14	16	18	20	22	24	26	28	30	32	34	36	38	40
Keff	1.2047	1.1883	1.1712	1.1536	1.1364	1.1199	1.1104	1.0890	1.0742	1.0597	1.0454	1.0312	1.0171	1.0031	0.9893	0.9756	0.9622	0.9490	0.9360	0.9234	0.9111
Ko	1.1113	1.1076	1.1029	1.0970	1.0907	1.0844	1.0780	1.0712	1.0637	1.0555	1.0462	1.0359	1.0248	1.0130	1.0007	0.9881	0.9754	0.9628	0.9502	0.9378	0.9257
Kkmax-CS	1.1289 (46)	1.1213 (46)	1.1136 (46)	1.1059 (46)	1.0983 (46)	1.0907 (46)	1.0834 (46)	1.0763 (46)	1.0697 (46)	1.0635 (46)	1.0579 (46)	1.0528 (46)	1.0483 (46)	1.0442 (46)	1.0405 (46)	1.0371 (46)	1.0339 (46)	1.0310 (46)	1.0283 (46)	1.0258 (46)	1.0234 (46)
βeff	0.007199	0.006911	0.006660	0.006451	0.006273	0.006118	0.005982	0.005859	0.005748	0.005647	0.005554	0.005468	0.005388	0.005314	0.005243	0.005177	0.005115	0.005056	0.005000	0.004946	0.004895

Table 2.10. Parameters Evolution in the Process of Fuel Irradiation. MOX LTA 4.4/3.0/2.4

Irradiation Point →	Burnup, GWd/t																			
Parameters ↓	0	2	4	6	8	10	12	14	16	18	20	22	24	26	28	30	32	34	36	38	40
Keff	1.2313	1.2100	1.1895	1.1693	1.1497	1.1311	1.1133	1.0962	1.0798	1.0640	1.0487	1.0338	1.0193	1.0051	0.9913	0.9779	0.9647	0.9519	0.9394	0.9272	0.9038
Ko	1.2439	1.2170	1.1911	1.1698	1.1502	1.1318	1.1143	1.0977	1.0818	1.0665	1.0518	1.0375	1.0237	1.0104	0.9975	0.9849	0.9727	0.9609	0.9495	0.9384	0.9172
Kkmax-CS	1.1898	1.1394	1.0979	1.0924	1.0878	1.0831	1.0781	1.0737	1.0751	1.0798	1.0841	1.0881	1.0917	1.0950	1.0980	1.1006	1.1029	1.1049	1.1065	1.1079	1.1112

Table 2.11. Parameters Evolution in the Process of Fuel Irradiation. MOX LTA 4.4/3.0/2.0

Irradiation Point →	Burnup, GWd/t																			
Parameters ↓	0	2	4	6	8	10	12	14	16	18	20	22	24	26	28	30	32	34	36	38	40
Keff	1.2306	1.2091	1.1886	1.1682	1.1487	1.1300	1.1121	1.0951	1.0786	1.0628	1.0474	1.0325	1.0180	1.0039	0.9901	0.9766	0.9634	0.9506	0.9381	0.9259	0.9140
Ko	1.2384	1.2090	1.1853	1.1640	1.1444	1.1260	1.1087	1.0923	1.0765	1.0614	1.0469	1.0329	1.0193	1.0061	0.9934	0.9811	0.9691	0.9575	0.9461	0.9353	0.9247
Kkmax-CS	1.1027 (46)	1.1016 (46)	1.0984 (46)	1.0941 (46)	1.0896 (46)	1.0849 (46)	1.0802 (46)	1.0760 (46)	1.0810 (206)	1.0856 (206)	1.0896 (206)	1.0936 (206)	1.0971 (206)	1.1002 (206)	1.1031 (136)	1.1056 (136)	1.1076 (136)	1.1091 (136)	1.1103 (206)	1.1114 (206)	1.1122 (206)
βeff	0.005978	0.005804	0.005650	0.005523	0.005415	0.005322	0.005241	0.005170	0.005107	0.005050	0.004998	0.004951	0.004908	0.004868	0.004831	0.004796	0.004763	0.004733	0.004704	0.004676	0.004650

Table 2.12. Parameters Evolution in the Process of Fuel Irradiation. MOX LTA 4.4/3.2/2.0

Irradiation Point →	Burnup, GWd/t																			
Parameters ↓	0	2	4	6	8	10	12	14	16	18	20	22	24	26	28	30	32	34	36	38	40
Keff	1.2311	1.2098	1.1893	1.1690	1.1495	1.1308	1.1130	1.0960	1.0796	1.0638	1.0484	1.0335	1.0190	1.0049	0.9911	0.9776	0.9645	0.9517	0.9391	0.9269	0.9151
Ko	1.2407	1.2116	1.1881	1.1670	1.1475	1.1293	1.1121	1.0957	1.0800	1.0649	1.0504	1.0364	1.0228	1.0097	0.9969	0.9846	0.9725	0.9609	0.9495	0.9385	0.9278
Kkmax-CS	1.1020 (46)	1.1007 (46)	1.0974 (46)	1.0931 (46)	1.0885 (46)	1.0837 (46)	1.0787 (46)	1.0740 (46)	1.0718 (206)	1.0768 (206)	1.0815 (206)	1.0857 (206)	1.0896 (206)	1.0932 (206)	1.0964 (206)	1.0994 (206)	1.1019 (206)	1.1042 (206)	1.1061 (206)	1.1077 (206)	1.1090 (206)
βeff	0.005972	0.005798	0.005645	0.005518	0.005410	0.005318	0.005237	0.005165	0.005102	0.005045	0.004993	0.004946	0.004903	0.004864	0.004827	0.004792	0.004760	0.004730	0.004701	0.004674	0.004648

Table 2.13. Parameters Evolution in the Process of Fuel Irradiation. MOX LTA 4.2/3.0/2.0

Irradiation Point →	Burnup, GWd/t																			
Parameters ↓	0	2	4	6	8	10	12	14	16	18	20	22	24	26	28	30	32	34	36	38	40
Keff	1.2300	1.2081	1.1871	1.1664	1.1465	1.1275	1.1094	1.0921	1.0755	1.0595	1.0440	1.0290	1.0144	1.0002	0.9863	0.9728	0.9596	0.9468	0.9343	0.9221	0.9103
Ko	1.2361	1.2062	1.1820	1.1603	1.1403	1.1217	1.1041	1.0874	1.0714	1.0560	1.0413	1.0271	1.0134	1.0001	0.9872	0.9748	0.9627	0.9511	0.9398	0.9288	0.9182
Kkmax-CS	1.1043 (46)	1.1030 (46)	1.0997 (46)	1.0955 (46)	1.0910 (46)	1.0863 (46)	1.0816 (46)	1.0769 (46)	1.0723 (46)	1.0693 (206)	1.0734 (206)	1.0770 (206)	1.0803 (206)	1.0833 (206)	1.0859 (206)	1.0882 (206)	1.0902 (206)	1.0919 (206)	1.0933 (206)	1.0944 (206)	1.0963 (253)
βeff	0.005985	0.005810	0.005656	0.005529	0.005421	0.005329	0.005248	0.005177	0.005113	0.005056	0.005005	0.004957	0.004914	0.004874	0.004837	0.004803	0.004763	0.004739	0.004710	0.004682	0.004656

Table 3.1. Power peaking factors for various FA arrangements depending on the boundary conditions

Variant	Fuel	Kk_{max}-CS	Variant	Fuel	Kk_{max}-CS
V1	UO_2	1.301 1.266	V2	UO_2	1.305 1.266
	1/3 MOX	1.393 1.327		1/3 MOX	1.451 1.327
V3	UO_2	1.509 1.281	V4	UO_2	1.560 1.359
	1/3 MOX	1.529 1.331		1/3 MOX	1.617 1.379
V5	UO_2	1.405 1.377	V6	UO_2	1.404 1.377
	1/3 MOX	1.445 1.418		1/3 MOX	1.444 1.418

Table 3.2. Power peaking factors in system with non-zonned MOX FA at x_{Pu^f} = 3.7 %

T (EFPD)	K_{Kmax}-CS	K_{Kmax}-CA	$K\overline{kmax}$ - CA	K_{Kmax}-CS	K_{Kmax}-CA	$K\overline{kmax}$ - CA
		V1			**V2**	
0	*1.451*	*1.451*	*1.150*	*1.452*	*1.452*	*1.150*
50	*1.426*	*1.426*	*1.134*	*1.426*	*1.426*	*1.133*
100	*1.414*	*1.414*	*1.129*	*1.414*	*1.414*	*1.130*
150	*1.406*	*1.406*	*1.129*	*1.406*	*1.406*	*1.131*
200	*1.400*	*1.400*	*1.130*	*1.398*	*1.398*	*1.130*
250	*1.394*	*1.394*	*1.131*	*1.391*	*1.391*	*1.132*
292	*1.387*	*1.387*	*1.133*	*1.385*	*1.385*	*1.133*
		V3			**V4**	
0	*1.462*	*1.462*	*1.147*	*1.615*	*1.615*	*1.210*
50	*1.436*	*1.436*	*1.333*	*1.567*	*1.567*	*1.188*
100	*1.424*	*1.424*	*1.128*	*1.534*	*1.534*	*1.179*
150	*1.415*	*1.415*	*1.128*	*1.509*	*1.509*	*1.175*
200	*1.408*	*1.408*	*1.129*	*1.488*	*1.488*	*1.173*
250	*1.402*	*1.402*	*1.131*	*1.469*	*1.469*	*1.170*
292	*1.395*	*1.395*	*1.132*	*1.454*	*1.454*	*1.169*
		V5			**V6**	
0	*1.687*	*1.687*	*1.260*	*1.687*	*1.687*	*1.260*
50	*1.630*	*1.630*	*1.233*	*1.630*	*1.630*	*1.233*
100	*1.591*	*1.591*	*1.219*	*1.591*	*1.591*	*1.219*
150	*1.560*	*1.560*	*1.209*	*1.560*	*1.560*	*1.209*
200	*1.534*	*1.534*	*1.202*	*1.534*	*1.534*	*1.203*
250	*1.511*	*1.511*	*1.197*	*1.511*	*1.511*	*1.197*
292	*1.494*	*1.494*	*1.193*	*1.494*	*1.494*	*1.193*

Table 3.3. Power peaking factors in system with zonned MOX FA at x_{Pu^f} = 4.4 %/3.4 %/2.6 %

T (EFPD)	K_{Kmax}-CS	K_{Kmax}-CA	$K\overline{kmax}$ - CA	K_{Kmax}-CS	K_{Kmax}-CA	$K\overline{kmax}$ - CA
		V1			**V2**	
0	1.300	1.280	1.147	1.300	1.281	1.147
50	1.287	1.247	1.131	1.287	1.247	1.130
100	1.267	1.225	1.125	1.268	1.225	1.124
150	1.247	1.223	1.125	1.247	1.223	1.125
200	1.229	1.224	1.124	1.229	1.224	1.125
250	*1.229*	*1.229*	*1.128*	*1.227*	*1.229*	*1.126*
292	*1.229*	*1.229*	*1.127*	*1.228*	*1.228*	*1.126*
		V3			**V4**	
0	1.307	1.290	1.147	*1.426*	*1.426*	*1.205*
50	1.294	1.255	1.129	*1.371*	*1.371*	*1.183*
100	1.274	1.234	1.124	*1.331*	*1.331*	*1.174*
150	1.254	1.227	1.123	1.302	1.297	1.168
200	1.235	1.228	1.124	1.277	1.272	1.165
250	*1.230*	*1.230*	*1.124*	*1.269*	*1.269*	*1.163*
292	*1.232*	*1.232*	*1.125*	*1.266*	*1.266*	*1.160*
		V5			**V6**	
0	*1.492*	*1.492*	*1.255*	*1.491*	*1.491*	*1.254*
50	*1.426*	*1.426*	*1.226*	*1.426*	*1.426*	*1.227*
100	*1.379*	*1.379*	*1.211*	*1.379*	*1.379*	*1.211*
150	*1.340*	*1.340*	*1.201*	*1.340*	*1.340*	*1.201*
200	*1.307*	*1.307*	*1.193*	*1.307*	*1.307*	*1.193*
250	*1.289*	*1.289*	*1.187*	*1.288*	*1.288*	*1.187*
292	*1.285*	*1.285*	*1.183*	*1.285*	*1.285*	*1.183*

Table 3.4. Power peaking factors in system with zonned MOX FA at x_{Pu^f} = 4.5 %/3.4 %/2.4 %

T (EFPD)	K_{Kmax}-CS	K_{Kmax}-CA	$K\overline{kmax}$ - CA	K_{Kmax}-CS	K_{Kmax}-CA	$K\overline{kmax}$ - CA
		V1			**V2**	
0	1.298	1.250	1.148	1.298	1.250	1.148
50	1.286	1.231	1.131	1.286	1.231	1.131
100	1.266	1.226	1.125	1.265	1.227	1.126
150	1.246	1.227	1.124	1.246	1.227	1.124
200	*1.232*	*1.232*	*1.127*	*1.230*	*1.230*	*1.126*
250	*1.232*	*1.232*	*1.126*	*1.233*	*1.233*	*1.126*
292	*1.234*	*1.234*	*1.126*	*1.234*	*1.234*	*1.126*
		V3			**V4**	
0	1.305	1.258	1.147	1.379	1.374	1.206
50	1.292	1.242	1.131	1.358	1.319	1.183
100	1.273	1.237	1.124	1.329	1.294	1.173
150	1.252	1.237	1.123	1.300	1.288	1.169
200	*1.241*	*1.241*	*1.124*	*1.283*	*1.283*	*1.164*
250	*1.242*	*1.242*	*1.125*	*1.281*	*1.281*	*1.162*
292	*1.246*	*1.246*	*1.127*	*1.278*	*1.278*	*1.160*
		V5			**V6**	
0	*1.437*	*1.437*	*1.254*	*1.436*	*1.436*	*1.254*
50	*1.372*	*1.372*	*1.225*	*1.372*	*1.372*	*1.225*
100	*1.342*	*1.342*	*1.210*	*1.342*	*1.342*	*1.210*
150	*1.313*	*1.313*	*1.200*	*1.313*	*1.313*	*1.200*
200	*1.306*	*1.306*	*1.192*	*1.306*	*1.306*	*1.192*
250	*1.301*	*1.301*	*1.186*	*1.301*	*1.301*	*1.186*
292	*1.297*	*1.297*	*1.181*	*1.297*	*1.297*	*1.181*

Table 3.5. Power peaking factors in system with zonned MOX FA at x_{Pu^f} = 4.6 %/3.4 %/2.2 %

T (EFPD)	K_{Kmax}-CS	K_{Kmax}-CA	$K\overline{kmax - CA}$	K_{Kmax}-CS	K_{Kmax}-CA	$K\overline{kmax - CA}$
		V1			**V2**	
0	1.299	1.253	1.142	1.299	1.253	1.141
50	1.285	1.236	1.125	1.285	1.235	1.125
100	1.264	1.231	1.120	1.264	1.230	1.119
150	1.244	1.231	1.118	1.244	1.231	1.118
200	*1.234*	*1.234*	*1.119*	*1.234*	*1.234*	*1.119*
250	*1.238*	*1.238*	*1.121*	*1.238*	*1.238*	*1.121*
292	*1.239*	*1.239*	*1.121*	*1.239*	*1.239*	*1.120*
		V3			**V4**	
0	1.305	1.262	1.140	1.380	1.333	1.199
50	1.292	1.245	1.124	1.355	1.310	1.177
100	1.270	1.241	1.119	1.325	1.298	1.167
150	1.249	1.243	1.119	1.295	1.291	1.162
200	*1.246*	*1.246*	*1.119*	*1.288*	*1.288*	*1.159*
250	*1.246*	*1.246*	*1.119*	*1.285*	*1.285*	*1.156*
292	*1.248*	*1.248*	*1.119*	*1.282*	*1.282*	*1.112*
		V5			**V6**	
0	1.394	1.382	1.247	1.393	1.382	1.247
50	1.370	1.339	1.218	1.370	1.339	1.218
100	1.338	1.325	1.203	1.338	1.325	1.203
150	*1.316*	*1.316*	*1.192*	*1.316*	*1.316*	*1.193*
200	*1.310*	*1.310*	*1.184*	*1.310*	*1.310*	*1.185*
250	*1.305*	*1.305*	*1.178*	*1.305*	*1.305*	*1.178*
292	*1.301*	*1.301*	*1.173*	*1.301*	*1.301*	*1.174*

Table 3.6. Power peaking factors in system with zonned MOX FA at x_{Pu^f} = 4.7 %/3.4 %/2.0 %

T (EFPD)	K_{Kmax}-CS	K_{Kmax}-CA	$K\overline{kmax}$ - CA	K_{Kmax}-CS	K_{Kmax}-CA	$K\overline{kmax}$ - CA
		V1			V2	
0	1.302	1.263	1.140	1.302	1.262	1.140
50	1.289	1.245	1.122	1.289	1.246	1.123
100	1.269	1.242	1.117	1.268	1.244	1.119
150	1.248	1.245	1.117	1.249	1.244	1.116
200	*1.248*	*1.248*	*1.116*	*1.247*	*1.247*	*1.116*
250	*1.251*	*1.251*	*1.117*	*1.250*	*1.250*	*1.117*
292	*1.254*	*1.254*	*1.118*	*1.253*	*1.253*	*1.118*
		V3			V4	
0	1.308	1.281	1.139	1.384	1.354	1.197
50	1.296	1.264	1.122	1.362	1.330	1.174
100	1.276	1.259	1.115	1.331	1.320	1.165
150	*1.262*	*1.262*	*1.115*	*1.315*	*1.315*	*1.160*
200	*1.265*	*1.265*	*1.116*	*1.310*	*1.310*	*1.156*
250	*1.267*	*1.267*	*1.117*	*1.308*	*1.308*	*1.153*
292	*1.270*	*1.270*	*1.118*	*1.305*	*1.305*	*1.151*
		V5			V6	
0	1.398	1.388	1.245	1.397	1.388	1.245
50	1.375	1.361	1.216	1.375	1.361	1.216
100	*1.347*	*1.347*	*1.201*	*1.347*	*1.347*	*1.201*
150	*1.339*	*1.339*	*1.191*	*1.339*	*1.339*	*1.191*
200	*1.334*	*1.334*	*1.183*	*1.334*	*1.334*	*1.183*
250	*1.328*	*1.328*	*1.177*	*1.328*	*1.328*	*1.177*
292	*1.325*	*1.325*	*1.172*	*1.325*	*1.325*	*1.172*

Table 3.7. Fuel reloading schemes

	1	2	3	4
UO_2	101→201	101→202	101→201	101→202
UO_2	102→202	102→201	102→202	102→201
MOX	103→203	103→203	103→203	103→203
UO_2	201→301	201→301	201→302	201→302
UO_2	202→302	202→302	202→301	202→301
MOX	203→303	203→303	203→303	203→303

Table 3.8. Effect of fuel reloading scheme on the K_K-CS value. Cycle № 5. x_{Pu^f} = 4.6 %/3.4 %/2.2 %

T (EFPD)	1	2	3	4	1	2	3	4
		V1				**V2**		
0	1.307	1.308	1.308	1.308	1.308	1.307	1.308	1.308
50	1.282	1.283	1.283	1.283	1.283	1.283	1.283	1.284
100	1.262	1.262	1.262	1.262	1.262	1.261	1.262	1.262
150	1.241	1.241	1.241	1.242	1.242	1.241	1.241	1.242
200	1.233	1.231	1.233	1.232	1.232	1.232	1.232	1.232
250	1.236	1.235	1.235	1.235	1.235	1.236	1.234	1.235
292	1.238	1.237	1.237	1.237	1.237	1.237	1.237	1.237
		V3				**V4**		
0	1.314	1.314	1.314	1.314	1.406	1.404	1.405	1.407
50	1.289	1.289	1.289	1.287	1.362	1.361	1.362	1.363
100	1.268	1.268	1.268	1.268	1.329	1.328	1.329	1.330
150	1.247	1.247	1.247	1.247	1.300	1.298	1.299	1.301
200	1.241	1.242	1.243	1.242	1.293	1.291	1.292	1.294
250	1.244	1.245	1.244	1.245	1.290	1.288	1.291	1.291
292	1.247	1.245	1.246	1.245	1.287	1.285	1.289	1.289
		V5				**V6**		
0	1.417	1.418	1.418	1.416	1.418	1.417	1.418	1.418
50	1.377	1.376	1.377	1.377	1.377	1.377	1.377	1.377
100	1.343	1.344	1.345	1.345	1.344	1.344	1.345	1.345
150	1.322	1.322	1.324	1.324	1.322	1.323	1.323	1.324
200	1.316	1.316	1.318	1.317	1.315	1.316	1.317	1.317
250	1.311	1.311	1.313	1.312	1.310	1.311	1.312	1.312
292	1.307	1.307	1.308	1.308	1.306	1.307	1.308	1.308

Table 4.1. Limiting parameters for VVER-1000

Criterion	Limiting Value	Remarks
Kq	<=1.35	For nominal power W=3000 MW
Kr	<=1.60	For nominal power W=3000 MW
$K_{o\text{-}total}$	Tabl. 3.2	For nominal power W=3000 MW
MTC	< 0	
MDC	> 0	
RO stop	<= -2000 pcm	t=20°C, Xe=0, Sm=Smh, Cb=16000 ppm, all control rods extracted
RCT	< 220°C	
$(RO)_{AP\text{-}1}$	> 5500 pcm	In full power

Table 4.2. Limits recommended for total power peaking factor $K_{o\text{-}total}$ for VVER-1000

Layer (from bottom to top)	1	2	3	4	5	6	7	8	9	10
$K_{o\text{-}total}$	2.24	2.24	2.24	2.24	2.24	2.14	1.96	1.80	1.69	1.58

Table 4.3. Recommended limiting parameters for VVER-1000 with 3 MOX LTAs.

Criterion	Limiting Value	Remarks
Kq	<=1.35	
Kr	<=1.55	In MOX assemblies. For nominal power W=3000 MW
$K_{o\text{-}total}$	Tabl. 3.4	In MOX assemblies. For nominal power W=3000 MW
MTC	< 0	
MDC	> 0	
RO stop	<= -2000 pcm	t=20°C, Xe=0, Sm=Smh, Cb=16000 ppm, all control rods extracted
RCT	< 210°C	
$(RO)_{AP\text{-}1}$	> 5500 pcm	In full power

Table 4.4. Limits recommended for total power peaking factor $K_{o\text{-}total}$ in MOX assemblies for VVER-1000 with 3 MOX LTAs

Layer (from bottom to top)	1	2	3	4	5	6	7	8	9	10
$K_{o\text{-}total}$	2.17	2.17	2.17	2.17	2.17	2.07	1.90	1.74	1.64	1.53

Table 4.5. Evolution of main neutronics parameters in Uranium reference core . Equilibrium cycle

Sim = 60 , Xe = 1 , Sm = 3

№	T EFPD	$H_{reg.}$ cm	t_{entry} °C	W MW	$Cb^{crit.}$ ppm	G m^3/h	Kq	Nk	Kq^{MOX}	Nk	Kv	Nk	Nz	$\bar{B}_U$ MW•d/kg	$\bar{B}_{MOX}$ MW•d/kg	MDC pcm• $(g/cm^3)^{-1}$	MTC pcm• $°C^{-1}$	DTC pcm• $°C^{-1}$	DTC* pcm• $°C^{-1}$	DPC pcm• MW^{-1}	DRo/DCb pcm• ppm^{-1}	$\beta_{ef.}$ pcm	$l_{im.}$ $•10^5$ sec
1	0.0	283.2	287.0	3000	5657	84000	1.31	19	0.00	0	1.61	19	4	14.14	0.00	12293	−25.94	−2.96	−2.46	−0.29	−1.55	650	2.24
2	20.0	283.2	287.0	3000	5318	84000	1.31	19	0.00	0	1.58	19	4	15.00	0.00	12894	−26.94	−2.96	−2.47	−0.29	−1.55	639	2.24
3	40.0	283.2	287.0	3000	4899	84000	1.31	19	0.00	0	1.56	19	4	15.85	0.00	14000	−29.20	−2.94	−2.48	−0.29	−1.56	630	2.25
4	60.0	283.2	287.0	3000	4473	84000	1.31	19	0.00	0	1.53	19	3	16.70	0.00	15191	−31.69	−2.93	−2.50	−0.29	−1.57	622	2.27
5	80.0	283.2	287.0	3000	4047	84000	1.31	19	0.00	0	1.52	19	3	17.55	0.00	16400	−34.24	−2.93	−2.52	−0.29	−1.58	613	2.29
6	100.0	283.2	287.0	3000	3631	84000	1.31	19	0.00	0	1.51	19	3	18.41	0.00	17590	−36.77	−2.94	−2.55	−0.29	−1.59	606	2.31
7	120.0	283.2	287.0	3000	3215	84000	1.30	19	0.00	0	1.50	19	3	19.26	0.00	18775	−39.30	−2.96	−2.58	−0.29	−1.60	598	2.33
8	140.0	283.2	287.0	3000	2813	84000	1.30	19	0.00	0	1.49	19	3	20.11	0.00	19928	−41.77	−2.97	−2.60	−0.29	−1.62	591	2.35
9	160.0	283.2	287.0	3000	2411	84000	1.30	19	0.00	0	1.48	19	3	20.96	0.00	21077	−44.25	−2.99	−2.63	−0.29	−1.63	585	2.37
10	180.0	283.2	287.0	3000	2023	84000	1.30	19	0.00	0	1.47	19	2	21.82	0.00	22203	−46.69	−3.02	−2.66	−0.29	−1.64	578	2.40
11	200.0	283.2	287.0	3000	1634	84000	1.30	19	0.00	0	1.47	19	2	22.67	0.00	23333	−49.16	−3.04	−2.69	−0.29	−1.66	573	2.42
12	220.0	283.2	287.0	3000	1254	84000	1.29	19	0.00	0	1.47	19	2	23.52	0.00	24457	−51.62	−3.06	−2.71	−0.29	−1.67	567	2.45
13	240.0	283.2	287.0	3000	874	84000	1.29	19	0.00	0	1.47	19	2	24.37	0.00	25592	−54.13	−3.08	−2.74	−0.30	−1.68	562	2.48
14	260.0	283.2	287.0	3000	500	84000	1.29	19	0.00	0	1.46	19	2	25.23	0.00	26727	−56.64	−3.09	−2.76	−0.30	−1.70	557	2.51
15	280.0	283.2	287.0	3000	127	84000	1.28	19	0.00	0	1.46	19	2	26.08	0.00	27869	−59.18	−3.11	−2.79	−0.30	−1.71	552	2.54
16	286.9	283.2	287.0	3000	0	84000	1.28	19	0.00	0	1.45	19	2	26.37	0.00	28260	−60.05	−3.12	−2.80	−0.30	−1.72	551	2.55

Table 4.6. Main neutronics parameters in zero power states. Reference Uranium Core Equilibrium Cycle

T	RO pcm	Cb ppm	Bank 10	Other banks↓↑	Xe	Sm	Tmod °C	MTC pcm/°C	MDC pcm/g/cc	DTC pcm/°C	DRO/DCB pcm/ppm	λm $*10^5 s$	βeff *100
BOC	0	8860	100% ↑	100% ↑	0	Smh	280	-1.23	2210	-2.93	-1.49	2.10	0.65
EOC	0	2000	100% ↑	100% ↑	eq	Sm eq	280	-27.52	18730	-3.31	-1.76	2.44	0.57
BOC	-14237 (RO_{STOP})	16000	100% ↑	100% ↑	0	Smh	20						

Table 4.7. Evolution of main neutronics parameters. First cycle with 3 MOX LTAs of "100%Pu" type

Sim =360 , Xe = 1 , Sm = 3

№	T EFPD	$H_{reg.}$ cm	t_{entry} °C	W MW	$Cb^{crit.}$ ppm	G m^3/h	Kq	Nk	Kq^{MOX}	Nk	Kv	Nk	Nz	$\bar{B}_U$ MW•d/kg	$\bar{B}_{MOX}$ MW•d/kg	MDC pcm• $(g/cm^3)^{-1}$	MTC pcm• $°C^{-1}$	DTC pcm• $°C^{-1}$	DTC* pcm• $°C^{-1}$	DPC pcm• MW^{-1}	DRo/DCb pcm• ppm^{-1}	$\beta_{ef.}$ pcm	$l_{im.}$ $•10^5$ sec
1	0.0	283.2	287.0	3000	5784	84000	1.32	38	1.03	8	1.61	38	4	14.26	0.00	12029	−25.00	−2.88	−2.49	−0.28	−1.55	642	2.23
2	20.0	283.2	287.0	3000	5439	84000	1.27	38	0.98	8	1.52	38	4	15.12	0.88	12614	−25.94	−2.89	−2.51	−0.28	−1.56	632	2.24
3	40.0	283.2	287.0	3000	5012	84000	1.27	38	0.95	8	1.49	11	4	15.97	1.71	13743	−28.28	−2.88	−2.52	−0.28	−1.57	624	2.26
4	60.0	283.2	287.0	3000	4585	84000	1.26	117	0.93	8	1.47	117	3	16.82	2.52	14944	−30.82	−2.88	−2.54	−0.28	−1.58	616	2.27
5	80.0	283.2	287.0	3000	4152	84000	1.26	92	0.92	150	1.45	92	3	17.68	3.32	16173	−33.43	−2.89	−2.56	−0.28	−1.59	608	2.29
6	100.0	283.2	287.0	3000	3725	84000	1.26	92	0.91	150	1.45	92	3	18.53	4.10	17390	−36.04	−2.90	−2.58	−0.28	−1.60	601	2.31
7	120.0	283.2	287.0	3000	3298	84000	1.27	92	0.91	88	1.45	92	3	19.38	4.88	18604	−38.65	−2.91	−2.61	−0.28	−1.61	594	2.33
8	140.0	283.2	287.0	3000	2887	84000	1.27	92	0.90	88	1.44	92	3	20.24	5.66	19785	−41.20	−2.93	−2.63	−0.28	−1.62	587	2.35
9	160.0	283.2	287.0	3000	2476	84000	1.27	92	0.90	88	1.44	124	3	21.09	6.42	20964	−43.75	−2.95	−2.65	−0.29	−1.64	581	2.38
10	180.0	283.2	287.0	3000	2072	84000	1.27	92	0.89	88	1.44	124	2	21.95	7.19	22131	−46.29	−2.97	−2.68	−0.29	−1.65	575	2.40
11	200.0	283.2	287.0	3000	1669	84000	1.27	124	0.89	88	1.45	124	2	22.80	7.95	23302	−48.86	−2.99	−2.70	−0.29	−1.66	569	2.43
12	220.0	283.2	287.0	3000	1276	84000	1.27	124	0.88	88	1.45	124	2	23.65	8.70	24460	−51.40	−3.01	−2.72	−0.29	−1.68	564	2.46
13	240.0	283.2	287.0	3000	883	84000	1.28	124	0.88	88	1.46	124	2	24.51	9.46	25627	−53.97	−3.03	−2.75	−0.29	−1.69	559	2.49
14	260.0	283.2	287.0	3000	491	84000	1.28	124	0.88	88	1.46	124	2	25.36	10.21	26802	−56.58	−3.04	−2.77	−0.29	−1.71	554	2.52
15	280.0	283.2	287.0	3000	111	84000	1.27	124	0.88	88	1.46	124	2	26.22	10.96	27960	−59.14	−3.06	−2.79	−0.29	−1.72	549	2.55
16	285.8	283.2	287.0	3000	0	84000	1.27	124	0.88	88	1.45	124	2	26.47	11.18	28297	−59.90	−3.07	−2.79	−0.29	−1.73	548	2.56

Table 4.8. Main neutronics parameters in zero power states. First cycle with 3 MOX LTAs of "100%Pu" type

T	RO pcm	Cb ppm	Bank 10	Other banks↓↑	Xe	Sm	Tmod °C	MTC pcm/°C	MDC pcm/g/cc	DTC pcm/°C	DRO/DCB pcm/ppm	λm $*10^5 s$	βeff pcm
BOC	0	8920	100% ↑	100% ↑	0	Smh	280	-0.99	2240	-2.97	-1.49	2.10	650
EOC	0	1980	100% ↑	100% ↑	eq	Sm eq	280	-27.59	18820	-3.32	-1.77	2.45	560
BOC	-13967 (RO_{STOP})	16000	100% ↑	100% ↑	0	Smh	20						

Table 4.9. Evolution of main neutronics parameters. Second cycle with 3 MOX LTAs of "100%Pu" type

β_{im} =360, Xe = 1, β_m = 3

№	T EFPD	$H_{eq.}$ cm	t_{water} °C	W MW	$Cb^{exit.}$ ppm	G m^3/h	Kq	Nk	Kq^{max}	Nk	Kv	Nk	Nz	$\bar{B}_U$ MW•d/kg	$\bar{B}_{max}$ MW•d/kg	MDC pcm• $(g/cm^3)^{-1}$	MTC pcm• $°C^{-1}$	DTC pcm• $°C^{-1}$	DTC* pcm• $°C^{-1}$	DPC pcm• MW^{-1}	DRo/DCb pcm• ppm^{-1}	$\beta_{ef.}$ pcm	l_{kin} $•10^5$ sec
1	0.0	283.2	287.0	3000	5666	84000	1.34	153	1.21	141	1.66	153	4	13.82	11.18	12450	−26.03	−2.89	−2.49	−0.28	−1.55	642	2.23
2	20.0	283.2	287.0	3000	5325	84000	1.28	153	1.20	141	1.56	153	4	14.67	12.21	13070	−27.06	−2.89	−2.50	−0.28	−1.55	632	2.24
3	40.0	283.2	287.0	3000	4904	84000	1.28	153	1.18	141	1.53	153	4	15.52	13.23	14186	−29.37	−2.88	−2.52	−0.28	−1.56	624	2.25
4	60.0	283.2	287.0	3000	4484	84000	1.28	153	1.17	141	1.50	153	3	16.37	14.23	15365	−31.85	−2.88	−2.53	−0.28	−1.57	616	2.27
5	80.0	283.2	287.0	3000	4055	84000	1.27	153	1.16	141	1.47	153	3	17.22	15.23	16573	−34.41	−2.88	−2.56	−0.28	−1.58	608	2.28
6	100.0	283.2	287.0	3000	3633	84000	1.26	153	1.16	18	1.45	47	3	18.07	16.22	17770	−36.96	−2.89	−2.58	−0.28	−1.60	601	2.30
7	120.0	283.2	287.0	3000	3212	84000	1.25	153	1.15	18	1.43	47	3	18.92	17.21	18964	−39.52	−2.90	−2.60	−0.28	−1.61	594	2.33
8	140.0	283.2	287.0	3000	2805	84000	1.25	110	1.14	18	1.41	47	3	19.77	18.19	20126	−42.02	−2.92	−2.62	−0.28	−1.62	587	2.35
9	160.0	283.2	287.0	3000	2398	84000	1.25	110	1.14	18	1.41	110	3	20.62	19.16	21284	−44.52	−2.93	−2.65	−0.28	−1.63	581	2.37
10	180.0	283.2	287.0	3000	2000	84000	1.25	110	1.13	18	1.41	110	2	21.47	20.13	22429	−47.00	−2.95	−2.67	−0.29	−1.65	575	2.40
11	200.0	283.2	287.0	3000	1602	84000	1.25	110	1.12	18	1.42	110	2	22.32	21.09	23578	−49.50	−2.97	−2.69	−0.29	−1.66	569	2.42
12	220.0	283.2	287.0	3000	1215	84000	1.26	110	1.12	18	1.42	110	2	23.17	22.05	24712	−51.98	−2.99	−2.72	−0.29	−1.67	564	2.45
13	240.0	283.2	287.0	3000	827	84000	1.26	110	1.12	18	1.43	110	2	24.02	23.00	25855	−54.49	−3.01	−2.74	−0.29	−1.69	559	2.48
14	260.0	283.2	287.0	3000	446	84000	1.26	110	1.11	18	1.43	110	2	24.87	23.96	26995	−57.00	−3.03	−2.76	−0.29	−1.70	554	2.51
15	280.0	283.2	287.0	3000	65	84000	1.26	110	1.11	18	1.43	56	2	25.72	24.90	28140	−59.54	−3.04	−2.78	−0.29	−1.71	550	2.54
16	283.5	283.2	287.0	3000	0	84000	1.26	110	1.11	18	1.43	56	2	25.87	25.07	28338	−59.98	−3.05	−2.79	−0.29	−1.72	549	2.54

Table 4.10. Main neutronics parameters in zero power states. Second cycle with 3 MOX LTAs of "100%Pu" type

T	RO pcm	Cb ppm	Bank 10	Other banks↓↑	Xe	Sm	Tmod °C	MTC pcm/°C	MDC pcm/g/cc	DTC pcm/°C	DRO/DCB pcm/ppm	λm $*10^5 s$	βeff *100
BOC	0	8800	100% ↑	100% ↑	0	Smh	280	-1.87	2710	-2.97	-1.49	2.10	0.64
EOC	0	1950	100% ↑	100% ↑	eq	Sm eq	280	-27.81	18930	-3.31	-1.77	2.44	0.56
BOC	-14110 (RO_{STOP})	16000	100% ↑	100% ↑	0	Smh	20						

Table 4.11. Evolution of main neutronics parameters. 3-d cycle with 3 MOX LTAs of "100%Pu" type

Sim =360 , Xe = 1 , Sm = 3

M	T EFPD	$H_{reg.}$ cm	t_{entry} °C	W MW	$Cb^{crit.}$ ppm	G m^3/h	Kq	Nk	Kq^{MOX}	Nk	Kv	Nk	Nz	$\bar{B}_U$ MW•d/kg	$\bar{B}_{MOX}$ MW•d/kg	MDC pcm• $(g/cm^3)^{-1}$	MTC pcm• $°C^{-1}$	DTC pcm• $°C^{-1}$	DTC' pcm• $°C^{-1}$	DPC pcm• MW^{-1}	DRo/DCb pcm• ppm^{-1}	$\beta_{ef.}$ pcm	l_{im} $•10^5$ sec
1	0.0	283.2	287.0	3000	5810	84000	1.33	126	1.04	111	1.64	126	4	13.36	25.07	11897	-24.77	-2.89	-2.48	-0.28	-1.55	647	2.23
2	20.0	283.2	287.0	3000	5472	84000	1.28	11	1.06	111	1.54	126	4	14.21	25.96	12560	-25.89	-2.88	-2.49	-0.28	-1.55	636	2.24
3	40.0	283.2	287.0	3000	5054	84000	1.28	11	1.05	111	1.51	11	4	15.06	26.86	13685	-28.21	-2.88	-2.51	-0.28	-1.56	628	2.25
4	60.0	283.2	287.0	3000	4629	84000	1.27	11	1.05	111	1.48	126	3	15.91	27.75	14883	-30.74	-2.87	-2.53	-0.28	-1.57	620	2.27
5	80.0	283.2	287.0	3000	4204	84000	1.26	11	1.04	111	1.46	126	3	16.76	28.64	16095	-33.31	-2.88	-2.55	-0.28	-1.58	612	2.28
6	100.0	283.2	287.0	3000	3779	84000	1.25	124	1.04	111	1.44	124	3	17.62	29.53	17306	-35.90	-2.89	-2.57	-0.28	-1.59	604	2.30
7	120.0	283.2	287.0	3000	3368	84000	1.25	124	1.04	111	1.44	124	3	18.47	30.42	18486	-38.42	-2.90	-2.60	-0.28	-1.61	597	2.32
8	140.0	283.2	287.0	3000	2958	84000	1.25	124	1.04	111	1.43	124	3	19.32	31.30	19661	-40.95	-2.91	-2.62	-0.28	-1.62	591	2.34
9	160.0	283.2	287.0	3000	2547	84000	1.25	124	1.04	111	1.42	124	3	20.17	32.18	20833	-43.48	-2.93	-2.64	-0.28	-1.63	584	2.37
10	180.0	283.2	287.0	3000	2150	84000	1.25	124	1.04	111	1.42	124	2	21.02	33.07	21979	-45.97	-2.95	-2.67	-0.29	-1.64	578	2.39
11	200.0	283.2	287.0	3000	1754	84000	1.25	134	1.04	111	1.42	124	2	21.88	33.95	23129	-48.47	-2.97	-2.69	-0.29	-1.66	572	2.42
12	220.0	283.2	287.0	3000	1357	84000	1.25	134	1.04	111	1.42	124	2	22.73	34.83	24284	-51.00	-2.99	-2.72	-0.29	-1.67	567	2.45
13	240.0	283.2	287.0	3000	974	84000	1.25	134	1.04	111	1.42	124	2	23.58	35.72	25422	-53.50	-3.01	-2.74	-0.29	-1.69	561	2.47
14	260.0	283.2	287.0	3000	591	84000	1.25	134	1.04	111	1.42	134	2	24.43	36.60	26568	-56.03	-3.02	-2.76	-0.29	-1.70	557	2.50
15	280.0	283.2	287.0	3000	208	84000	1.25	134	1.04	111	1.42	134	2	25.28	37.49	27720	-58.58	-3.04	-2.78	-0.29	-1.71	552	2.53
16	291.0	283.2	287.0	3000	0	84000	1.25	134	1.04	111	1.42	134	2	25.75	37.97	28351	-59.99	-3.05	-2.79	-0.29	-1.72	550	2.55

Table 4.12. Main neutronics parameters in zero power states. Third cycle with 3 MOX LTAs of "100%Pu" type

T	RO pcm	Cb ppm	Bank 10	Other banks↓↑	Xe	Sm	Tmod °C	MTC pcm/°C	MDC pcm/g/cc	DTC pcm/°C	DRO/DCB pcm/ppm	λm $*10^5 s$	βeff pcm
BOC	0	8830	100% ↑	100% ↑	0	Smh	280	-0.94	2170	-2.96	-1.49	2.10	650
EOC	0	1950	100% ↑	100% ↑	eq	Sm eq	280	-27.87	18960	-3.31	-1.77	2.44	560
BOC	-14107 (RO_{STOP})	16000	100% ↑	100% ↑	0	Smh	20						

Table 4.13. Pin Power Peaking Factors Attained During Fuel Cycle

T, EFPD	Kr							N (Kr)				Ko-total				N (Ko-total)				M(Ko-total)			
	UOX	MOX 1		MOX 2		MOX 3		UOX	MOX 1	MOX 2	MOX 3	UOX	MOX 1	MOX 2	MOX 3	UOX	MOX 1	MOX 2	MOX 3	UOX	MOX 1	MOX 2	MOX 3
	ALL CORE	ALL CORE	MOX FA	ALL CORE	MOX FA	ALL CORE	MOX FA					ALL CORE	ALL CORE	ALL CORE	ALL CORE								
0	1.51	1.47	1.28	1.49	1.37	1.48	1.25	19	38	153	126	1.86	1.79	1.85	1.83	19	38	153	126	4	4	4	4
20	1.49	1.40	1.22	1.43	1.36	1.42	1.27	19	38	110	126	1.80	1.68	1.72	1.71	19	38	153	126	4	4	4	4
40	1.48	1.40	1.19	1.41	1.34	1.41	1.25	19	40	110	126	1.76	1.65	1.68	1.67	19	38	153	126	4	4	4	4
60	1.47	1.39	1.16	1.40	1.33	1.39	1.25	19	92	153	126	1.72	1.62	1.64	1.63	19	117	153	126	3	3	3	3
80	1.45	1.39	1.15	1.39	1.32	1.38	1.23	19	32	153	117	1.69	1.60	1.61	1.60	19	92	153	137	3	3	3	3
100	1.44	1.38	1.14	1.38	1.31	1.37	1.23	19	32	153	126	1.66	1.58	1.59	1.57	19	32	153	12	3	3	3	3
120	1.43	1.37	1.14	1.37	1.30	1.36	1.22	19	32	153	126	1.64	1.57	1.57	1.55	19	32	47	12	3	3	3	3
140	1.42	1.37	1.13	1.36	1.29	1.35	1.22	19	32	153	126	1.62	1.56	1.55	1.53	19	124	126	137	3	3	3	3
160	1.41	1.36	1.13	1.35	1.29	1.34	1.21	19	124	126	126	1.60	1.55	1.53	1.52	19	124	35	137	3	3	3	3
180	1.39	1.36	1.12	1.35	1.28	1.33	1.21	19	124	126	126	1.58	1.54	1.51	1.50	19	124	126	137	3	2	2	3
200	1.38	1.35	1.11	1.34	1.27	1.32	1.21	19	124	126	126	1.57	1.54	1.51	1.49	19	124	110	124	2	2	2	2
220	1.37	1.35	1.10	1.33	1.26	1.32	1.20	19	124	126	137	1.56	1.54	1.50	1.48	19	124	110	124	2	2	2	2
240	1.36	1.34	1.10	1.32	1.26	1.31	1.20	19	124	110	137	1.55	1.53	1.50	1.48	19	124	110	124	2	2	2	2
260	1.35	1.34	1.10	1.31	1.25	1.30	1.19	19	124	110	137	1.54	1.53	1.49	1.47	19	124	110	134	2	2	2	2
280	1.34	1.33	1.10	1.31	1.25	1.29	1.19	6	124	110	154	1.53	1.52	1.49	1.47	19	124	56	134	2	2	2	2
EOC	1.34	1.33	1.10	1.31	1.25	1.29	1.19	6	124	110	152	1.52	1.52	1.49	1.46	19	124	56	134	2	2	2	2

Table 4.14. Core Subcriticality (Scram Margin) in different states in the process of Scram actuation

State parameters						RO, pcm							
						UOX		MOX 1er cycle		MOX 2nd cycle		MOX 3d cycle	
State Number	W, MW	t_{entry}, °C	Hreg, %	Positions of banks	Positions of the most eff.	BOC	EOC	BOC	EOC	BOC	EOC	BOC	EOC
1	3000	Nominal.	100	100	100	+522	+605	+483	+600	+434	+563	+449	+569
	Regulation margin of reactivity												
2	3000	Nominal.	50	100	100	0.	0.	0.	0.	0.	0.	0.	0.
	Scram actuation without sticking of the most effective CR												
3	3000	Nominal.	0	0	0	-8833	-9136	-8772	-9043	-8806	-9064	-8994	-9150
	Scram actuation with sticking of the most effective CR												
4	3000	Nominal.	0	0	100	-7970	-8262	-7964	-8178	-7889	-8153	-8671	-8282
	Doppler effect												
5	0	Nominal.	0	0	100	-6391	-6807	-6989	-7296	-6865	-7244	-7628	-7379
	Moderator temperature effect												
6	0	287	0	0	100	-5550	-5088	-5718	-5001	-5609	-5000	-6488	-5192
	Moderator temperature effect												
7	0	280	0	0	100	-5358	-4711	-5530	-4624	-5417	-4624	-6294	-4817
	Vapor effect ($\Delta\rho$ = 50 pcm)												
8	0	280	0	0	100	-5308	-4661	-5480	-4574	-5367	-4574	-6244	-4767
	Uncertainty of $(RO)_{\Delta P}$ calculation (10% of p. 4)												
9	0	280	0	0	100	-4511	-3835	-4684	-3756	-4578	-3759	-5377	-3939
	Uncertainty of temperature effect calculation ($\Delta\rho$ = 180 pcm)												
10	0	280	0	0	100	-4331	-3655	-4504	-3576	-4398	-3579	-5197	-3759
	Absorbent irradiation effect ($\Delta\rho$ = 100 pcm)												
11	0	280	0	0	100	**-4231**	**-3555**	**-4404**	**-3476**	**-4298**	**-3479**	**-5097**	**-3659**

Table 4.15a. Control rods worth calculation. States description

V1. BOC	V2. BOC	V3. BOC	V1. EOC	V1. EOC	V1. EOC
S1 Wnom, Xe=Xe eq, t_{entry}=287°C, Cb burnup 100 % 5↓* 30 % 10↓ **S2**: the same but 100% 1-10↓	**S1** MCL, Xe=0, t_{entry}=280°C Cb crit 30% 10↓ **S2**: the same but 100% 1-10↓	**S1** MCL, Xe=Xe eq, t_{entry}=280°C Cb crit 30% 10↓ **S2**: the same but 100% 1-10↓	**S1** Wnom, Xe=Xe eq, t_{entry}=287°C Cb burnup 100 % 5↓ 30% 10↓ **S2**: the same but 100% 1-10↓	**S1** MCL, Xe=Xe eq, t_{entry}=280°C Cb crit 100 % 5↓ 30 % 10↓ **S2**: the same but 100% 1-10↓	**S1** MCL, Xe=0, t_{entry}=280°C Cb crit 100 % 5↓ 30 % 10↓ **S2**: the same but 100% 1-10↓

Table 4.15b. Control rods worth in Uranium reference core and in 3 MOX LTAs loaded cores (pcm)

		Uranium Core			MOX-1			MOX-2			MOX-3		
	Variant	V1	V2	V3	V1	V2	V3	V1	V2	V3	V1	V2	V3
BOC	Stuck rod number	55	55	55	67	67	67	109	82	82	112	97	97
	$(RO)_{AP-1}$	7684	7281	7252	7672	7376	7350	7712	7321	7275	8070	7677	7631
EOC	Stuck rod number	55	55	55	97	97	97	55	97	97	97	55	55
	$(RO)_{AP-1}$	7931	6481	6475	7790	6326	6297	7819	6414	6417	7856	6531	6514

* X% N↓ means that the Bank N is X% inserted in core

Table 4.16. Core reactivity in the process of control rods movement

AP Position,% (Hreg=80%)	BOC							
	Uranium		MOX-1		MOX-2		MOX-3	
	No stuck	Stuck N 55	No stuck	Stuck N 67	No stuck	Stuck N 109	No stuck	Stuck N 112
100	0	0	0	0	0	0	0	0
90	-120	-120	-120	-120	-110	-110	-120	-120
80	-210	-210	-210	-210	-200	-200	-200	-200
70	-310	-310	-310	-310	-290	-290	-300	-300
60	-460	-460	-450	-450	-430	-430	-440	-440
50	-700	-700	-680	-680	-660	-660	-680	-680
40	-1150	-1140	-1110	-1100	-1070	-1070	-1090	-1090
30	-2000	-1990	-1920	-1910	-1860	-1850	-1900	-1900
20	-3620	-3590	-3490	-3470	-3430	-3400	-3480	-3480
10	-7050	-6810	-6930	-6730	-6900	-6660	-7010	-7010
0	-9150	-8330	-9060	-8300	-9060	-8180	-9250	-9250

AP Position,% (Hreg=80%)	EOC							
	Uranium		MOX-1		MOX-2		MOX-3	
	No stuck	Stuck N 55	No stuck	Stuck N 97	No stuck	Stuck N 97	No stuck	Stuck N 97
100	0	0	0	0	0	0	0	0
90	-140	-140	-140	-140	-130	-130	-140	-140
80	-190	-190	-190	-190	-190	-190	-190	-190
70	-260	-260	-260	-260	-250	-250	-260	-260
60	-360	-360	-360	-360	-350	-350	-350	-350
50	-530	-530	-530	-530	-520	-520	-530	-530
40	-880	-870	-870	-870	-850	-850	-860	-860
30	-1590	-1580	-1570	-1570	-1540	-1530	-1540	-1540
20	-3000	-2980	-2960	-2960	-2910	-2890	-2910	-2890
10	-6300	-6160	-6200	-6200	-6180	-6020	-6190	-6060
0	-9410	-8570	-9310	-9310	-9310	-8430	-9400	-8560

Table 4.17. Return Criticality Temperature

	UOX	MOX-1	MOX-2	MOX-3
RCT, °C	124	129	130	117

Figure 2.1. Simplified Design for Uranium Reference Assembly (Type A)

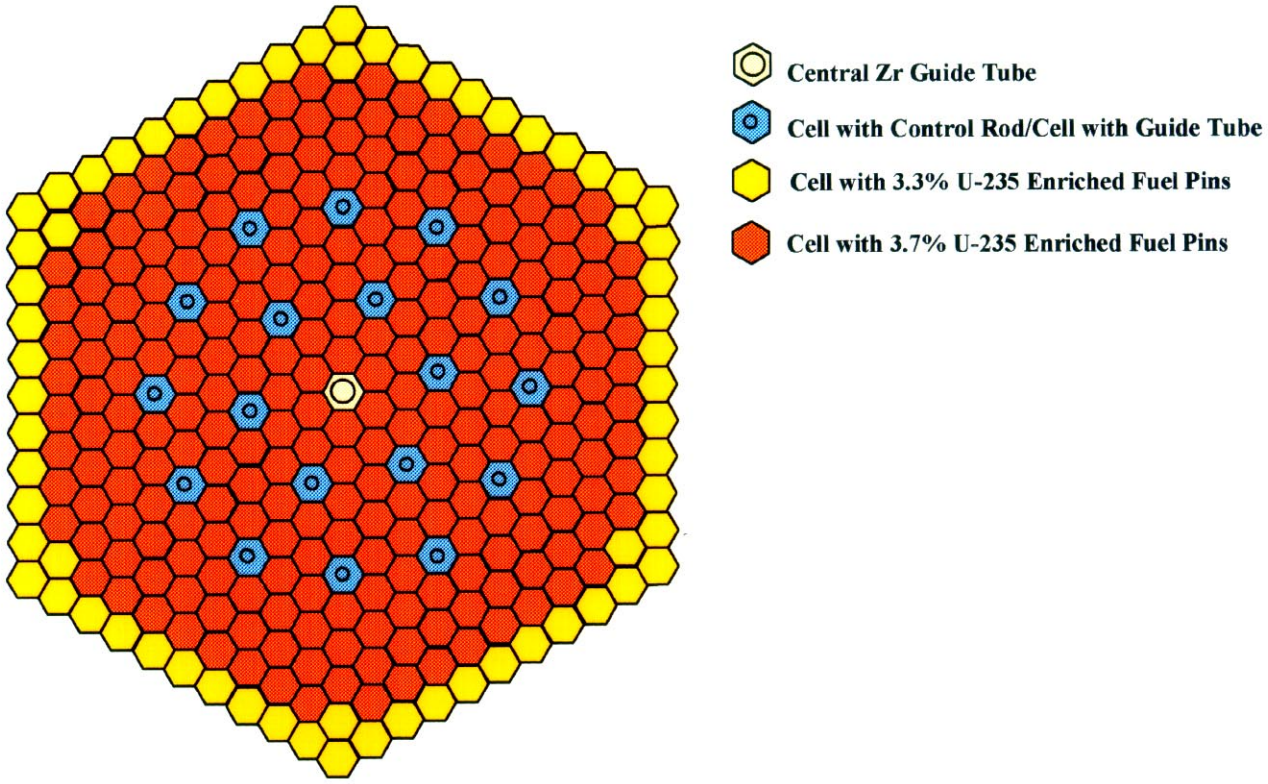

Figure 2.2. Calculational Model for Reference Uranium Assembly Surrounded by Uranium Assemblies. 60° Sector

26,
71,25,
71,71,25,
71,71,71,25,
71,71,71,71,25,
71,71,71,71,71,25,
29,71,71,71,71,71,25,
71,71,71,71,71,71,71,25,
71,71,71,29,71,71,71,71,25,
71,29,71,71,71,71,71,71,71,25,
71,71,71,71,71,71,71,71,71,71,25,
27,71,71,71,71,29,71,71,71,71,71,26,
71,71,71,29,71,71,71,71,71,71,71,25,64,
71,71,71,71,71,71,71,71,71,71,71,25,64,64,
71,71,29,71,71,71,29,71,71,71,71,25,64,50,50,
71,71,71,71,71,71,71,71,71,71,71,25,64,50,50,50,
29,71,71,71,71,29,71,71,71,71,71,25,64,50,50,50,50,
71,71,71,29,71,71,71,71,71,71,71,25,64,50,50,50,50,29,
71,71,71,71,71,71,71,71,71,71,71,25,64,50,50,50,50,50,50,
71,71,71,71,71,71,71,71,71,71,71,25,64,50,50,50,29,50,50,50,
71,71,71,71,71,71,71,71,71,71,71,25,64,50,50,50,50,50,50,50,50,
71,71,71,71,71,71,71,71,71,71,71,25,64,50,50,50,50,50,50,29,50,50,
26,25,25,25,25,25,25,25,25,25,25,26,64,64,50,50,50,29,50,50,50,50,27,

25 – side water cell
26 – corner water cell
27 – central tube cell
29 – guide tube cell / burnable absorber
50 – uranium 3.7% U-235 fuel rods
64 – uranium 3.3% U-235 fuel rods
71 – uranium 3.7% U-235 fuel rods

Figure 2.3. Simplified Design for Uranium Assembly (Types B and Ba)

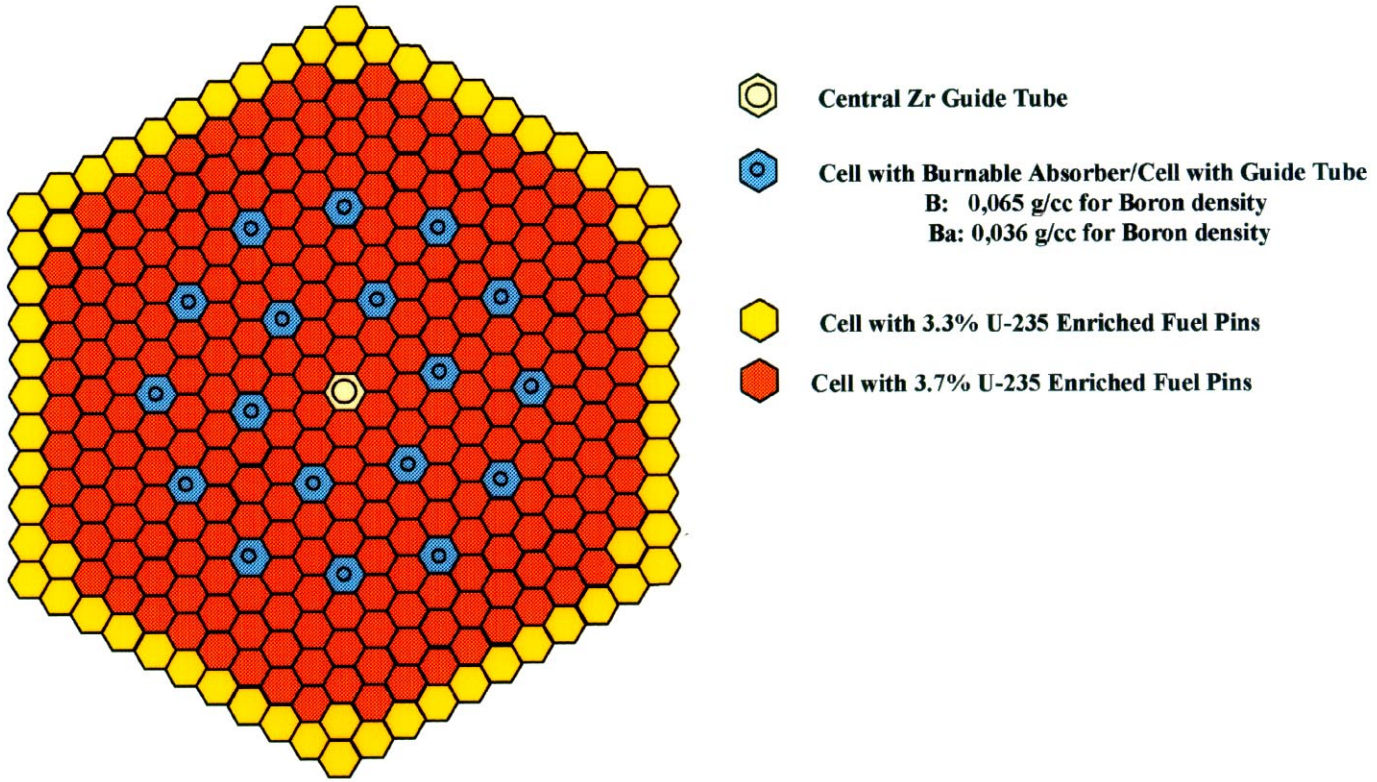

Figure 2.4. Simplified Design for Uranium Assembly (Type C)

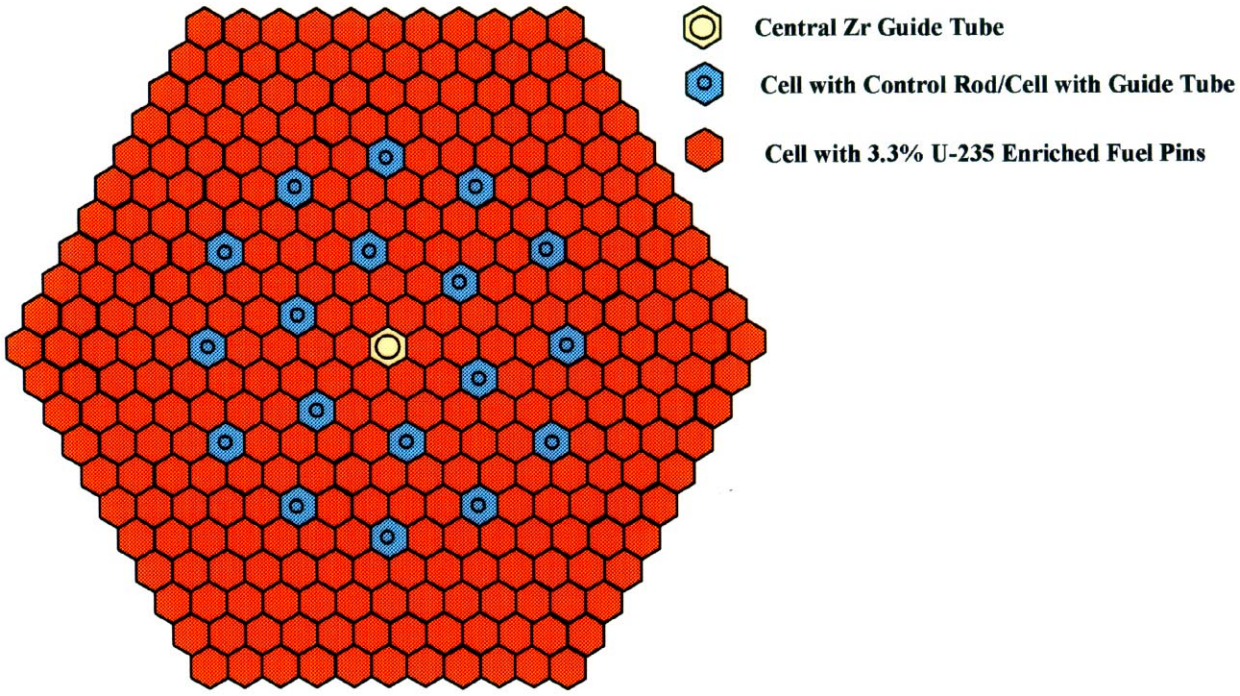

Figure 2.5. Simplified Design for 100 % Plutonium (3 Zones) MOX LTA

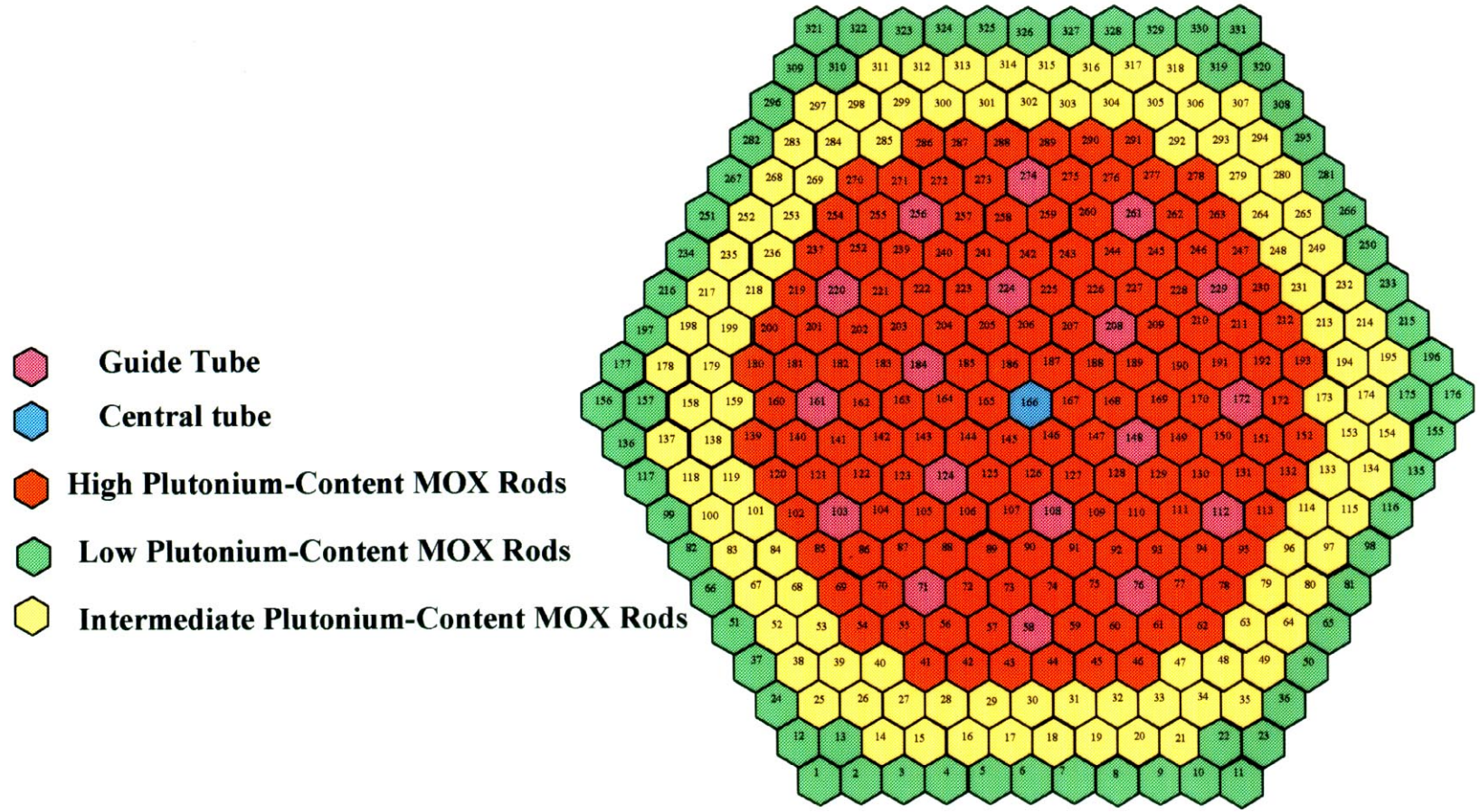

Figure 2.6. Calculational Model for 3-Zones (100 % Plutonium) MOX LTA Surrounded by Uranium Assemblies. 60° Sector

26,
71,25,
71,71,25,
71,71,71,25,
71,71,71,71,25,
71,71,71,71,71,25,
29,71,71,71,71,71,25,
71,71,71,71,71,71,71,25,
71,71,71,29,71,71,71,71,25,
71,29,71,71,71,71,71,71,71,25,
71,71,71,71,71,71,71,71,71,71,25,
27,71,71,71,71,29,71,71,71,71,71,26,
71,71,71,29,71,71,71,71,71,71,71,25,64,
71,71,71,71,71,71,71,71,71,71,71,25,64,64,
71,71,29,71,71,71,29,71,71,71,71,25,64,57,57,
71,71,71,71,71,71,71,71,71,71,71,25,64,57,57,57,
29,71,71,71,71,29,71,71,71,71,71,25,64,57,57,50,50,
71,71,71,29,71,71,71,71,71,71,71,25,64,57,57,50,50,29,
71,71,71,71,71,71,71,71,71,71,71,25,64,57,57,50,50,50,50,
71,71,71,71,71,71,71,71,71,71,71,25,64,57,57,50,29,50,50,50,
71,71,71,71,71,71,71,71,71,71,71,25,64,57,57,50,50,50,50,50,50,
71,71,71,71,71,71,71,71,71,71,71,25,64,57,57,50,50,50,50,29,50,50,
26,25,25,25,25,25,25,25,25,25,25,26,64,64,57,57,50,29,50,50,50,50,27,

25 – side water cell
26 – corner water cell
27 – central tube cell
29 – guide tube cell
50 – high plutonium-content fuel rods
57 – intermediate plutonium-content fuel rods
64 – low plutonium-content fuel rods
71 – uranium 3.7% U-235 fuel rods

Figure 2.7. Pins Numeration in CS Model

1 ,
2 , 3 ,
4, 5 , 6 ,
7 , 8 , 9 , 10 ,
11 , 12 , 13 , 14 , 15 ,
16 , 17 , 18 , 19 , 20 , 21 ,
22 , 23 , 24 , 25 , 26 , 27 , 28 ,
29 , 30 , 31 , 32 , 33 , 34 , 35 , 36 ,
37 , 38 , 39 , 40 , 41 , 42 , 43 , 44 , 45 ,
46 , 47 , 48 , 49 , 50 , 51 , 52 , 53 , 54 , 55 ,
56 , 57 , 58 , 59 , 60 , 61 , 62 ,63 , 64 , 65 , 66 ,
67 ,68 , 69 , 70 , 71 , 72 , 73 , 74 , 75 , 76 , 77, 78,
79 , 80 , 81 , 82 , 83 , 84 , 85 , 86 , 87 , 88 , 89 , 90, 91, .
92 , 93 , 94 , 95 , 96 , 97 , 98 , 99 ,100,101,102,103,104,105,
106,107,108,109,110,111,112,113,114,115,116,117,118,119,120, .
121,122,123,124,125,126,127,128,129,130,131,132,133,134,135,136,
137 ,138,139,140,141,142,143,144,145,146,147,148,149,150,151,152,153,
154,155,156,157,158,159,160,161,162,163,164,165,166,167,168,169,170,171,
172,173,174,175,176,177,178,179,180,181,182,183,184,185,186,187,188,189,190,
191,192,193,194,195,196,197,198,199,200,201,202,203,204,205,206,207,208,209,210,
211,212,213,214,215,216,217,218,219,220,221,222,223,224,225,226,227,228,229,230,231,
232,233,234,235,236,237,238,239,240,241,242,243,244,245,246,247,248,249,250,251,252,253,
254,255,256,257,258,259,260,261,262,263,264,265,266,267,268,269,270,271,272,273,274,275,276,

257 – side water cell
254 – corner water cell
276 – central tube cell
137 – guide tube cell / burnable absorber
223 –plutonium fuel rods
71 – uranium 3.7% U-235 fuel rods

Figure 2.8. Evolution of Ko in Plutonium-Uranium Super-Cells

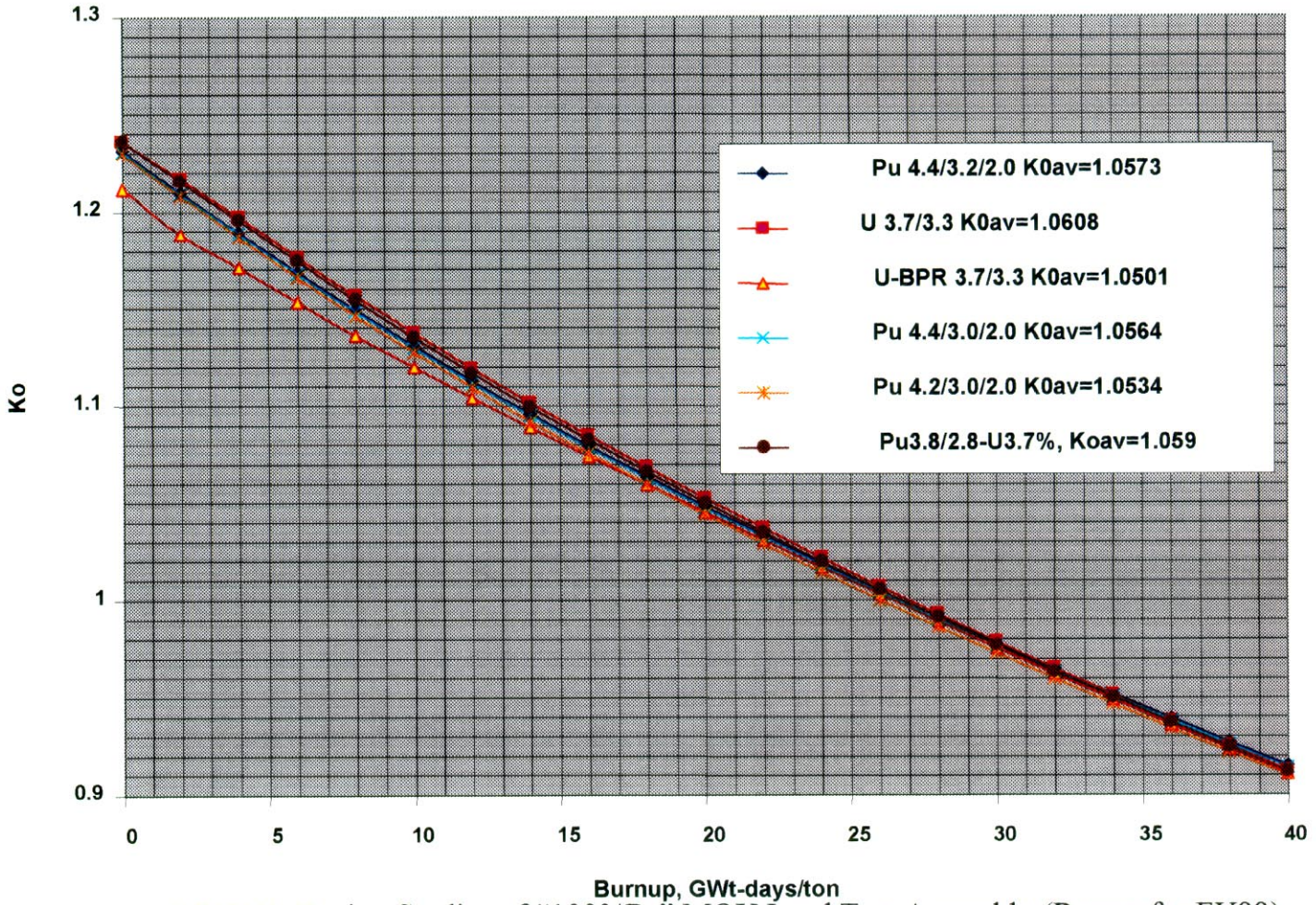

Figure 2.9. Evolution of Kk in Plutonium-Uranium Super-Cells

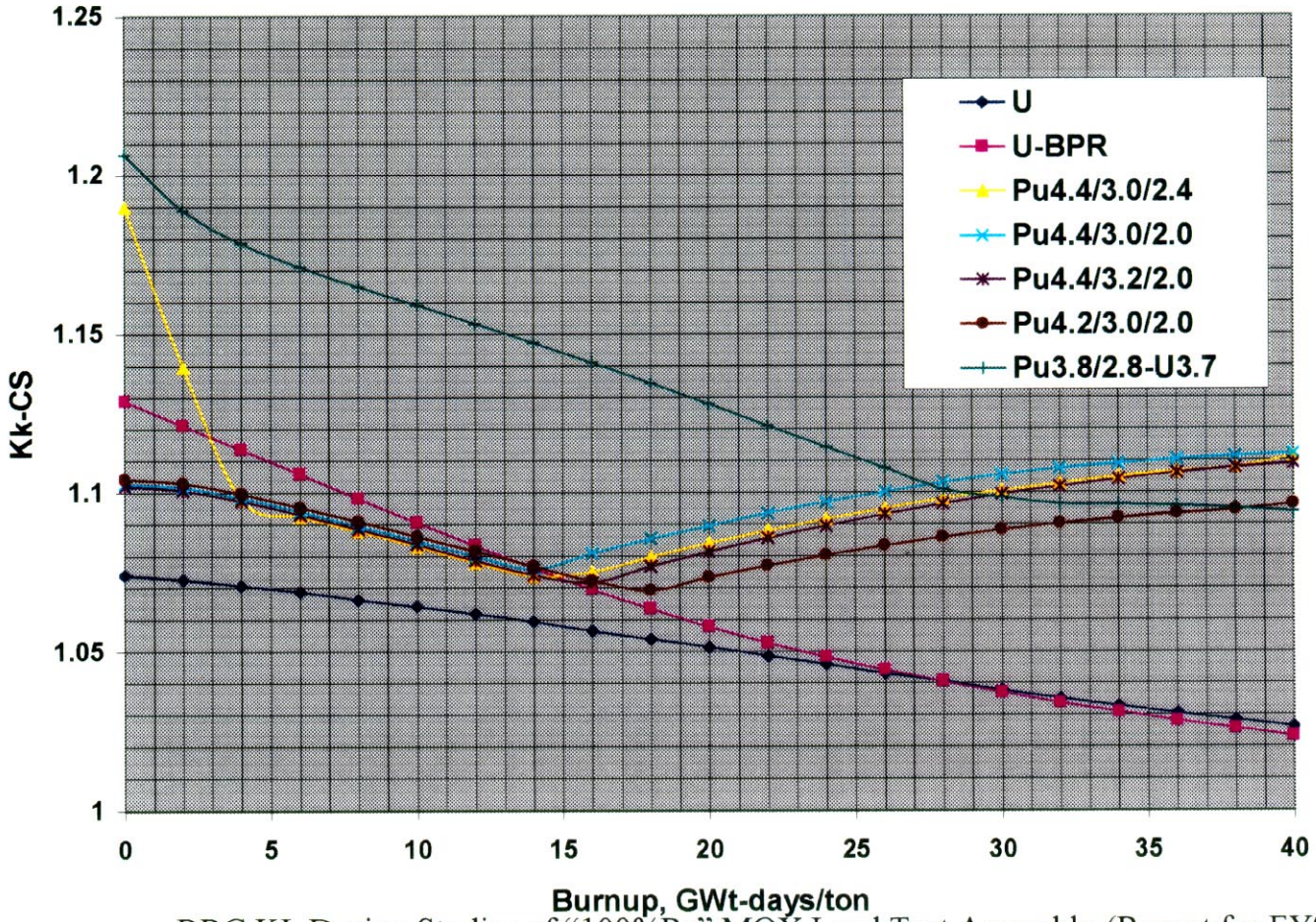

Figure 3.1. Symmetric element of the core

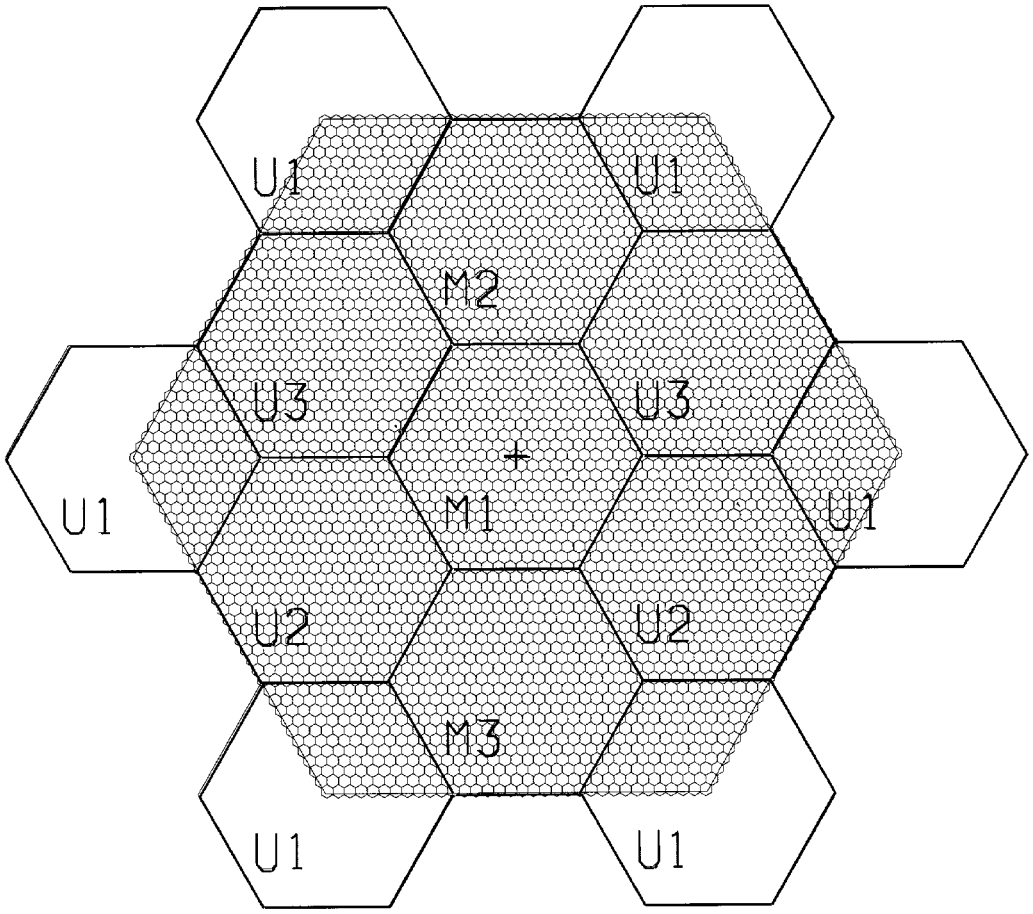

Figure 3.2. FA arrangements in symmetric element

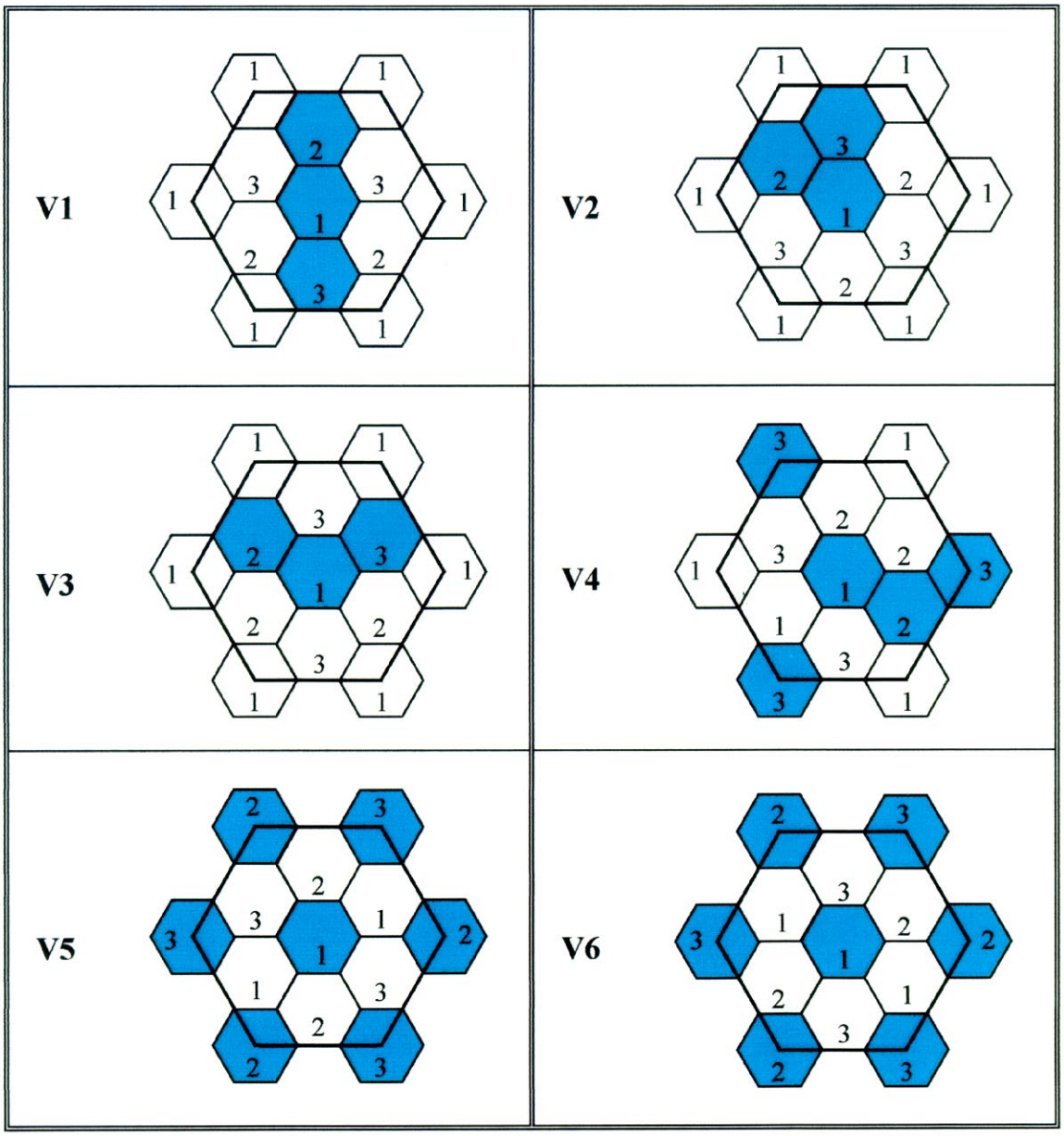

Figure 3.3. Power peaking factors K_{Kmax}–CS (Kk – CS) and K_{Kmax}–CA (K_K – CA) versus Pu content in a central FA

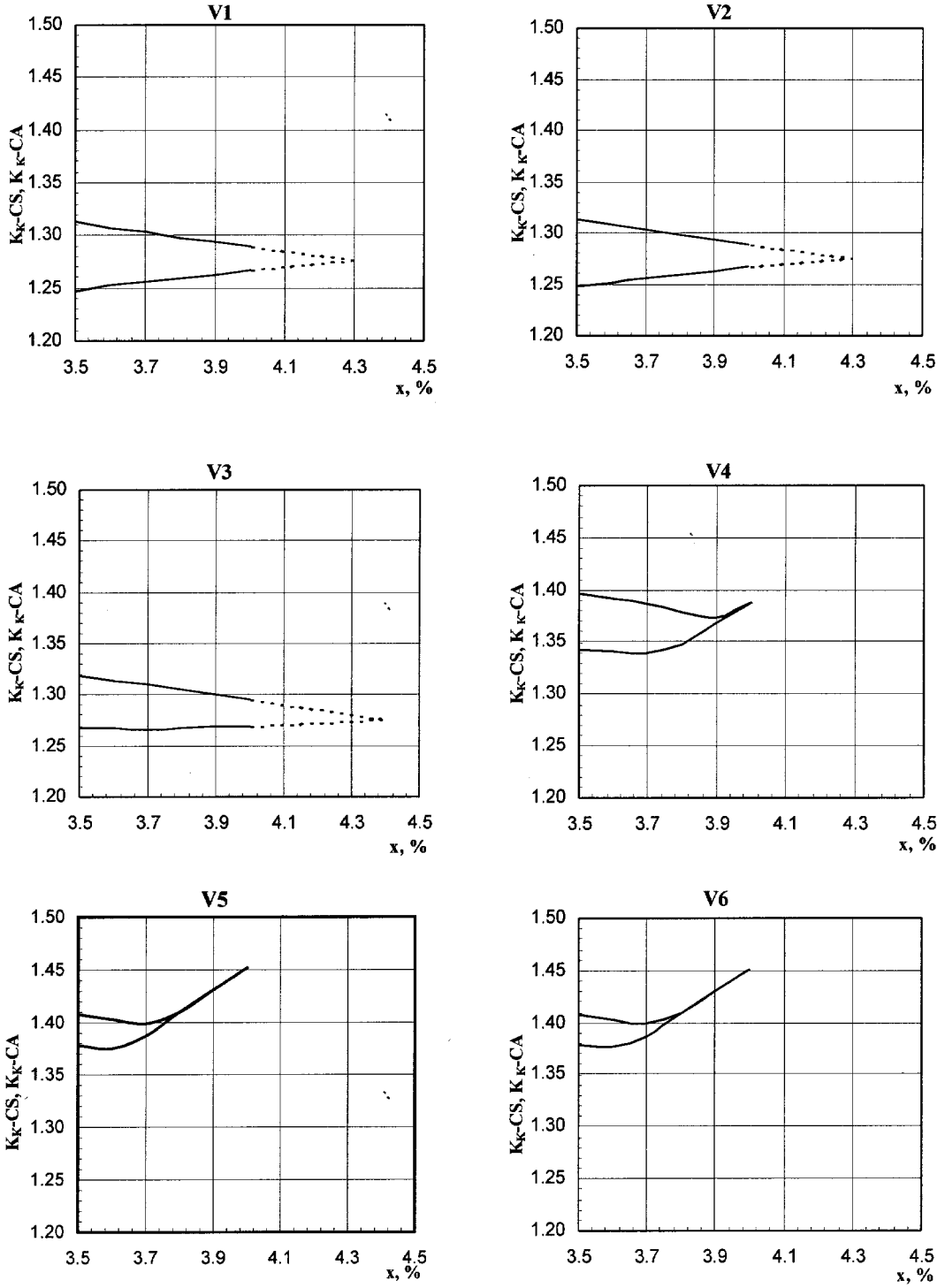

Fig. 3.4. FA arrangements in symmetric element

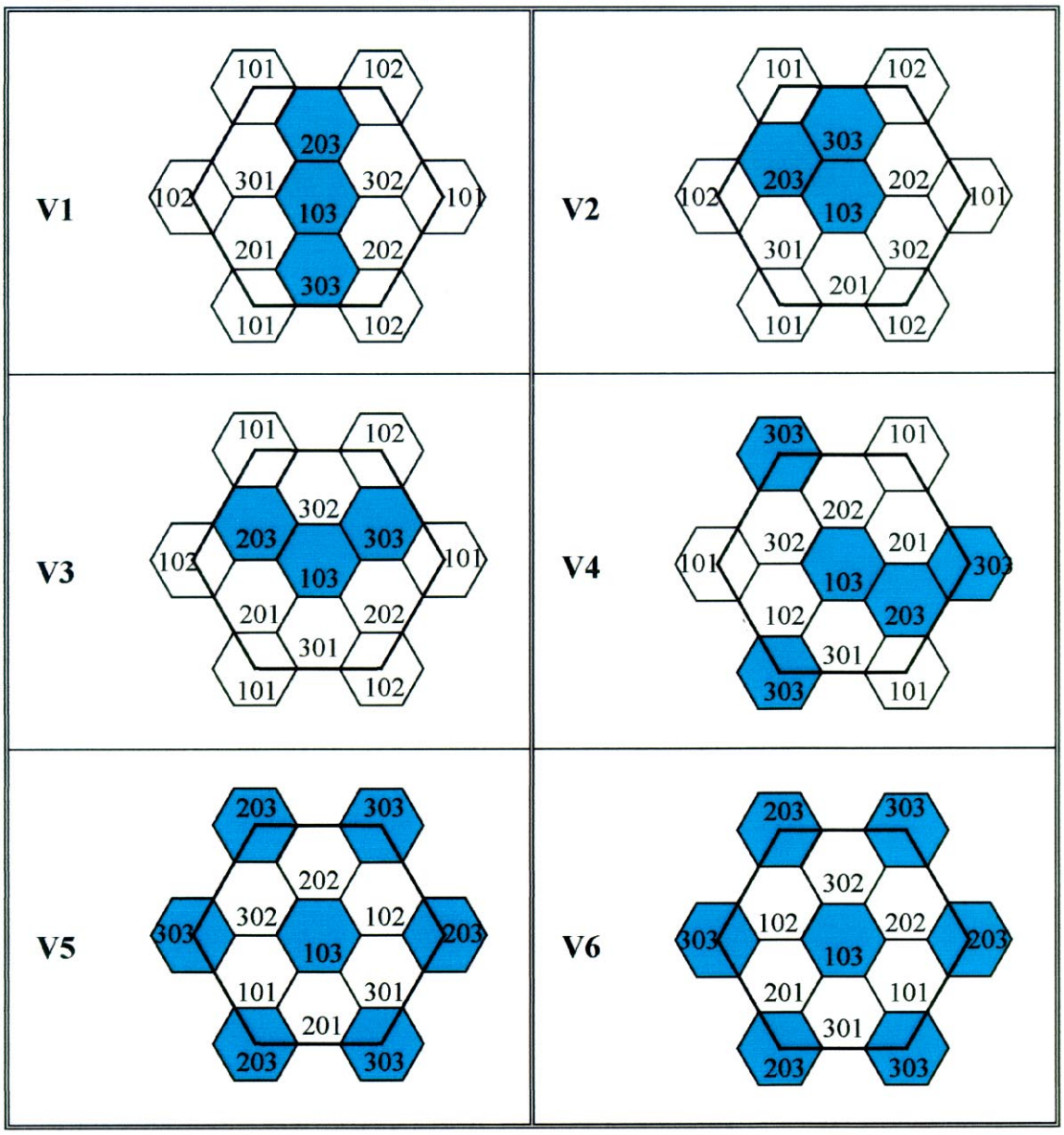

Fig. 3.5. Effect of fuel reloadings and burnups on K_{Kmax} - CS and K_{Kmax} - CA . CB=1200, ..., 0 ppm

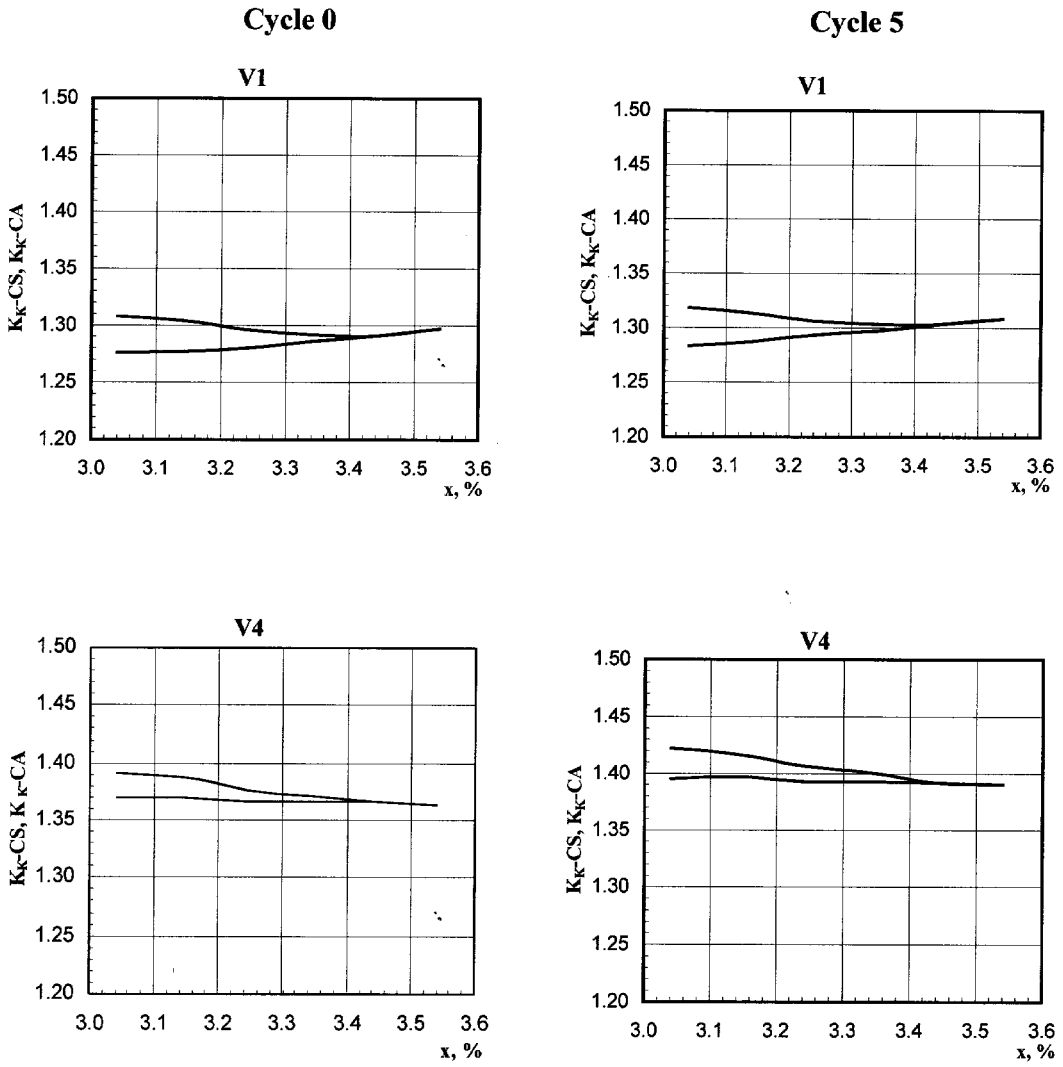

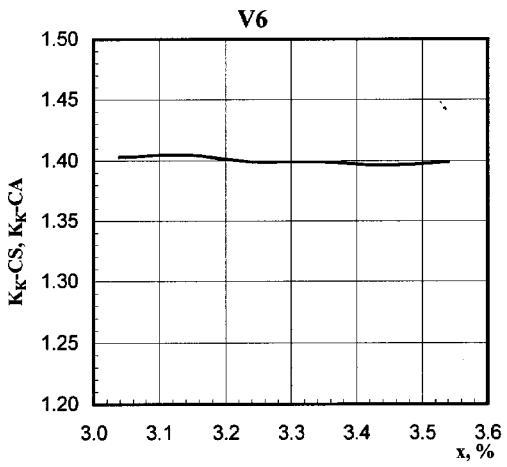
V6
1.50
1.45
1.40
1.35
1.30
1.25
1.20
K_K-CS, K_K-CA
3.0
3.1
3.2
3.3
3.4
3.5
3.6
x, %

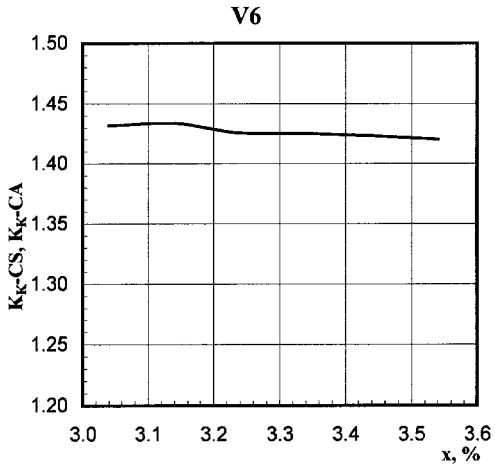
V6
1.50
1.45
1.40
1.35
1.30
1.25
1.20
K_K-CS, K_K-CA
3.0
3.1
3.2
3.3
3.4
3.5
3.6
x, %

Fig. 3.6. K_{Kmax} - CS and K_{Kmax} - CA versus from Pu content in a central FA

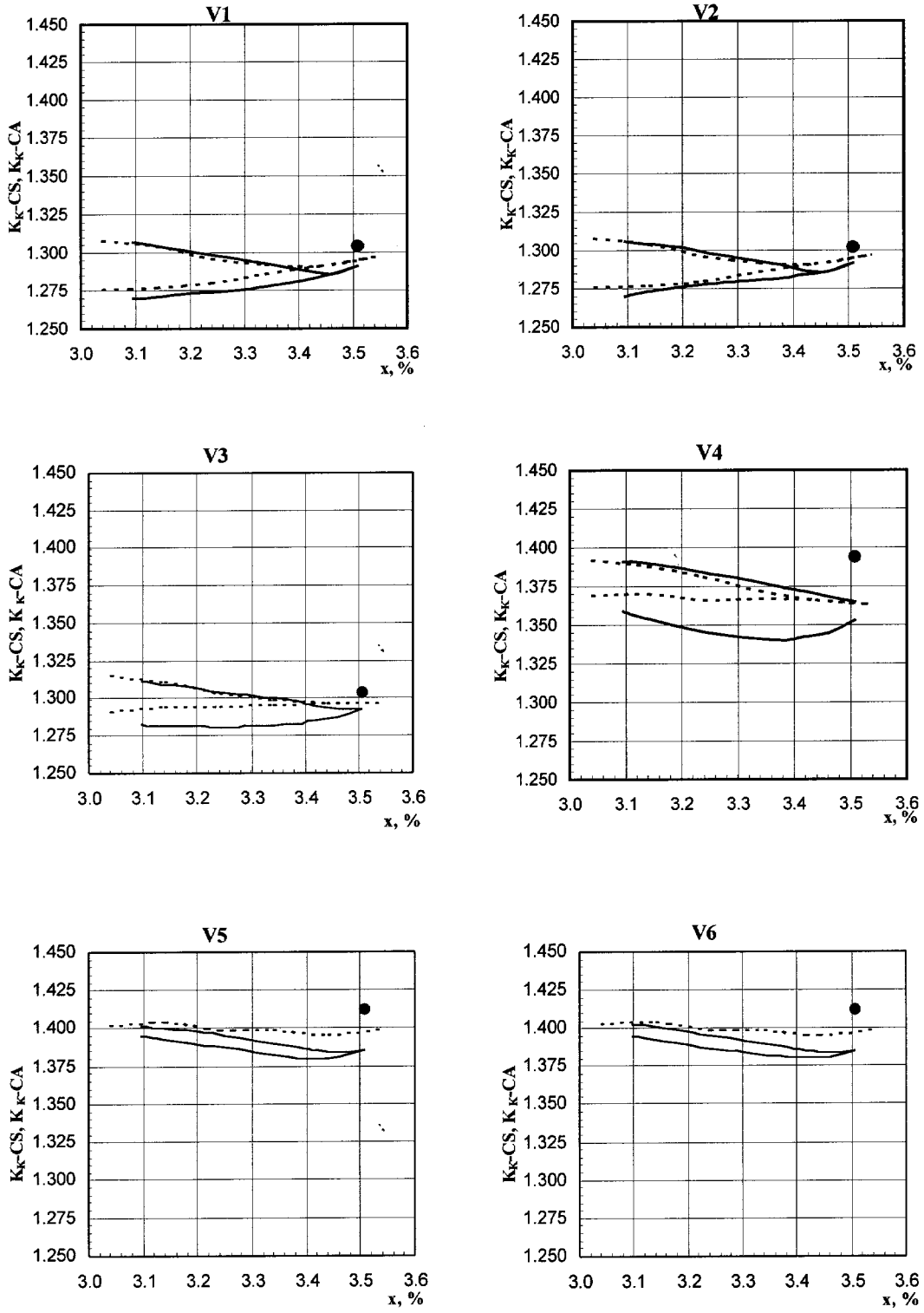

Fig. 3.7. Power distribution at the beginning of equilibrium cycle

Fig.4.1. Assembly-by-Assembly Burnup, Power and Temperature Drops Distributions. Equilibrium Cycle for Uranium Reference Core with Boron BPRs. Core 60° Sector

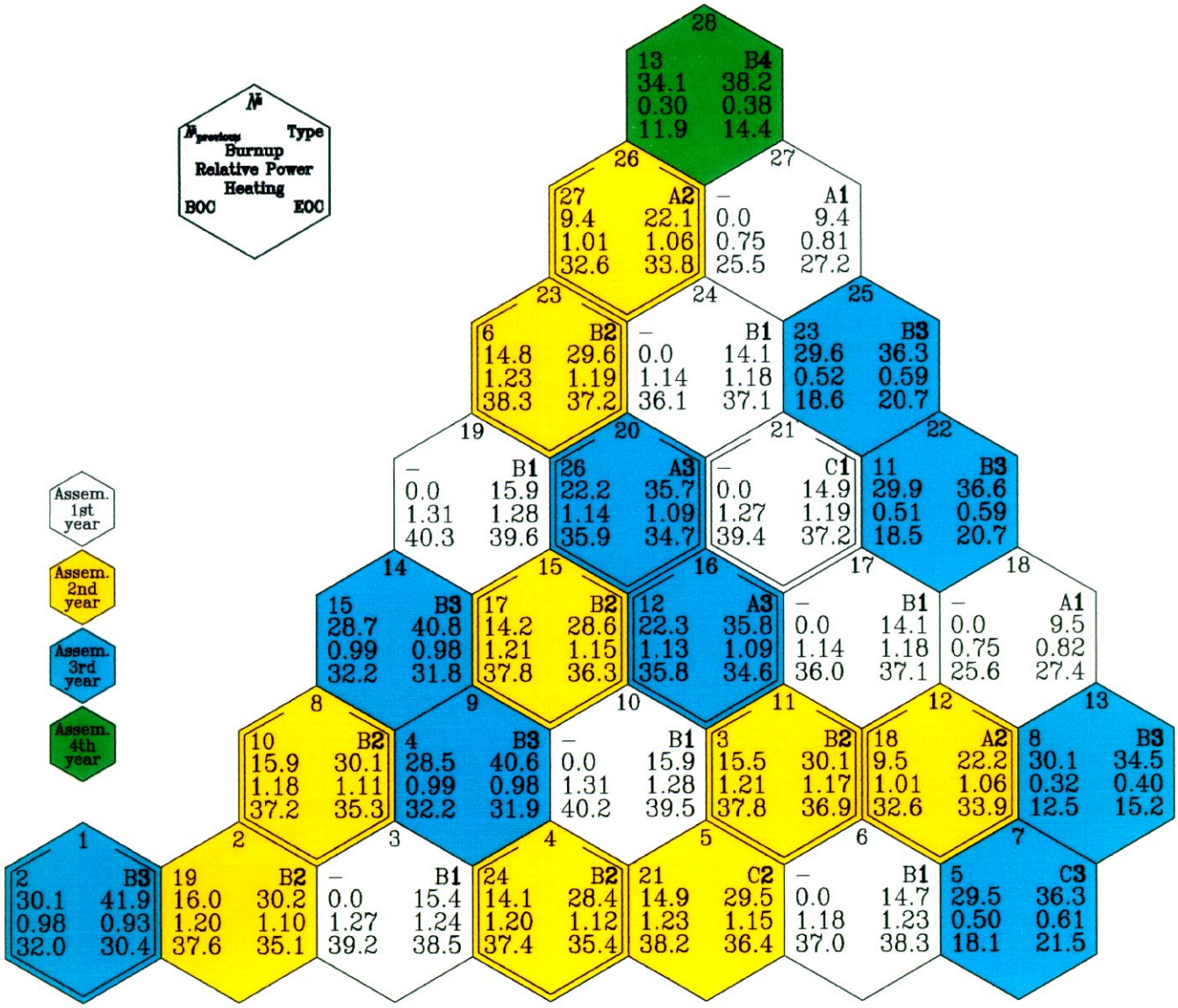

Fig.4.2. Assembly-by-Assembly Maximum Linear Pin Power Distribution in BOC. Equilibrium Cycle for Uranium Reference Core with Boron BPRs. Core 60° Sector

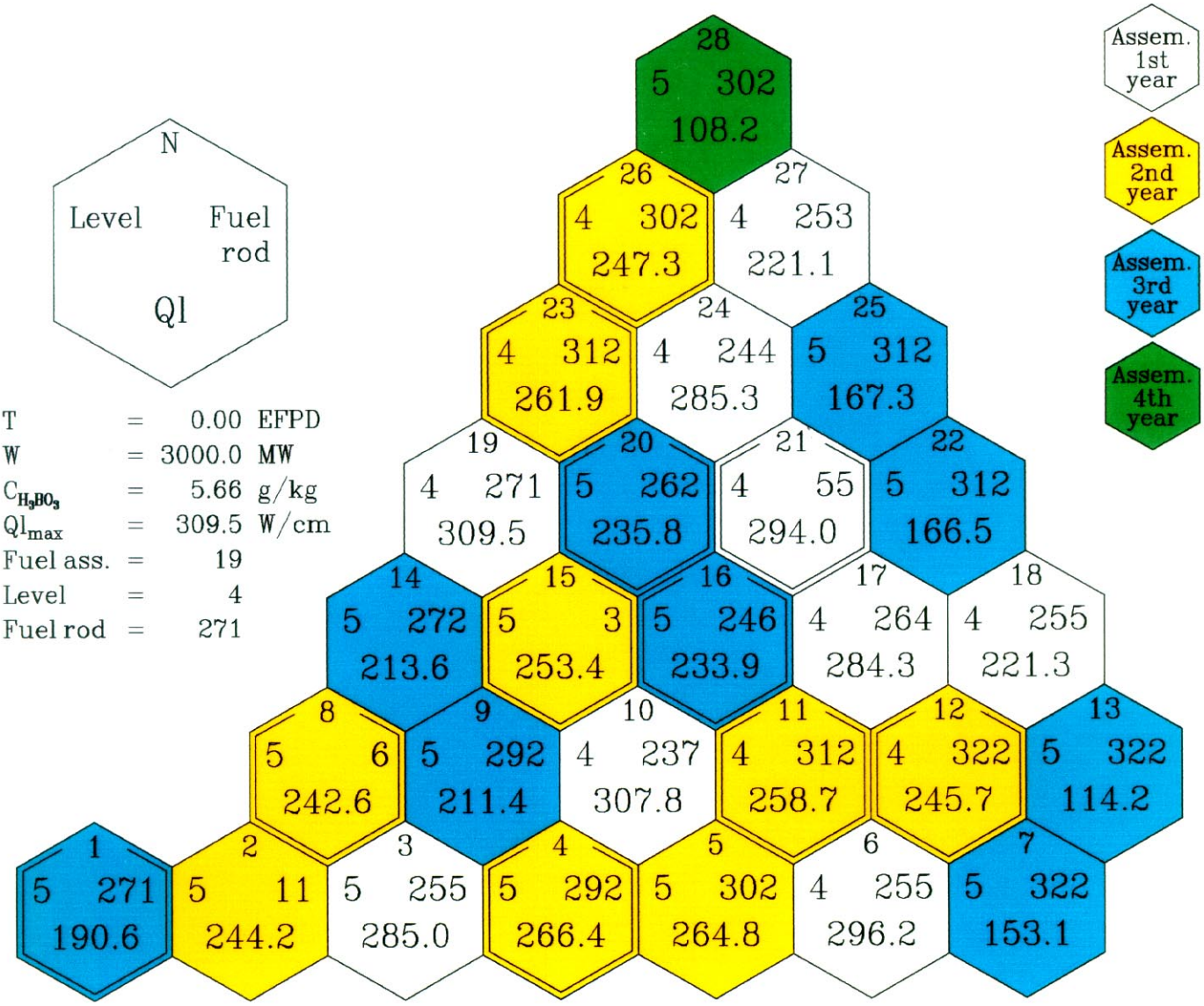

Fig.4.3. Assembly-by-Assembly Maximum Linear Pin Power Distribution in EOC. Equilibrium Cycle for Uranium Reference Core with Boron BPRs.Core 60° Sector

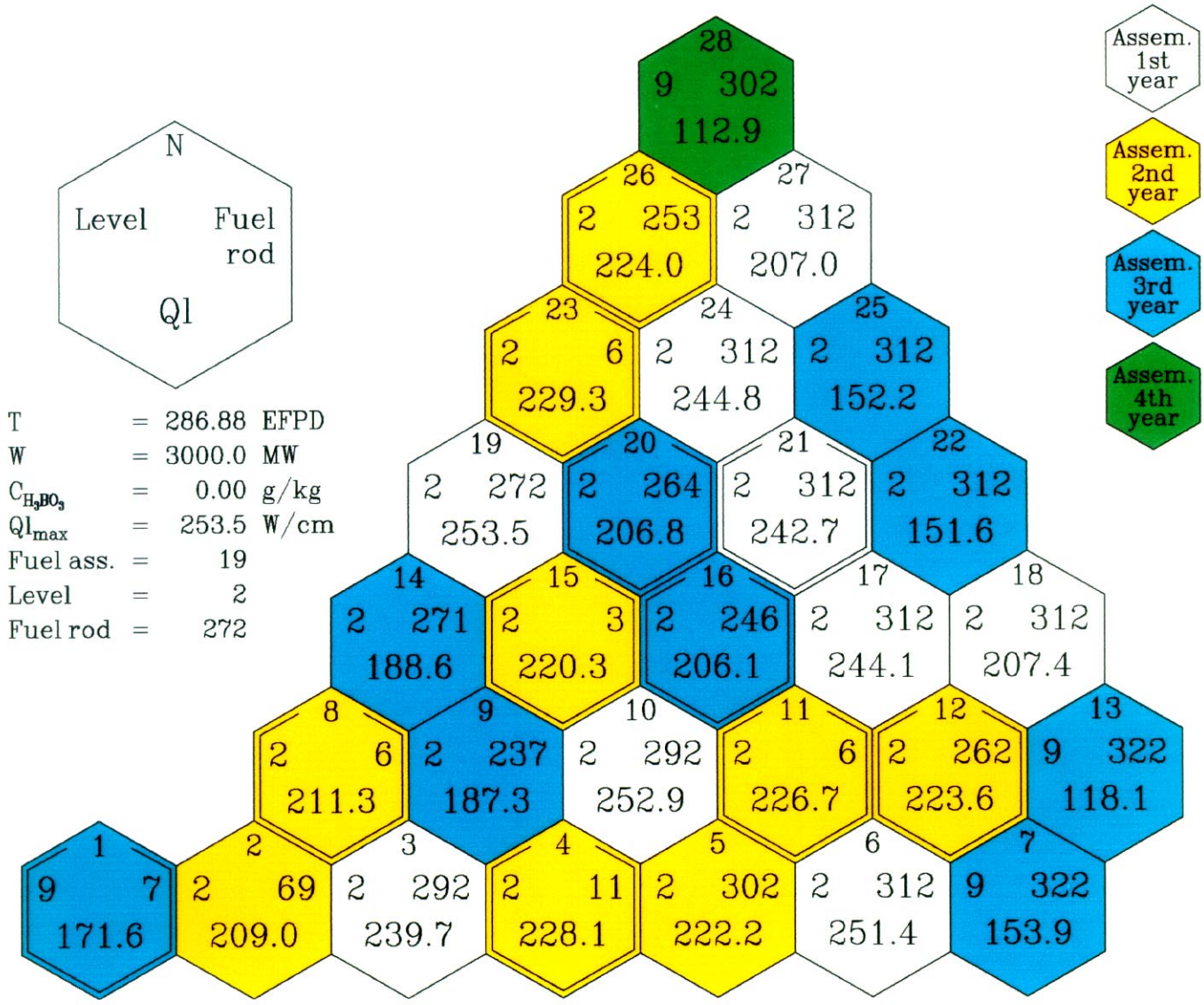

Fig.4.4. Pin-by-Pin Power Distribution in the Most Powered Assembly in BOC. Equilibrium Cycle for Uranium Reference Core with Boron BPRs

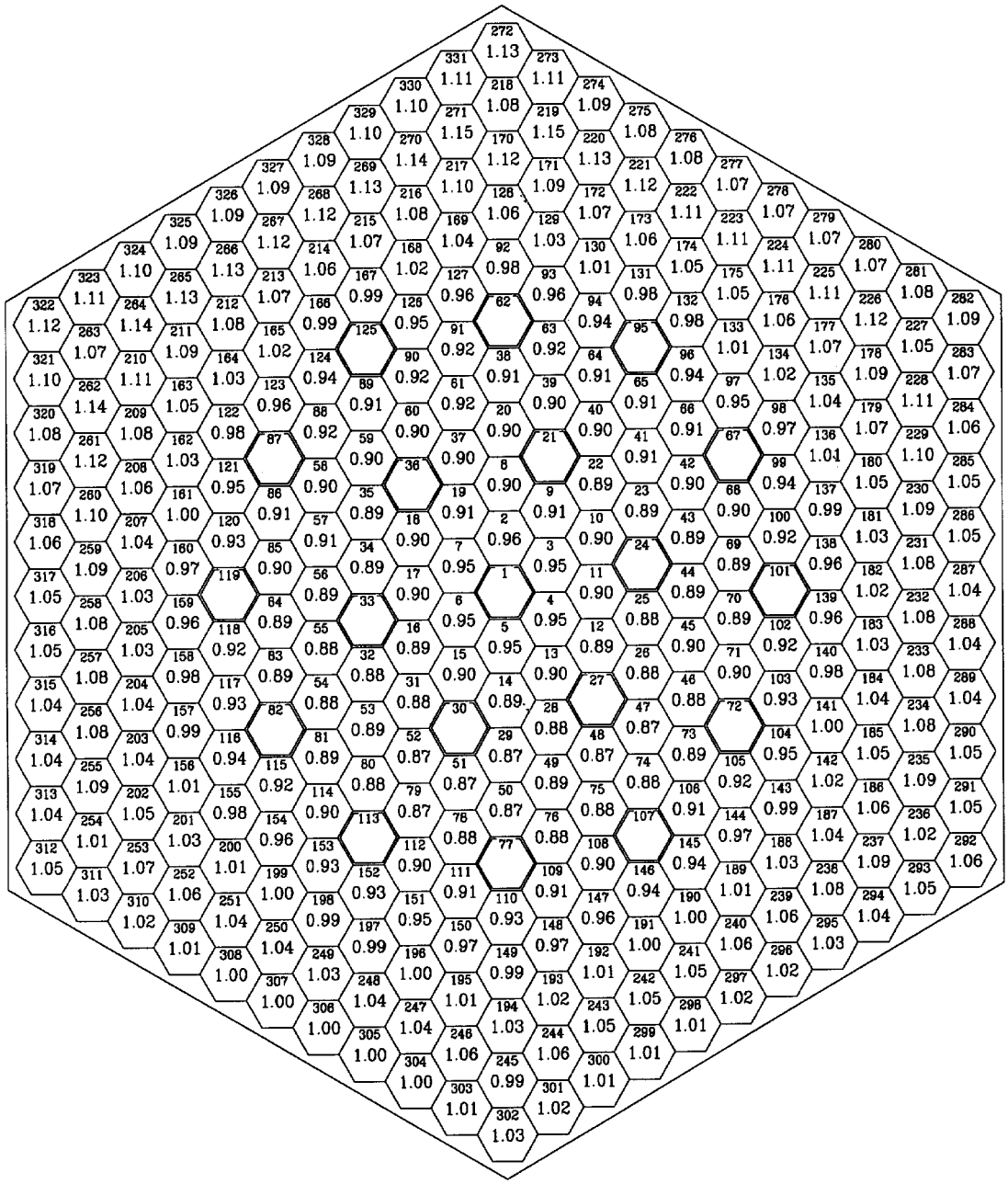

T	0.00	EFPD
W	3000.0	MW
$C_{H_3BO_3}$	5.66	g/kg
Ql_{max}	309.5	W/cm
Fuel assembly	19	
Level	4	
Fuel rod	271	
Kk_{max}	1.15	

Fig.4.5. Pin-by-Pin Power Distribution in the Most Powered Assembly in EOC. Equilibrium Cycle for Uranium Reference Core with Boron BPRs

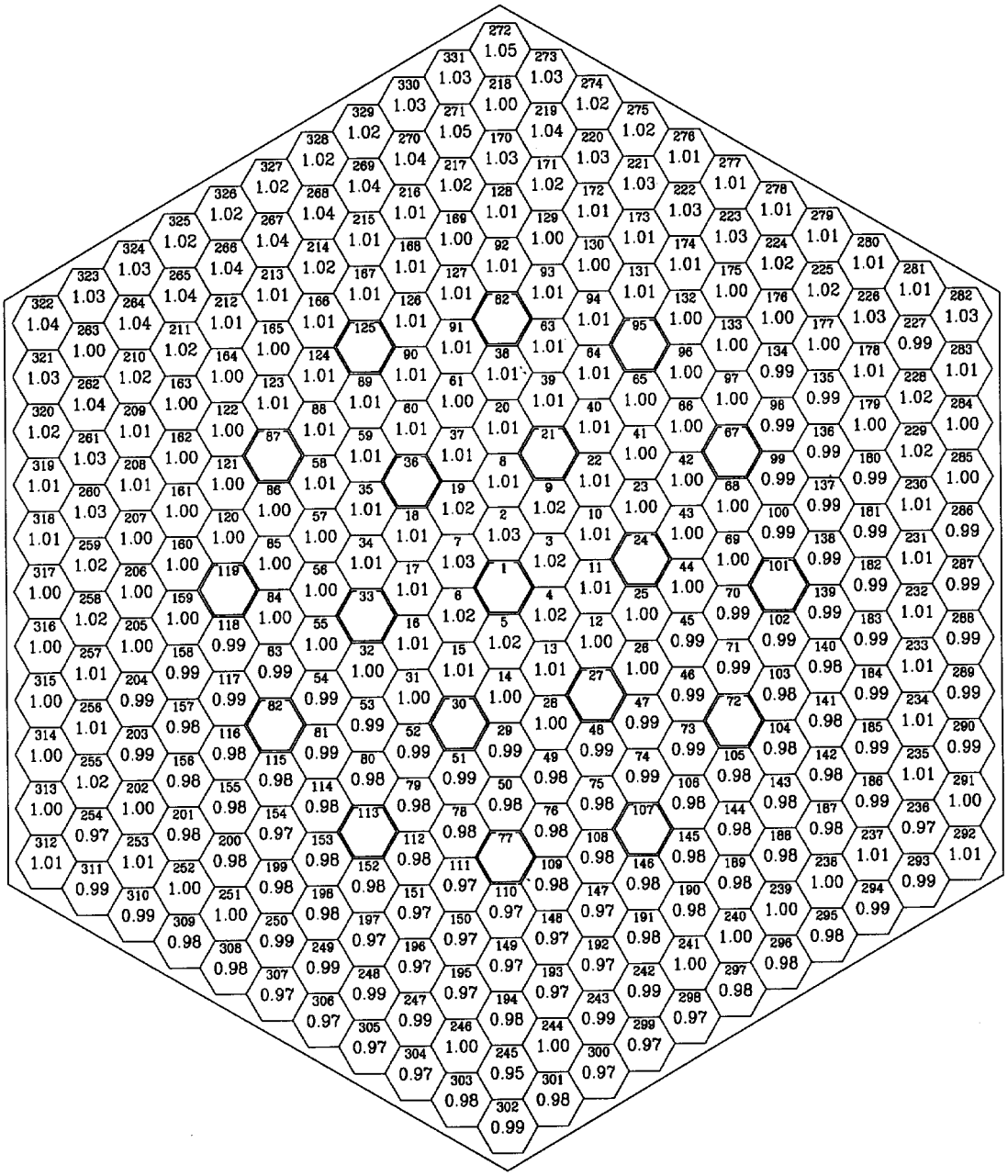

T	286.88	EFPD
W	3000.0	MW
$C_{H_3BO_3}$	0.00	g/kg
Ql_{max}	253.5	W/cm
Fuel assembly	19	
Level	2	
Fuel rod	272	
Kk_{max}	1.05	

Figure 4.6. Control Rods Grouping and Positions of In-core Self-Powered Detectors

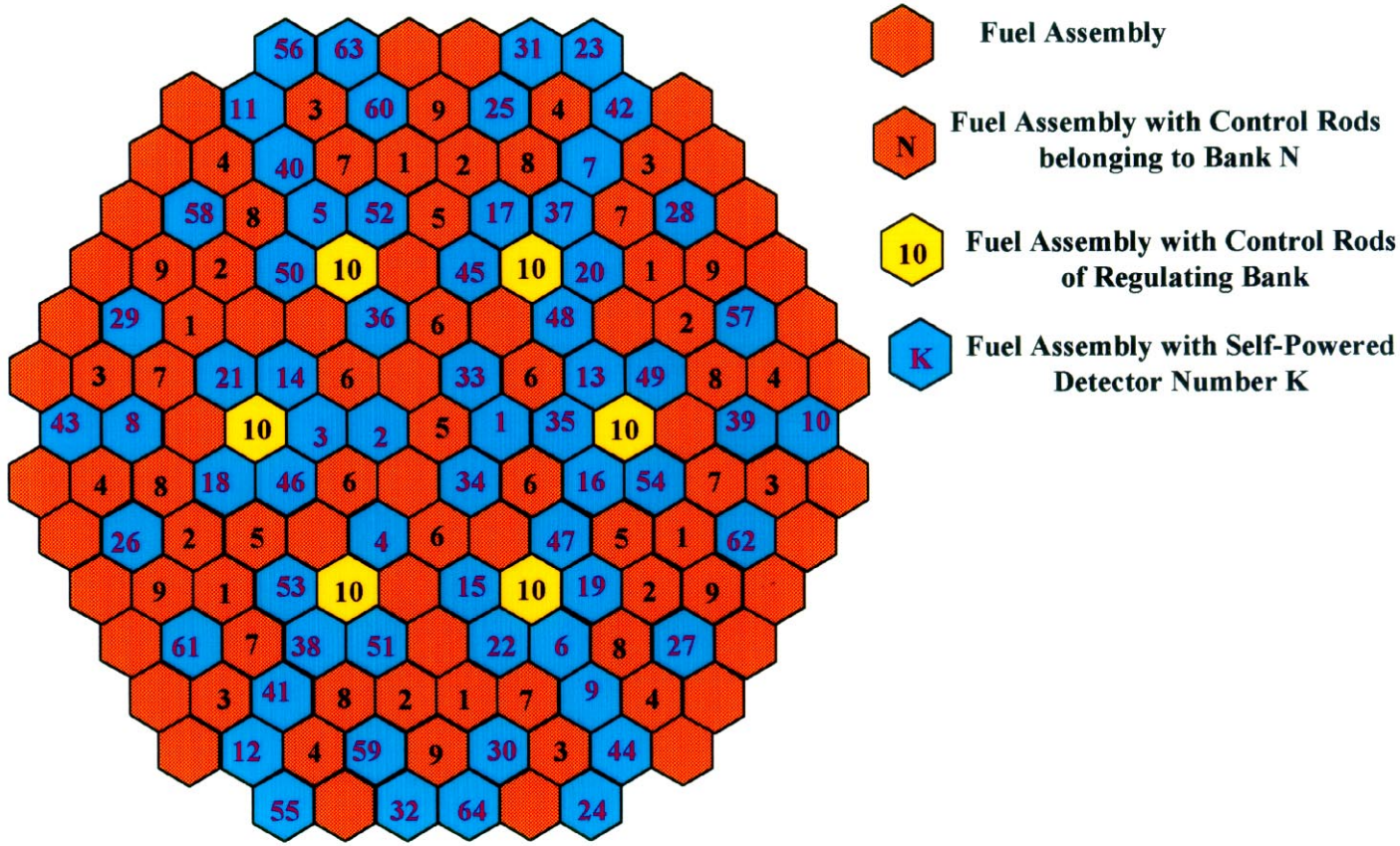

Fig.4.7. Reloading Scheme.
First Cycle with 3 MOX LTAs

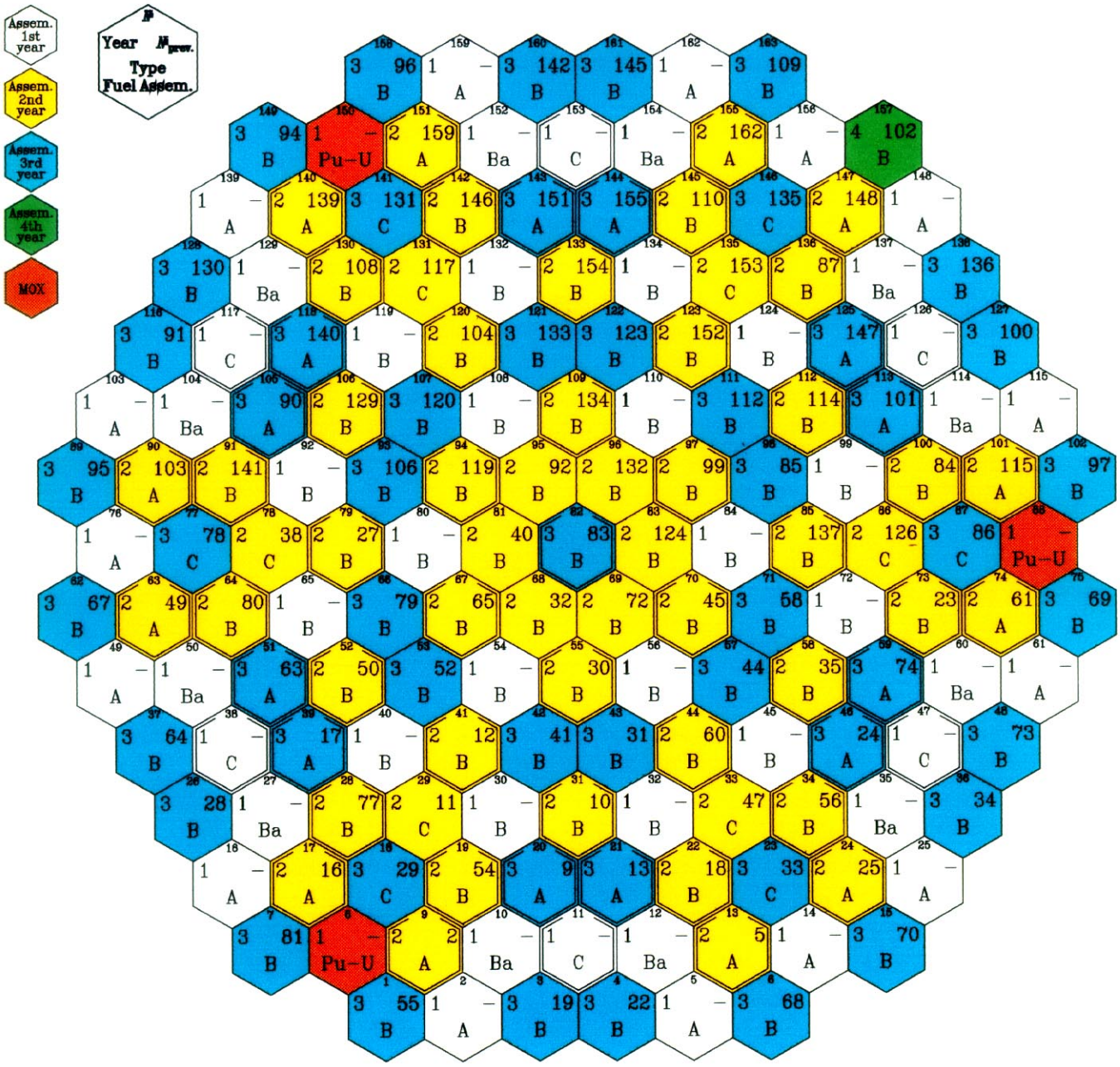

Fig.4.8. Assembly-by-Assembly Power Distribution.
First Cycle with 3 "100%Pu" MOX LTAs

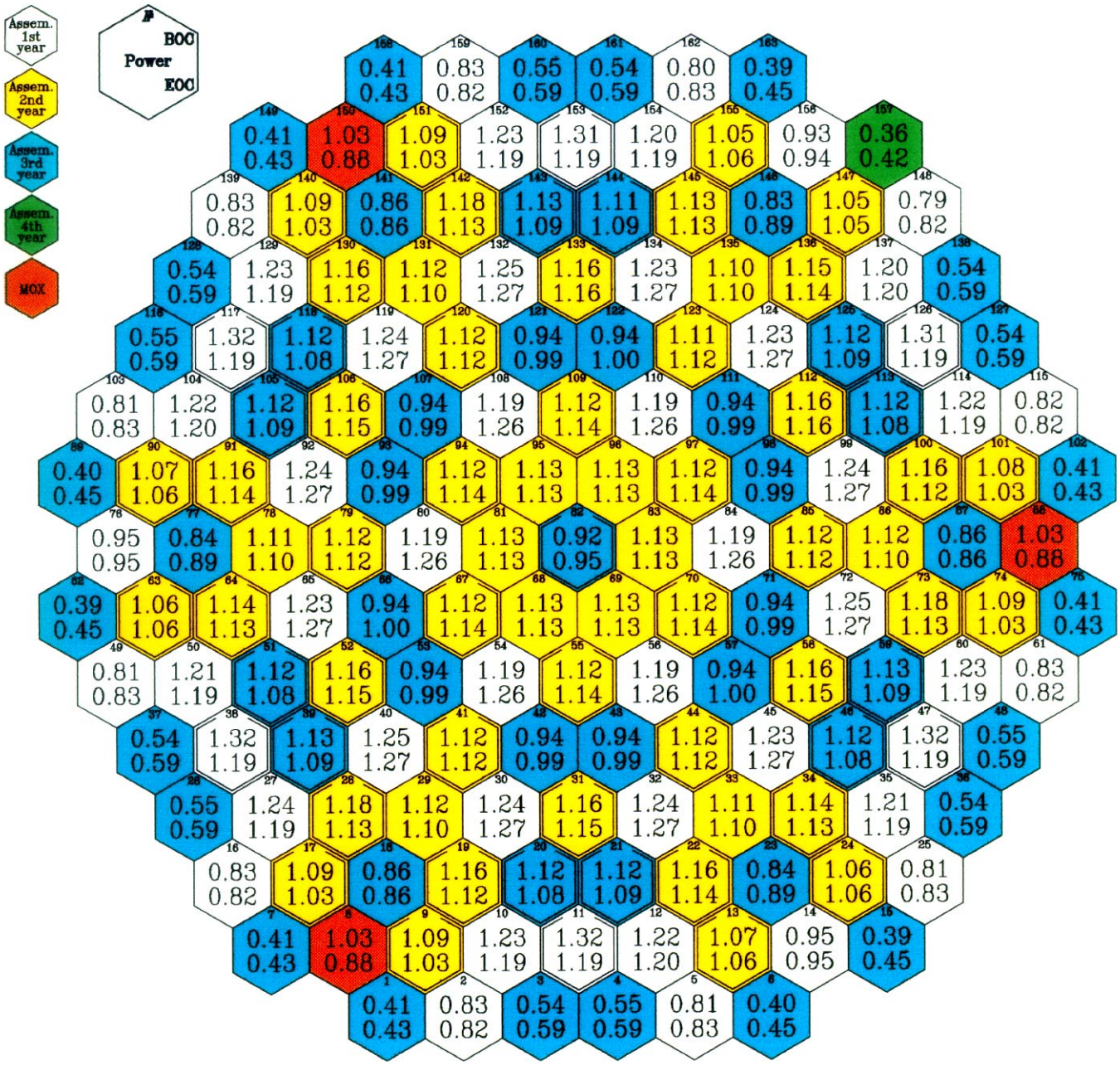

Fig.4.9. Assembly-by-Assembly Burnup Distribution.
First Cycle with 3 "100%Pu" MOX LTAs

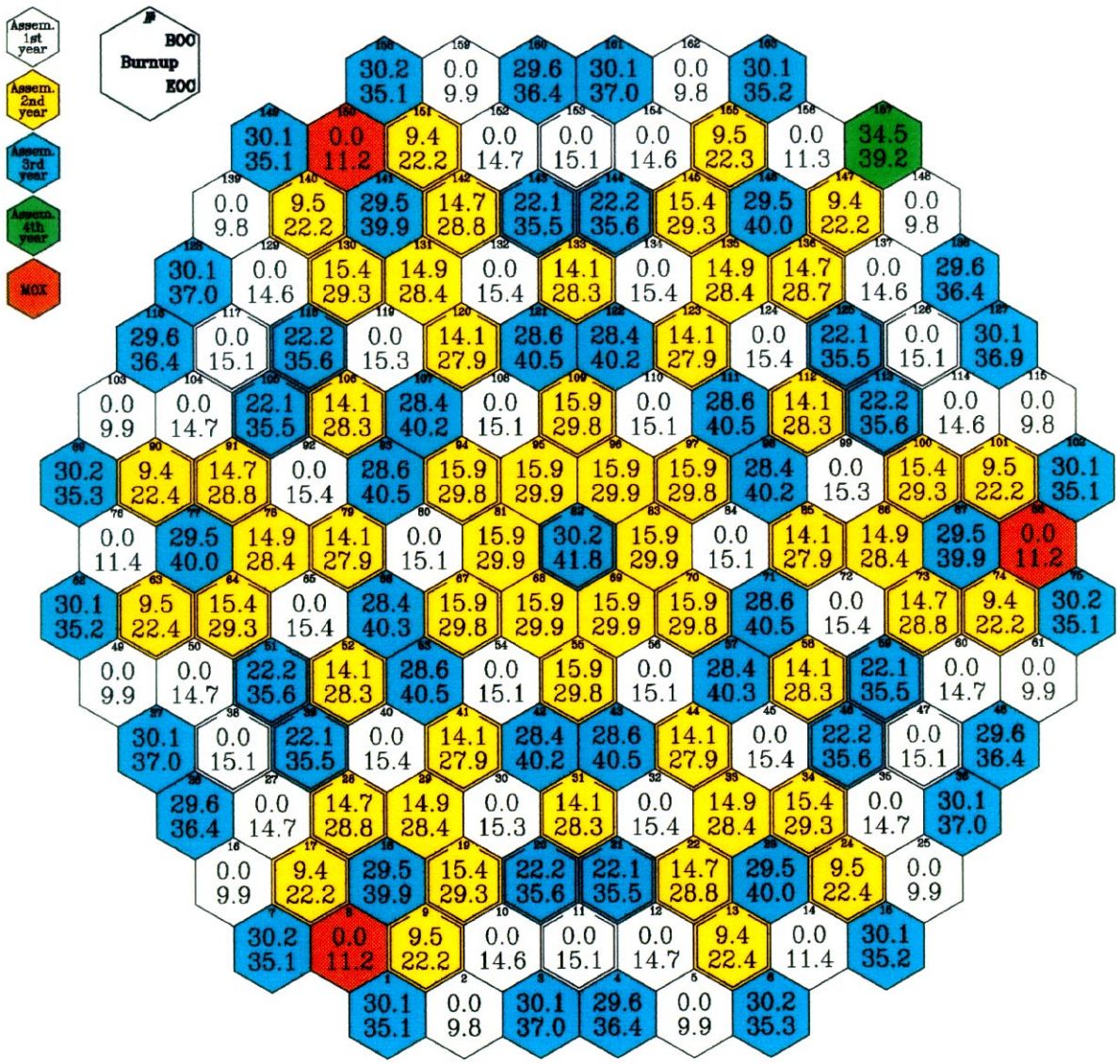

Fig.4.10. Assembly-by-Assembly Temperature Drop Distribution.
First Cycle with 3 "100%Pu" MOX LTAs

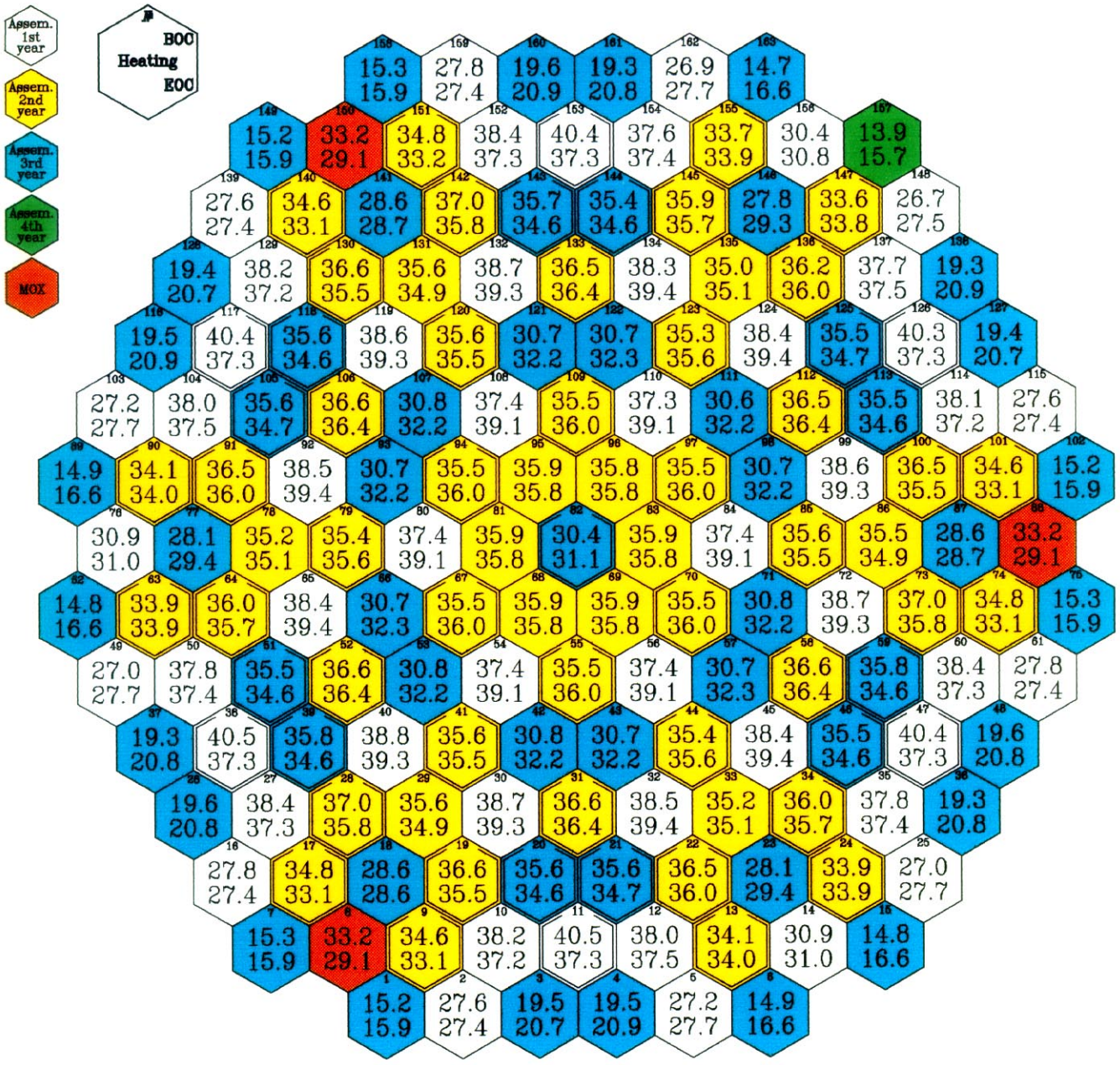

Fig.4.11. Assembly-by-Assembly Maximum Linear Power Distribution in BOC. First Cycle with 3 "100%Pu" MOX LTAs

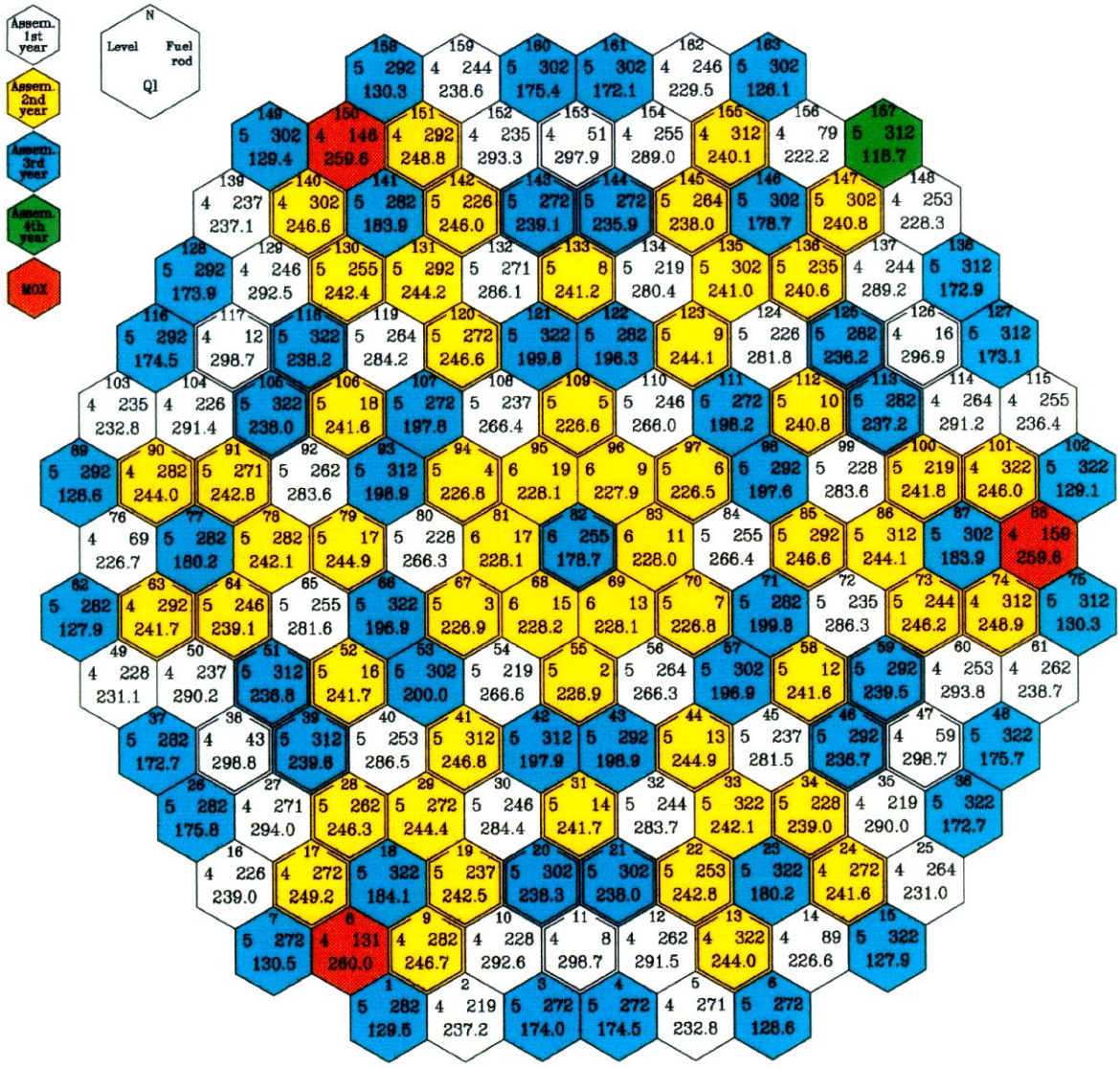

T	=	0.00 EFPD
W	=	3000.0 MW
$C_{H_3BO_3}$	=	5.78 g/kg
Ql_{max}	=	298.8 W/cm
Fuel ass.	=	38
Level	=	4
Fuel rod	=	43

Fig.4.12. Assembly-by-Assembly Maximum Linear Power Distribution in EOC. First Cycle with 3 "100%Pu" MOX LTAs

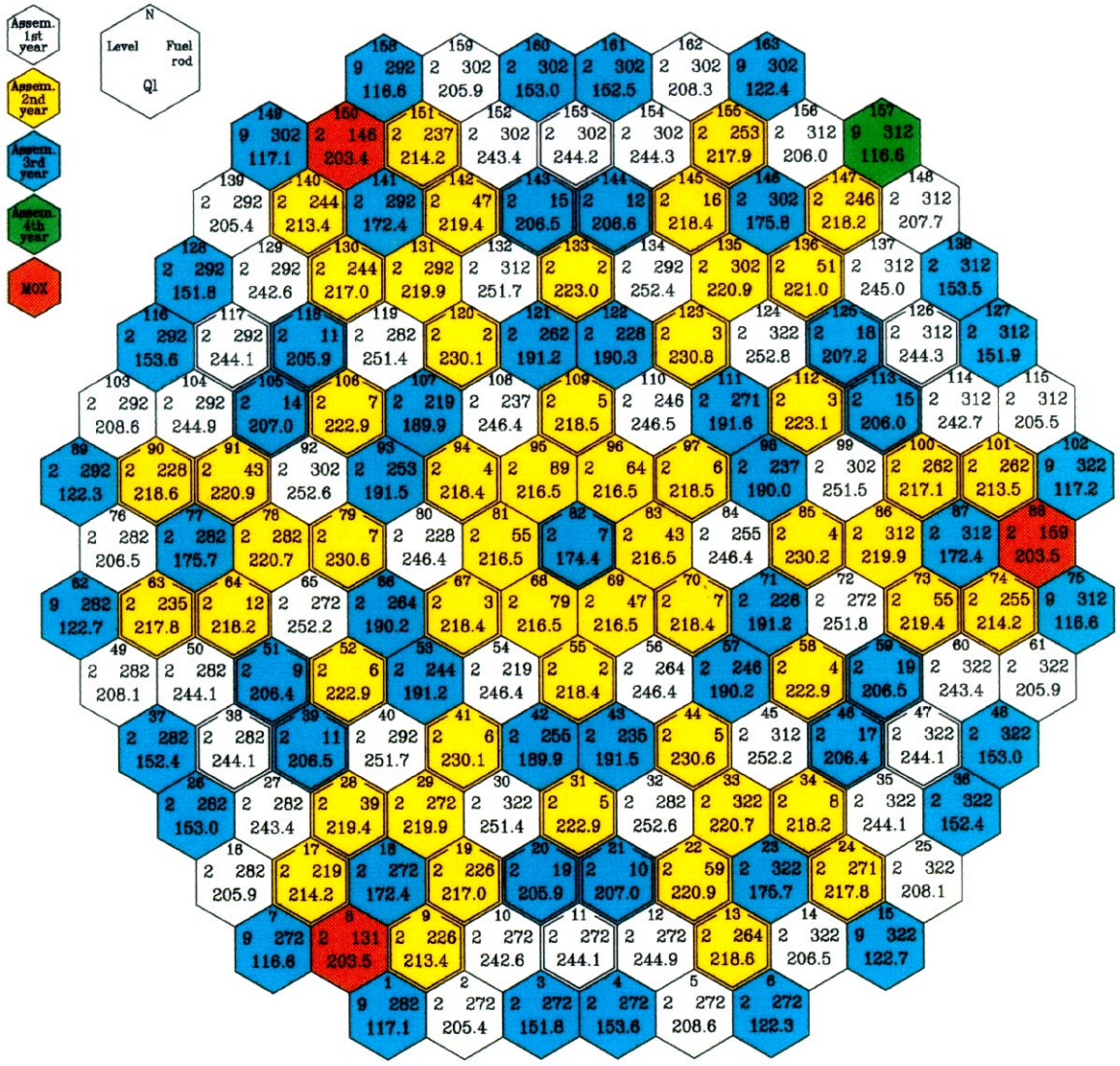

T	=	285.83 EFPD
W	=	3000.0 MW
$C_{H_3BO_3}$	=	0.00 g/kg
Ql_{max}	=	252.8 W/cm
Fuel ass.	=	124
Level	=	2
Fuel rod	=	322

Fig.4.13. Pin-by-Pin Power Distribution in the Most Powered Assembly in BOC. First Cycle with 3 "100%Pu" MOX LTAs

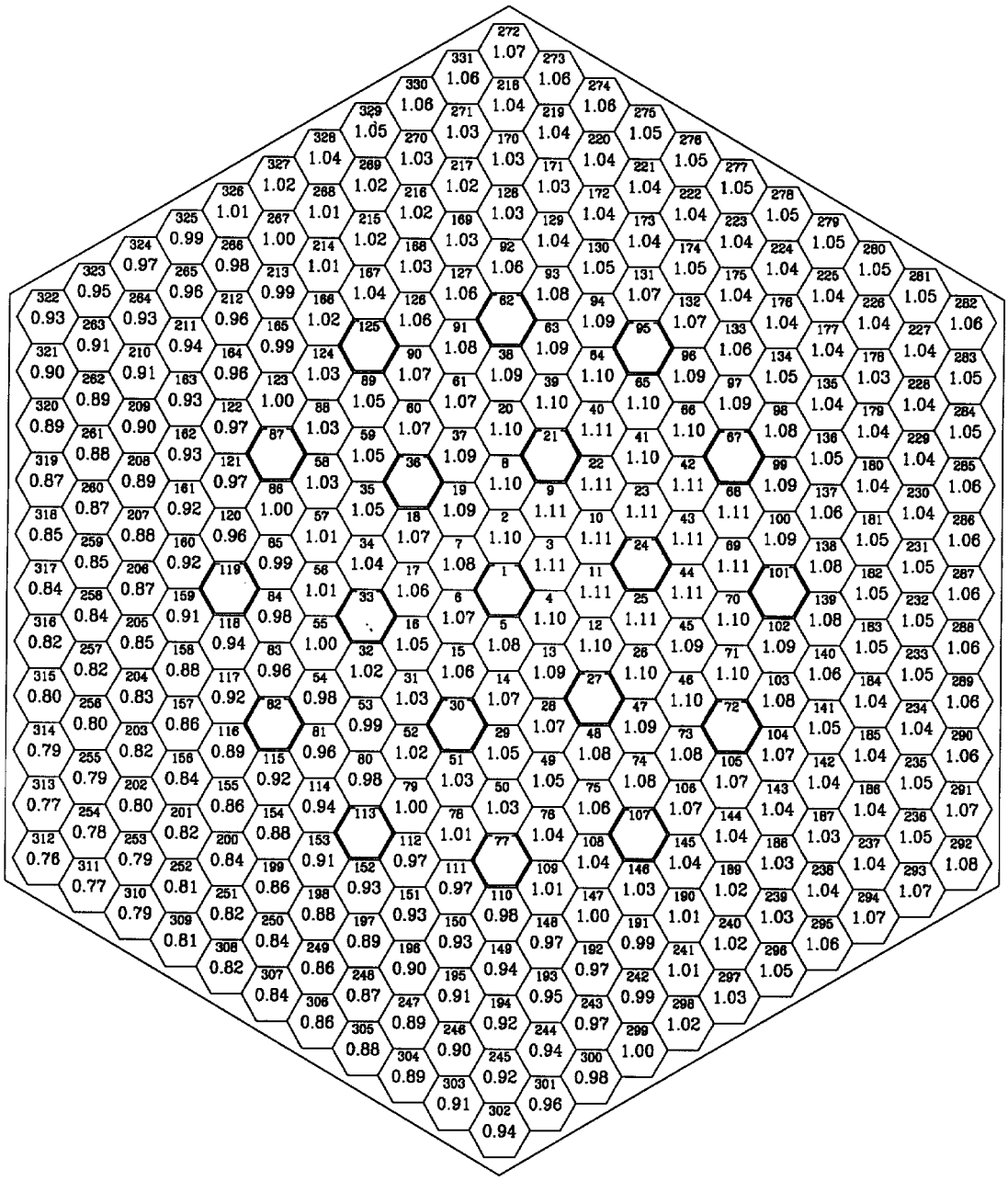

T	0.00	EFPD
W	3000.0	MW
$C_{H_3BO_3}$	5.78	g/kg
Ql	298.8	W/cm
Fuel assembly	38	
Level	4	
Fuel rod	43	
Kk_{max}	1.11	

Fig.4.14. Pin-by-Pin Power Distribution in the Most Powered Assembly in EOC. First Cycle with 3 "100%Pu" MOX LTAs

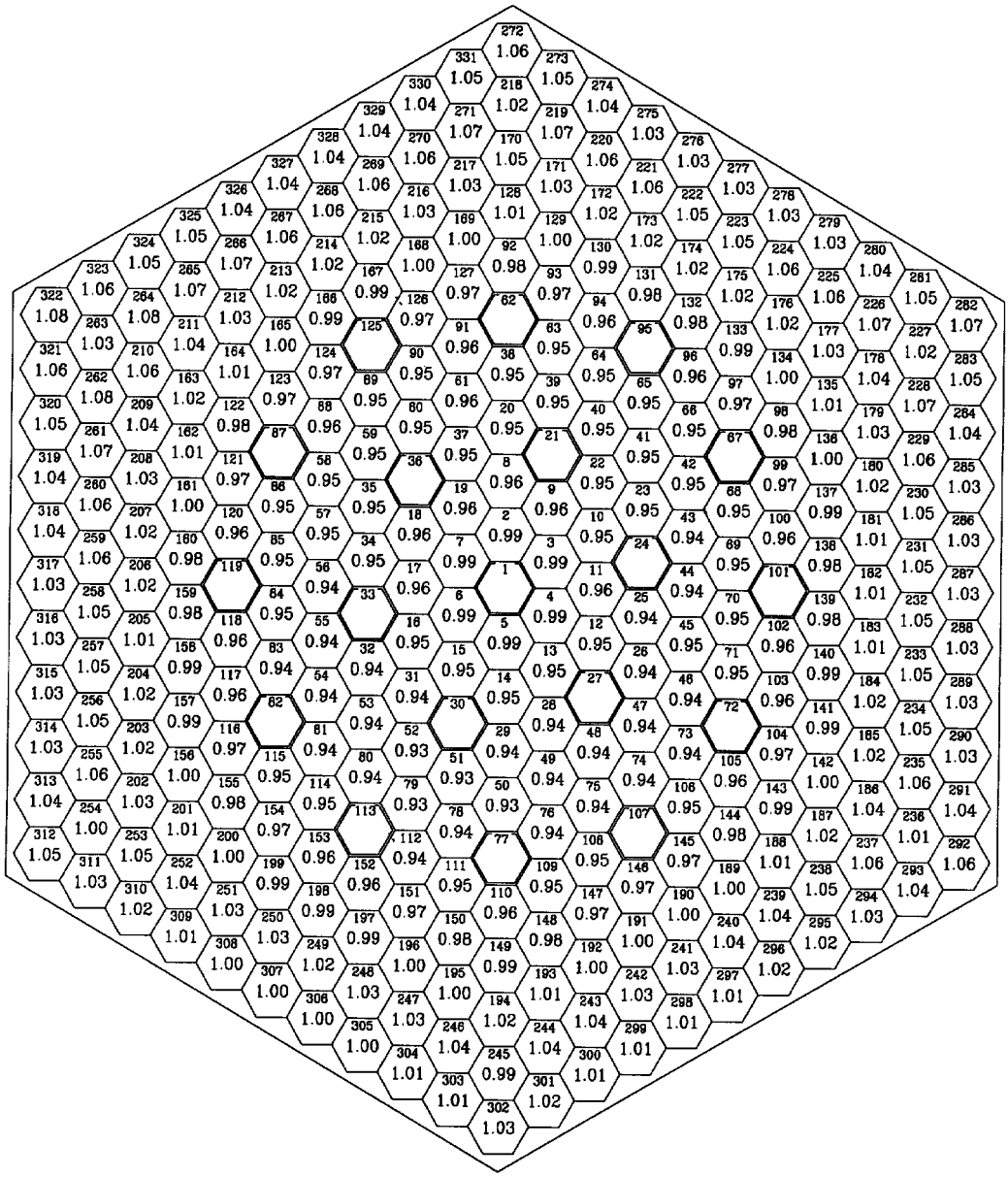

T	285.83	EFPD
W	3000.0	MW
$C_{H_3BO_3}$	0.00	g/kg
Burnup	18.8	
Fuel assembly	124	
Level	4	
Fuel rod	264	
Kb_{max}	1.08	

Fig.4.15. Pin-by-Pin Power Distribution in MOX LTA in BOC. First Cycle with 3 "100%Pu" MOX LTAs

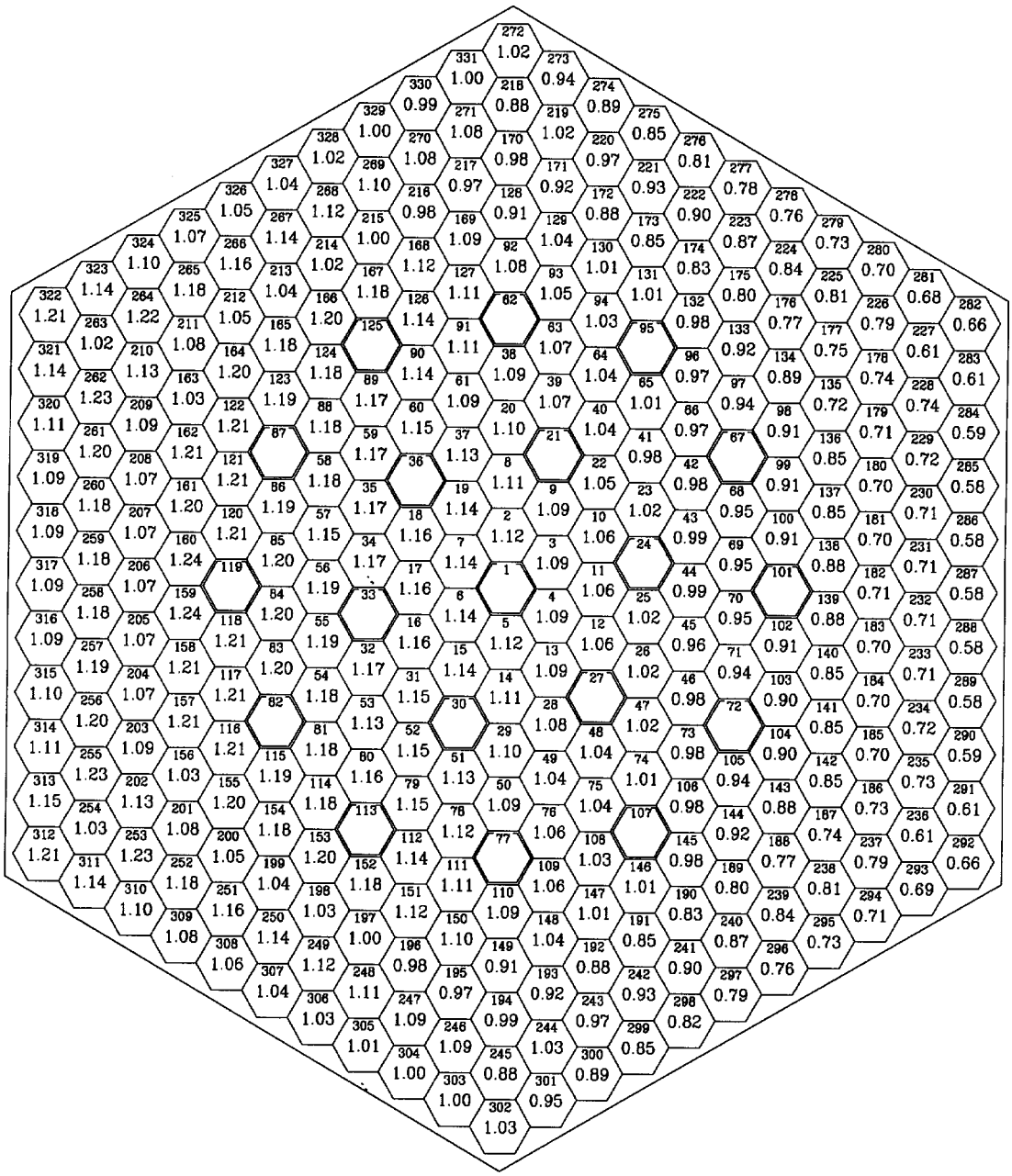

T	0.00	EFPD
W	3000.0	MW
$C_{H_3BO_3}$	5.78	g/kg
Ql	259.6	W/cm
Fuel assembly	88	
Level	4	
Fuel rod	159	
Kk_{max}	1.24	

Fig.4.16. Pin-by-Pin Power Distribution in MOX LTA in EOC. First Cycle with 3 MOX "100%Pu" MOX LTAs

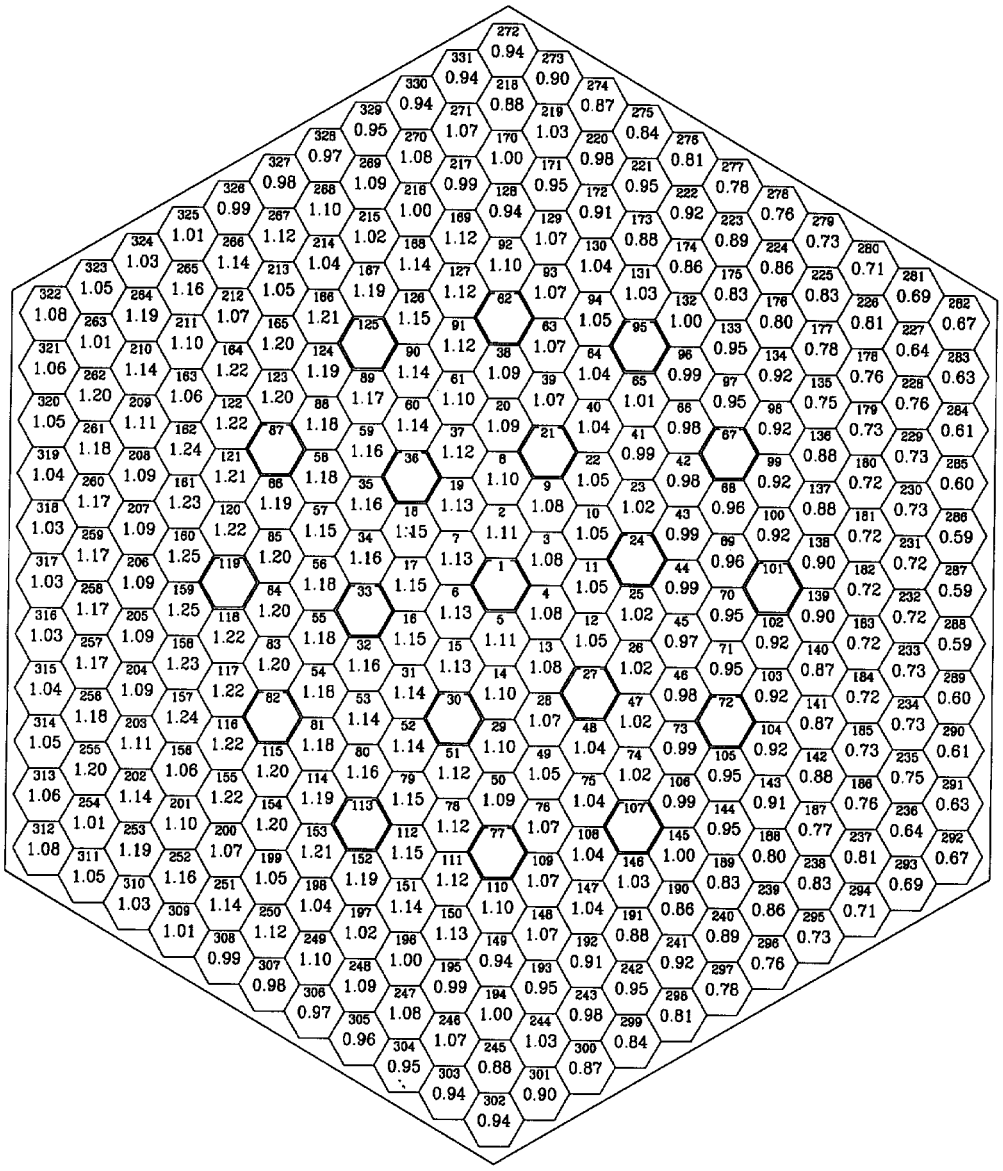

T	285.83	EFPD
W	3000.0	MW
$C_{H_3BO_3}$	0.00	g/kg
Ql	194.0	W/cm
Fuel assembly	88	
Level	4	
Fuel rod	159	
Kk_{max}	1.25	

Fig.4.17. Reloading Scheme.
Second Cycle with 3 MOX LTAs

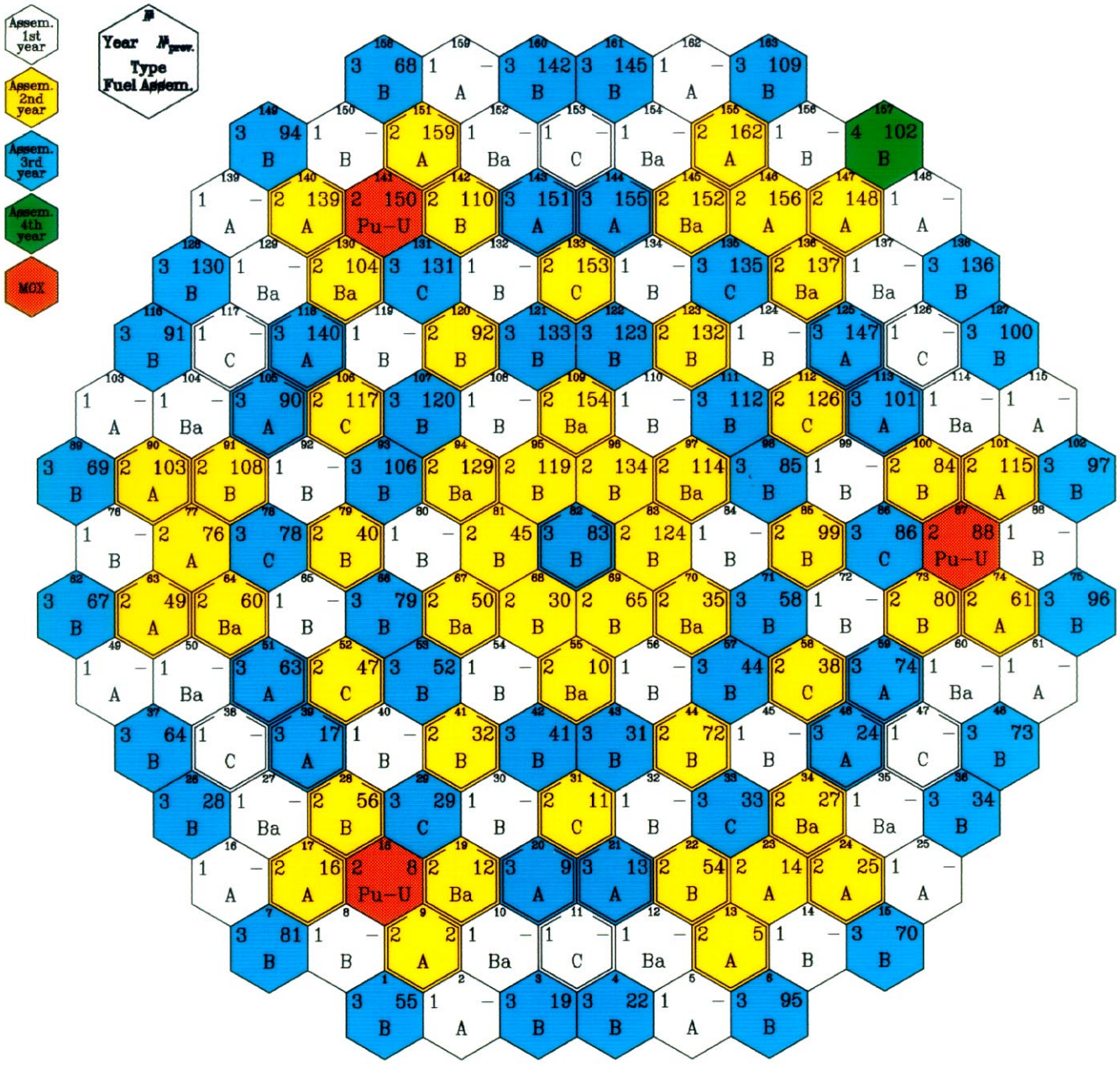

Fig.4.18. Assembly-by-Assembly Power Distribution.
Second Cycle with 3 MOX "100%Pu" MOX LTAs

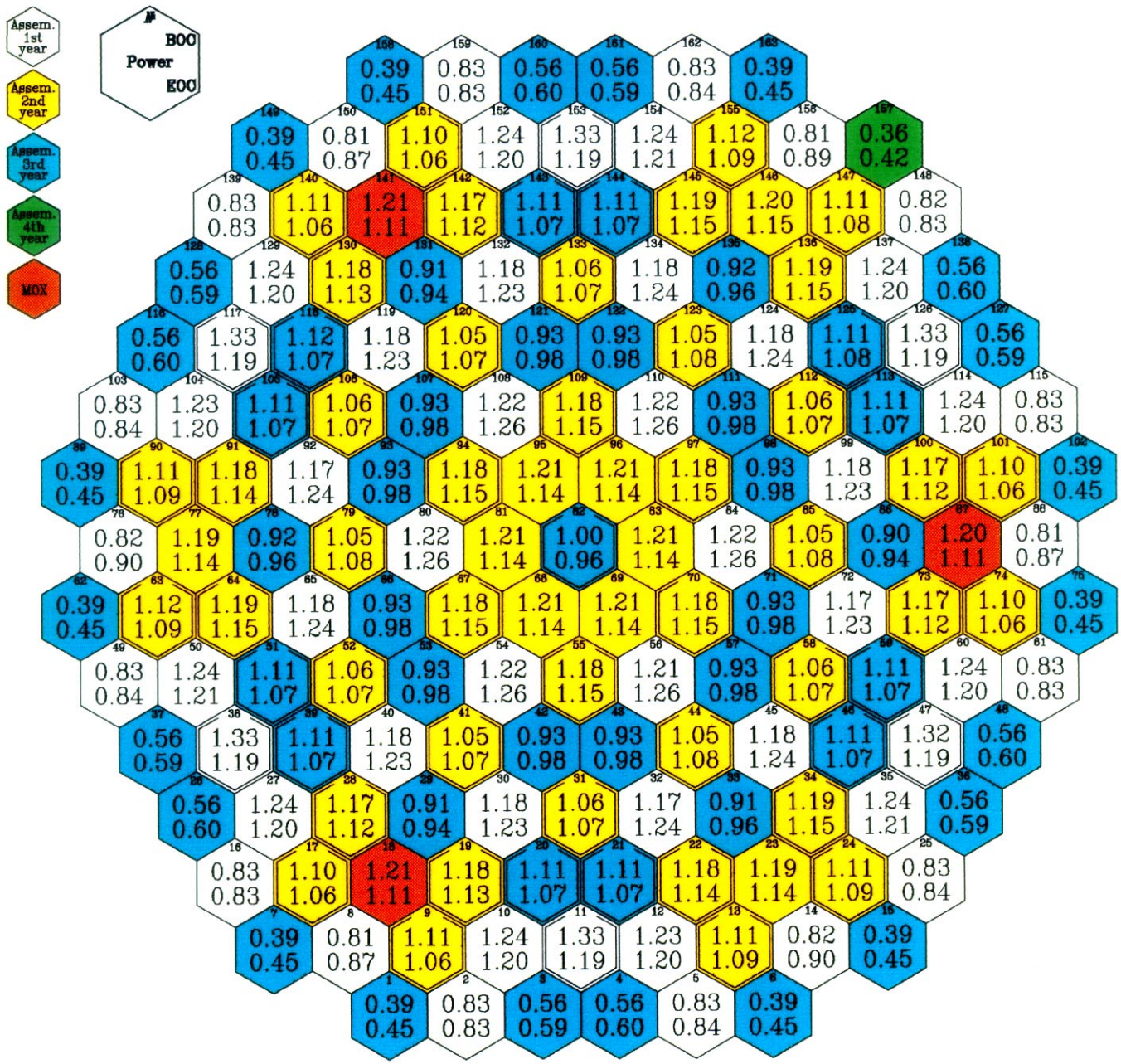

Fig.4.19. Assembly-by-Assembly Burnup Distribution. Second Cycle with 3 "100%Pu" MOX LTAs

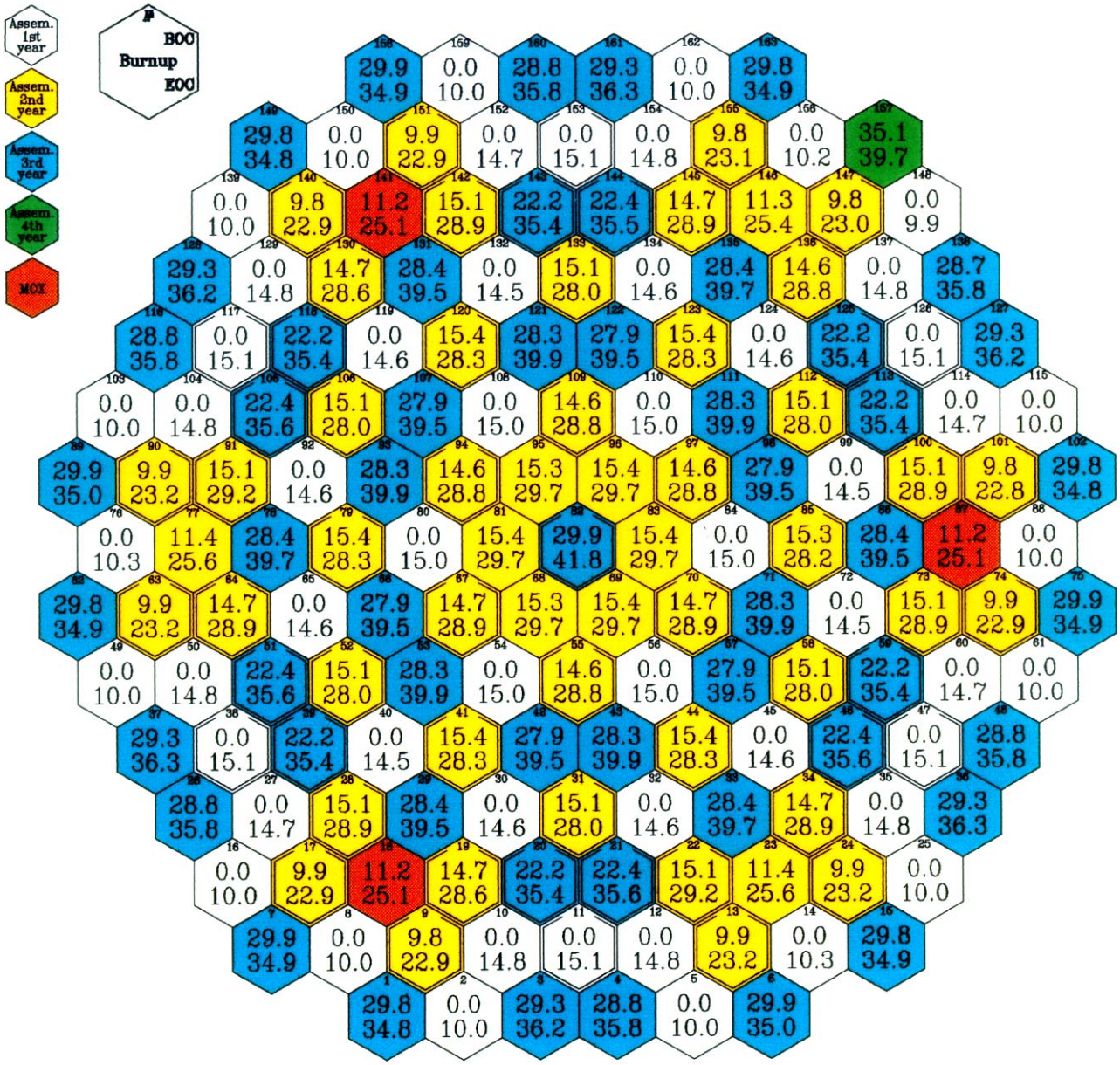

Fig.4.20. Assembly-by-Assembly Temperature Drop Distribution.
Second Cycle with 3 MOX "100%Pu" MOX LTAs

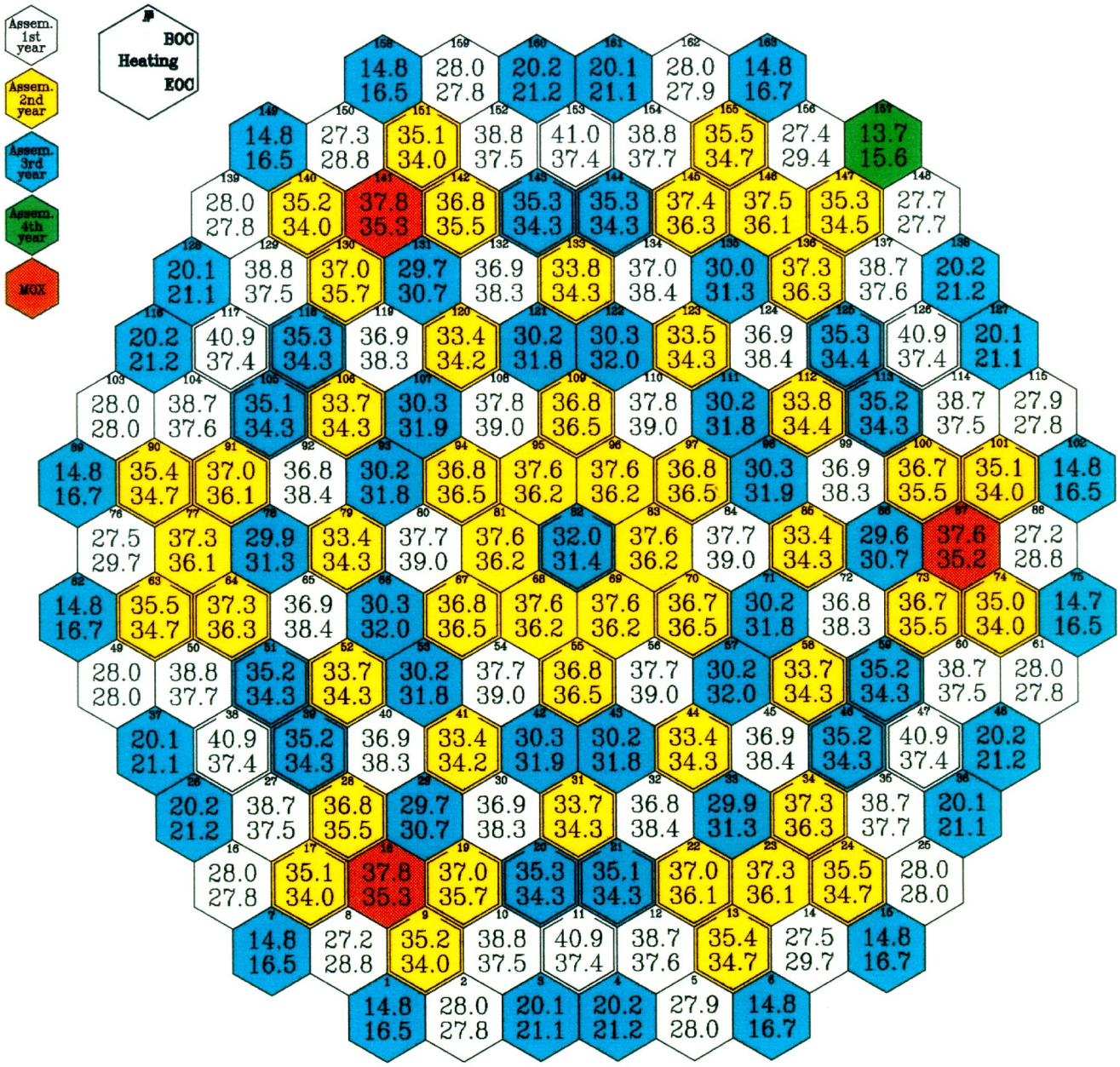

Fig.4.21. Assembly-by-Assembly Maximum Linear Pin Power Distribution in BOC. Second Cycle with 3 "100%Pu" MOX LTAs

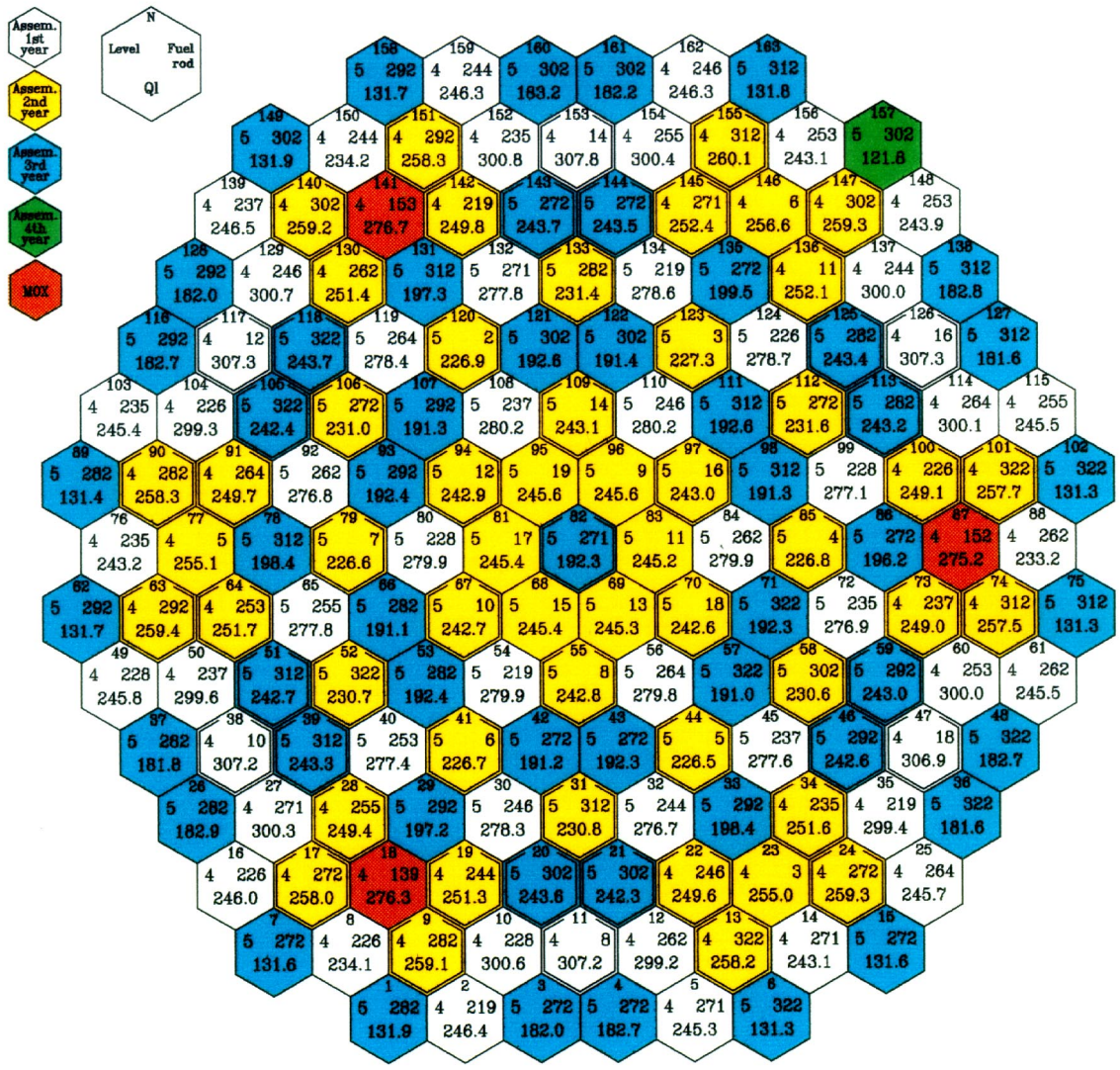

T	=	0.00 EFPD
W	=	3000.0 MW
$C_{H_3BO_3}$	=	5.67 g/kg
Ql_{max}	=	307.8 W/cm
Fuel ass.	=	153
Level	=	4
Fuel rod	=	14

Fig.4.22. Assembly-by-Assembly Maximum Linear Pin Power Distribution in EOC. Second Cycle with 3 "100%Pu" MOX LTAs

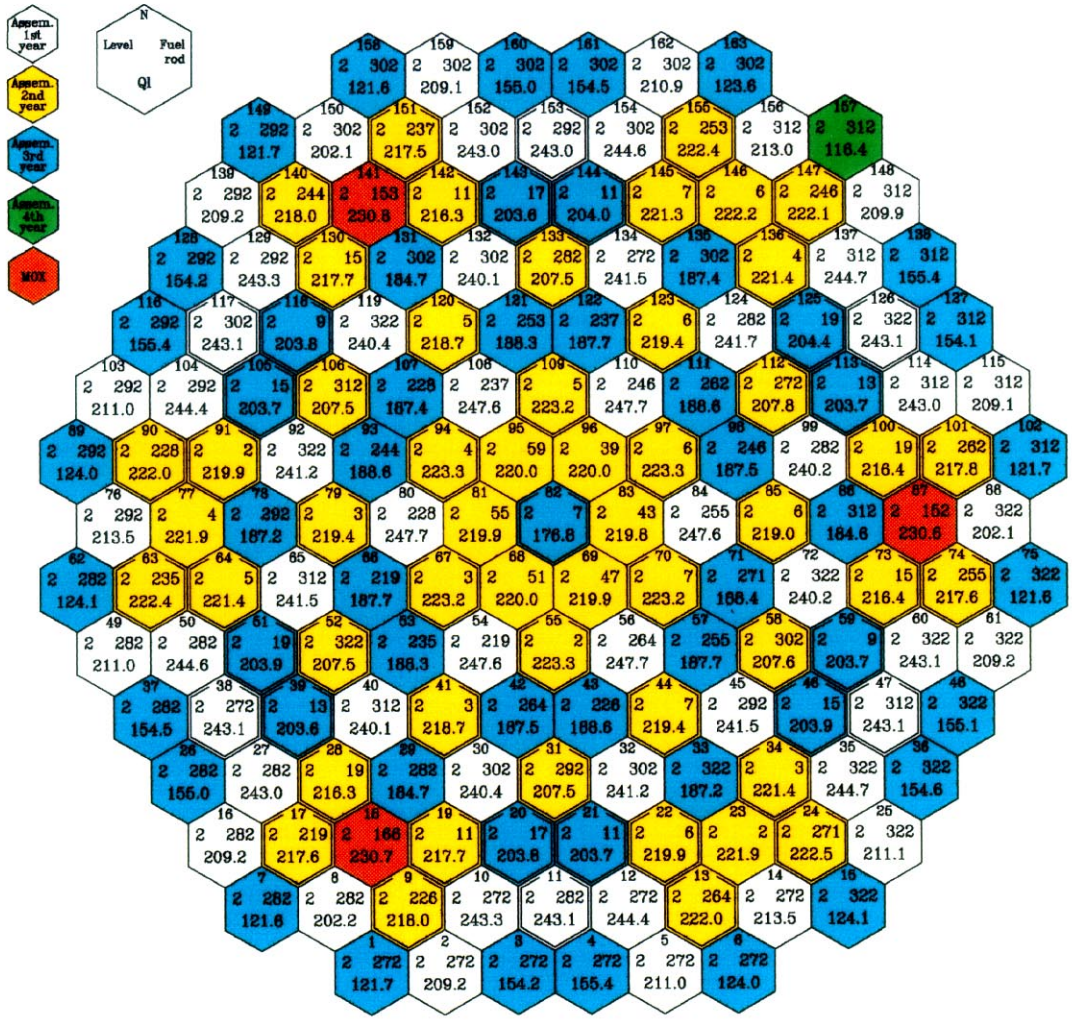

T	= 283.52	EFPD
W	= 3000.0	MW
$C_{H_3BO_3}$	= 0.00	g/kg
Ql_{max}	= 247.7	W/cm
Fuel ass.	= 56	
Level	= 2	
Fuel rod	= 264	

Fig.4.23. Pin-by-Pin Power Distribution in the Most Powered Assembly in BOC. Second Cycle with 3 "100%Pu" MOX LTAs

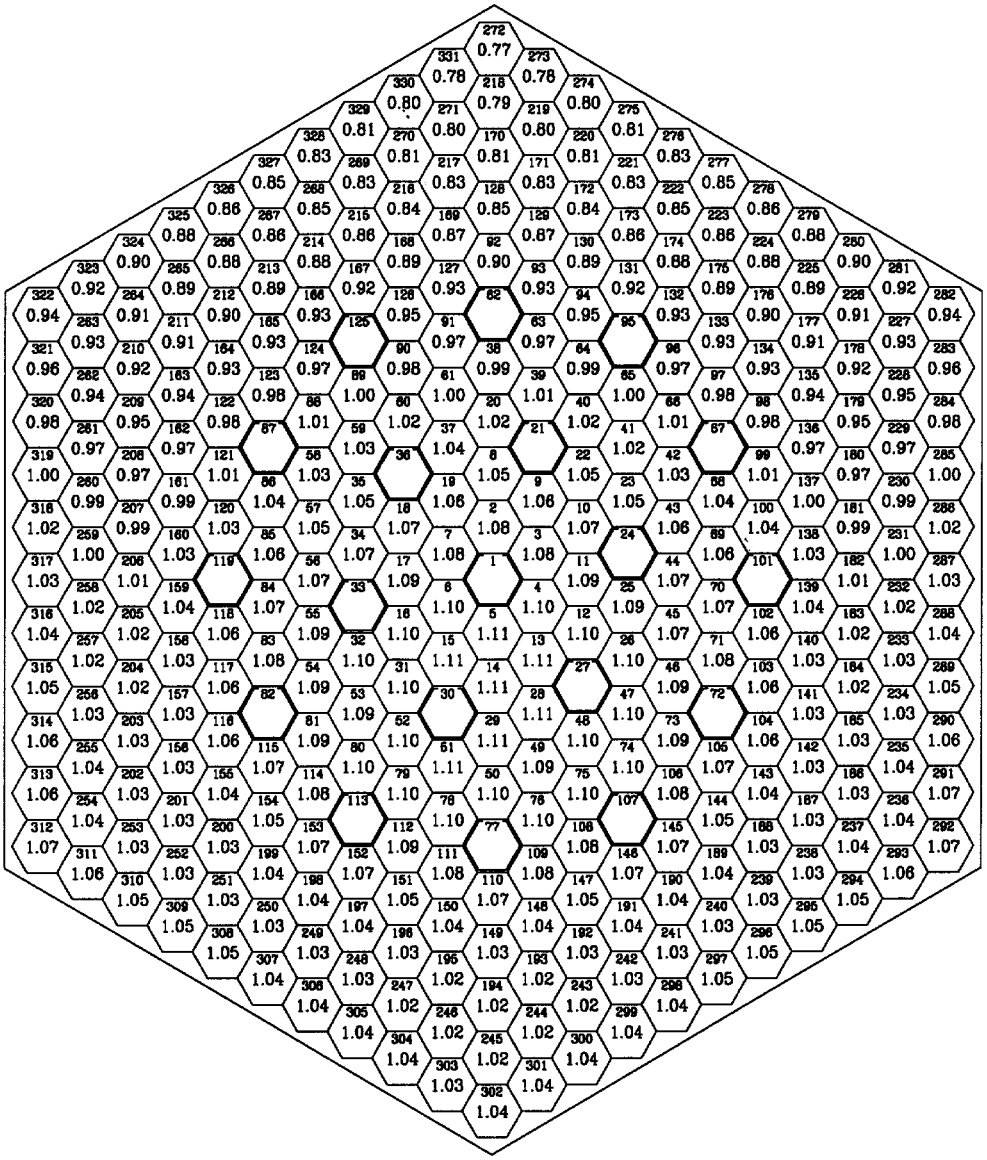

T	0.00	EFPD
W	3000.0	MW
$C_{H_3BO_3}$	5.67	g/kg
Ql_{max}	307.8	W/cm
Fuel assembly	153	
Level	4	
Fuel rod	14	
Kk_{max}	1.11	

Fig.4.24. Pin-by-Pin Power Distribution in the Most Powered Assembly in EOC. Second Cycle with 3 "100%Pu" MOX LTAs

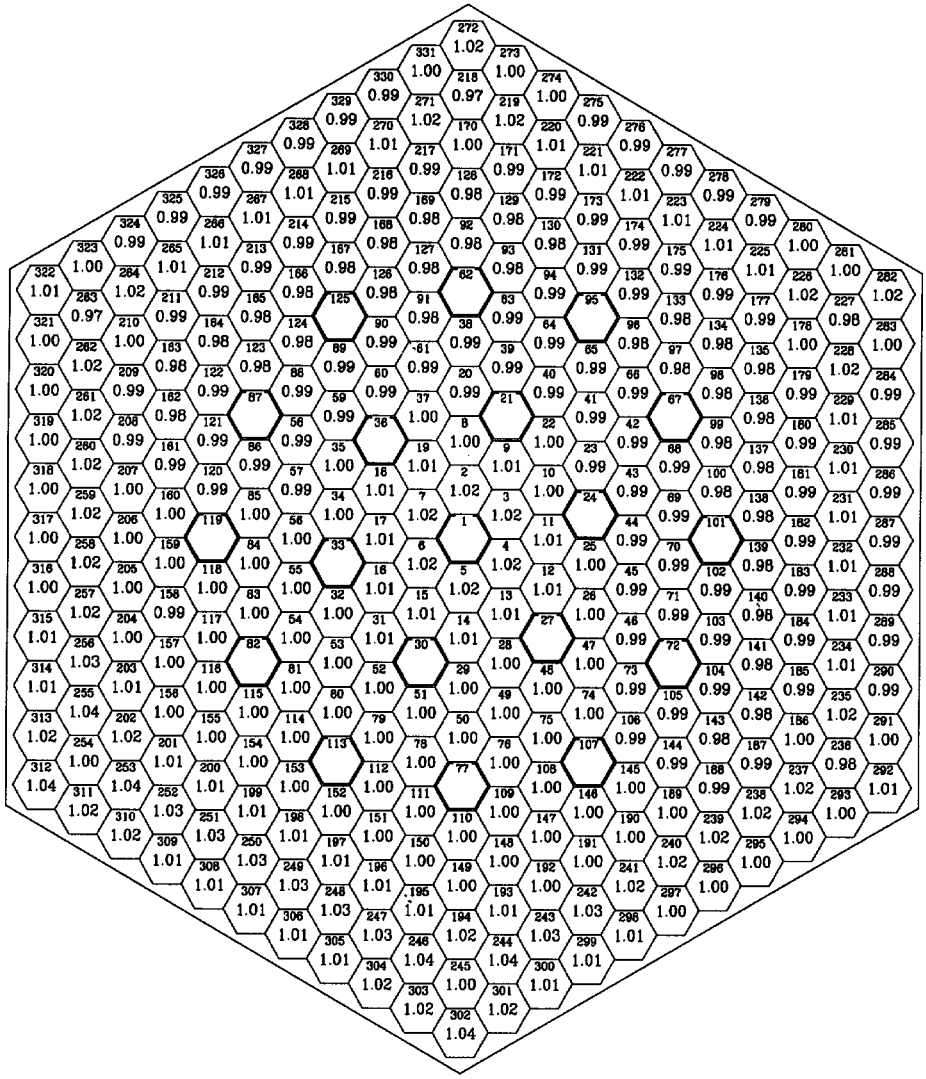

T	283.52	EFPD
W	3000.0	MW
$C_{H_3BO_3}$	0.00	g/kg
Ql	234.3	W/cm
Fuel assembly	110	
Level	4	
Fuel rod	246	
Kk_{max}	1.04	

Fig.4.25. Pin-by-Pin Power Distribution in MOX LTA in BOC. Second Cycle with 3 "100%Pu" MOX LTAs

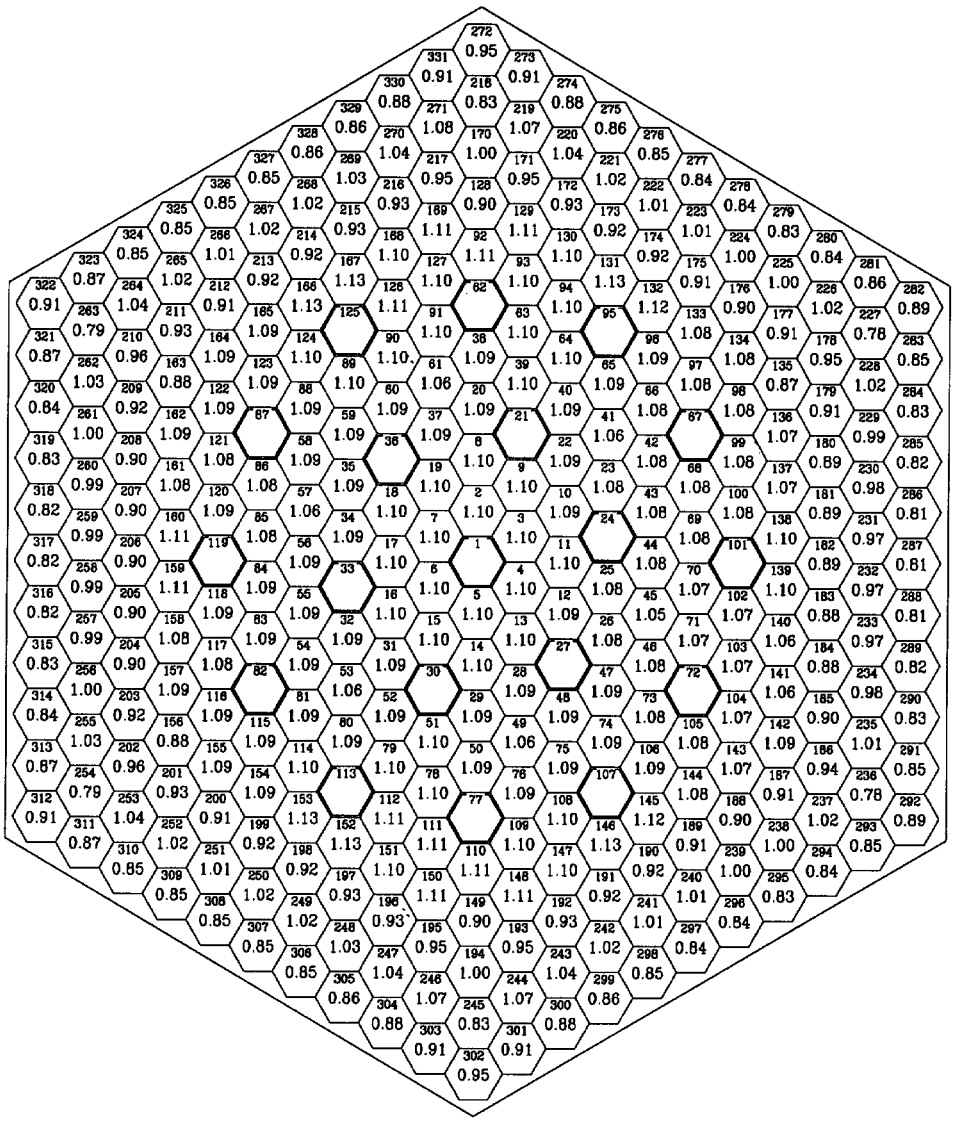

T	0.00	EFPD
W	3000.0	MW
$C_{H_3BO_3}$	5.67	g/kg
Ql	275.2	W/cm
Fuel assembly	87	
Level	4	
Fuel rod	152	
Kk_{max}	1.13	

Fig.4.26. Pin-by-Pin Power Distribution in MOX LTA in EOC. Second Cycle with 3 "100%Pu" MOX LTAs

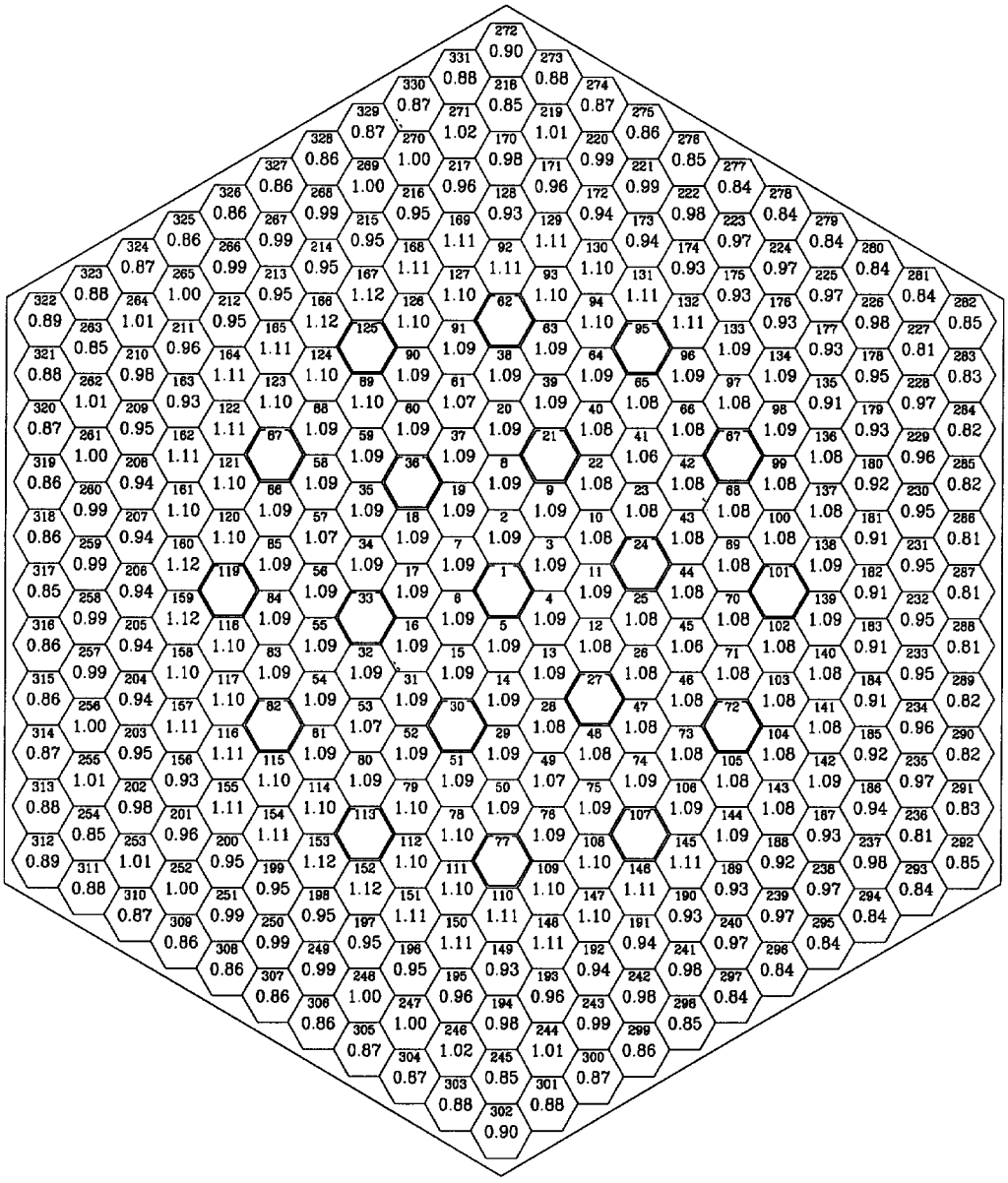

T	283.52	EFPD
W	3000.0	MW
$C_{H_3BO_3}$	0.00	g/kg
Ql	217.9	W/cm
Fuel assembly	87	
Level	4	
Fuel rod	152	
Kk_{max}	1.12	

Fig.4.27. Reloading scheme.
Third Cycle with 3 MOX LTAs

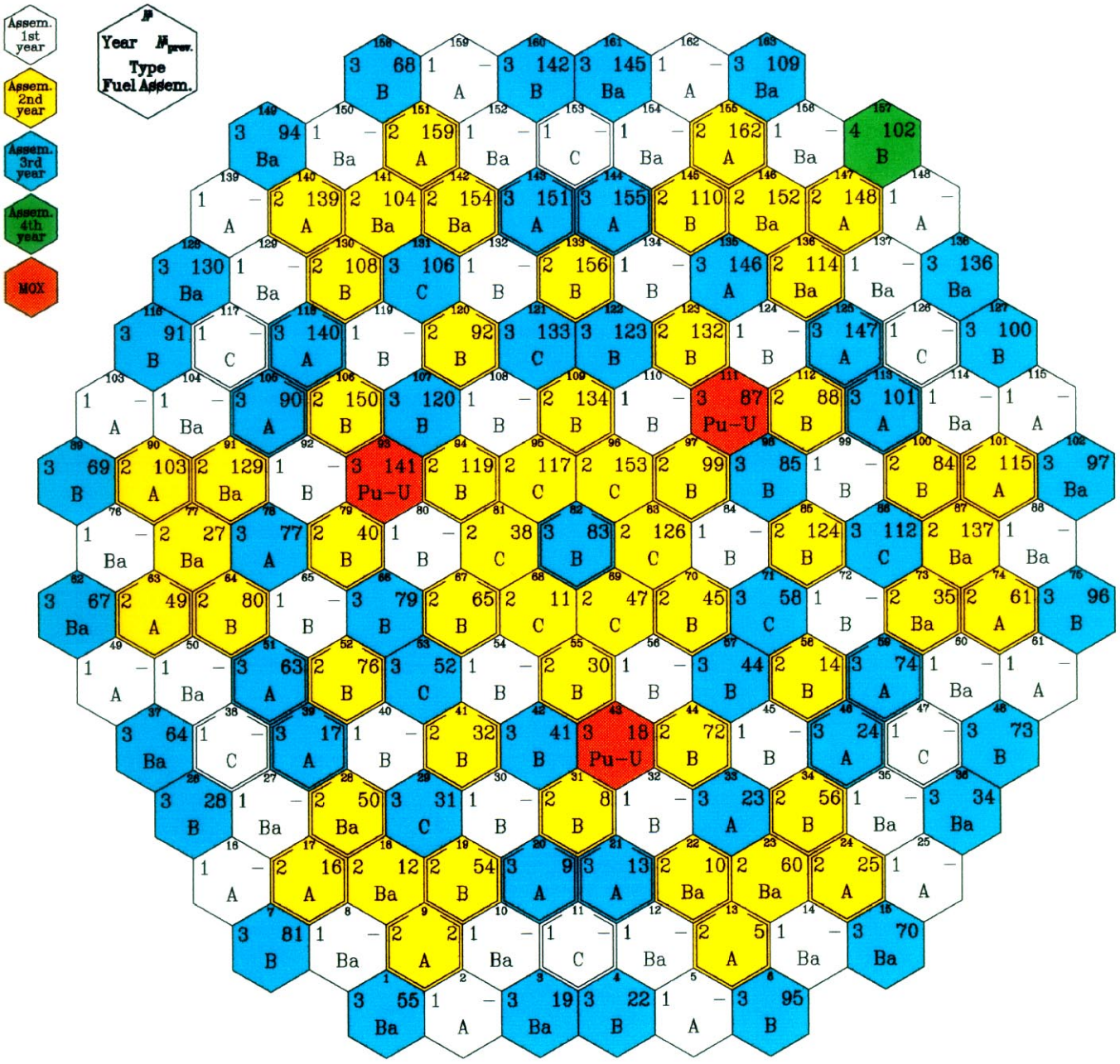

Fig.4.28. Assembly-by-Assembly Power Distribution.
Third Cycle with 3 "100%Pu" MOX LTAs

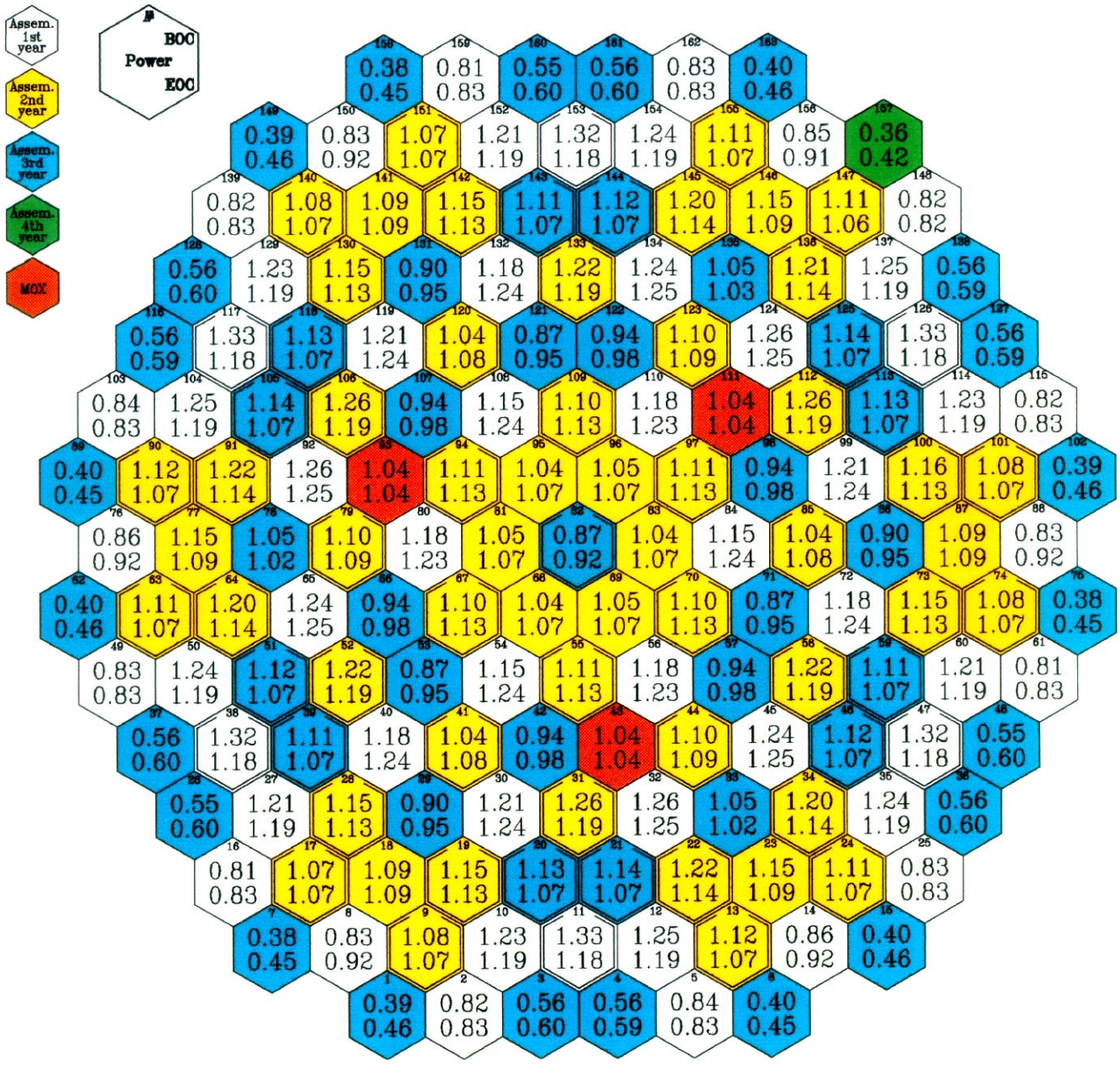

Fig.4.29. Assembly-by-Assembly Burnup Distribution.
Third Cycle with 3 "100%Pu" MOX LTAs

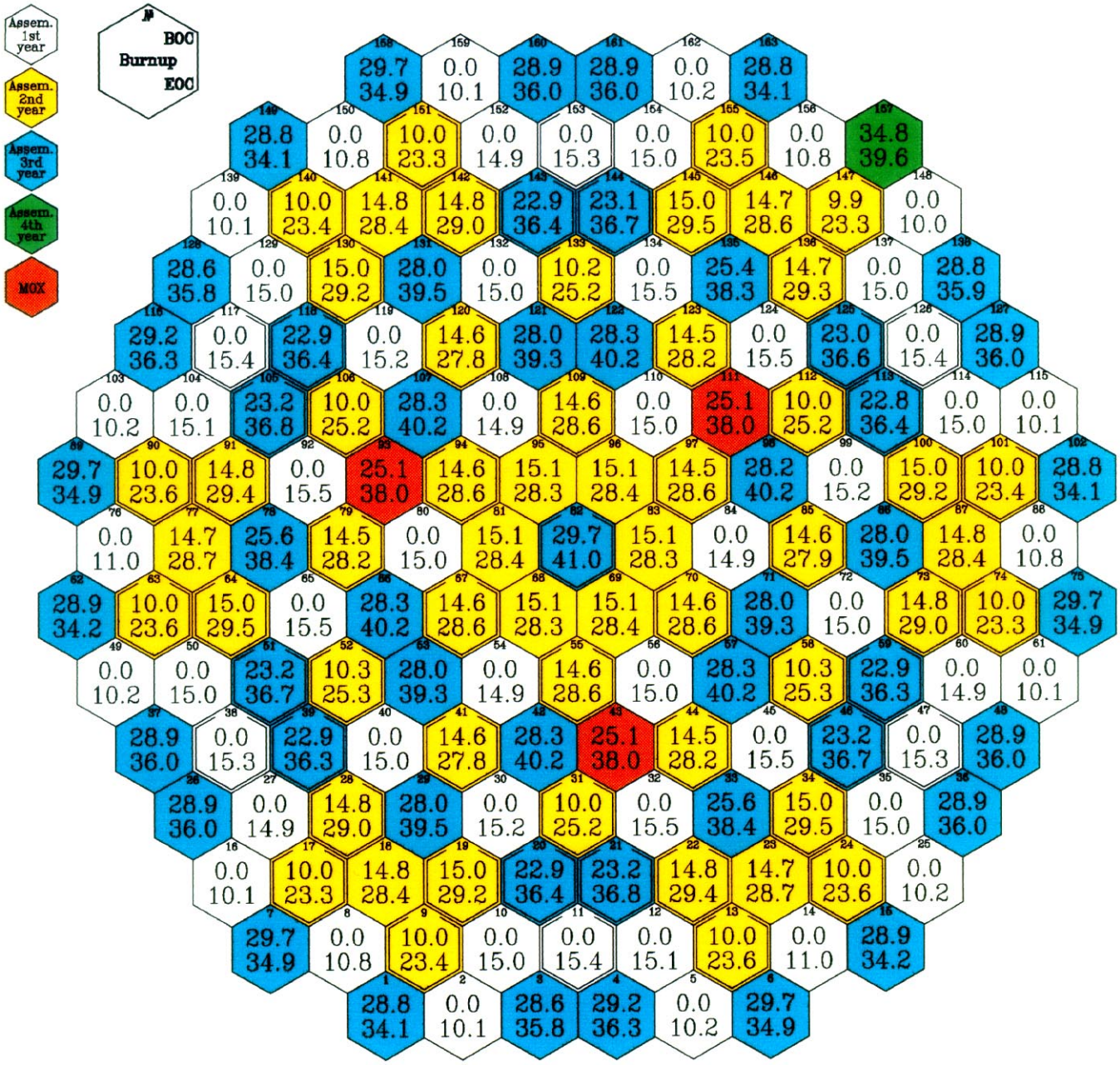

Fig.4.30. Assembly-by-Assembly Temperature Drop Distribution. Third Cycle with 3 "100%Pu" MOX LTAs

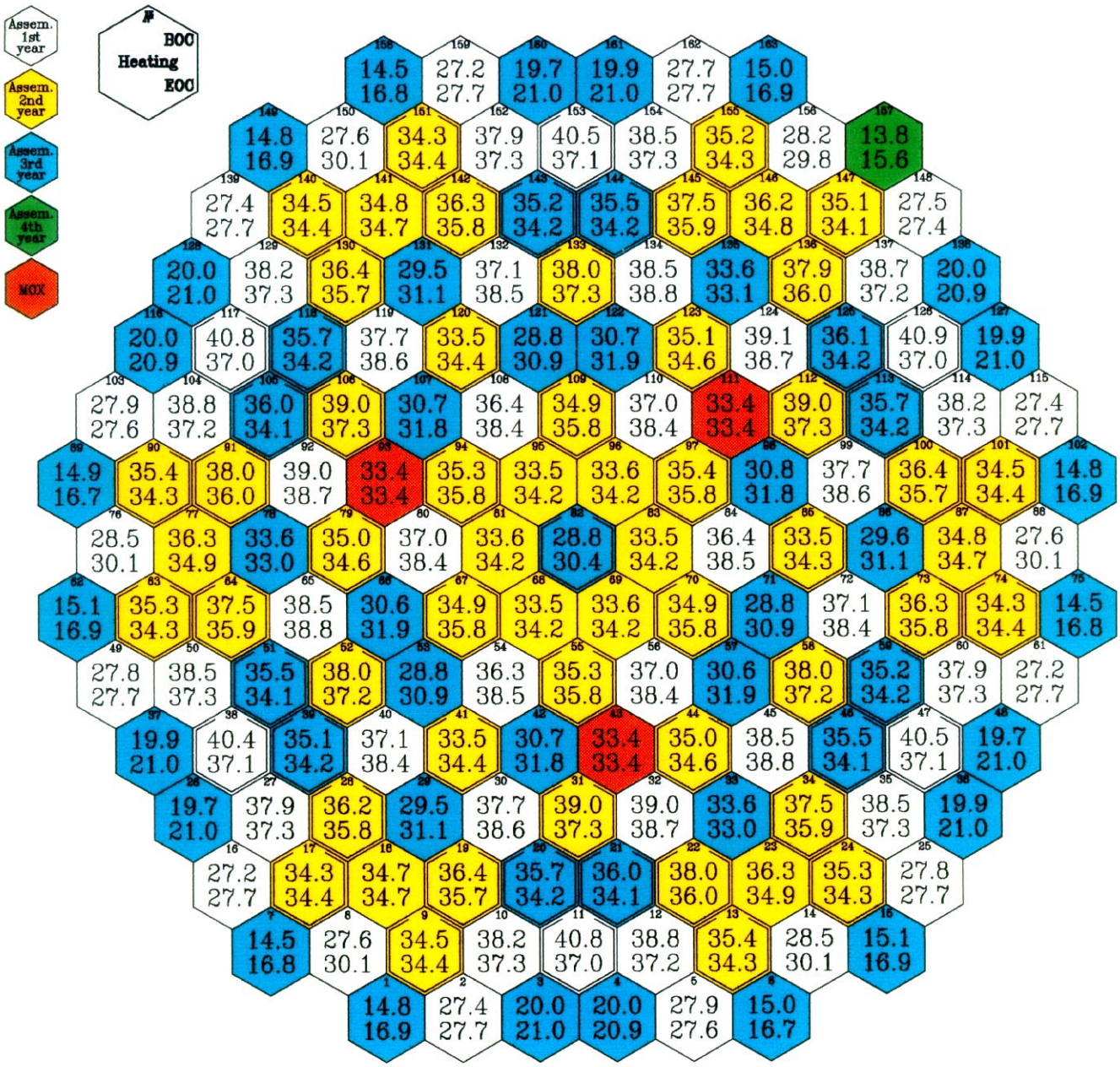

Fig.4.31. Assembly-by-Assembly Maximum Linear Power Distribution in BOC. Third Cycle with 3 "100%Pu" MOX LTAs

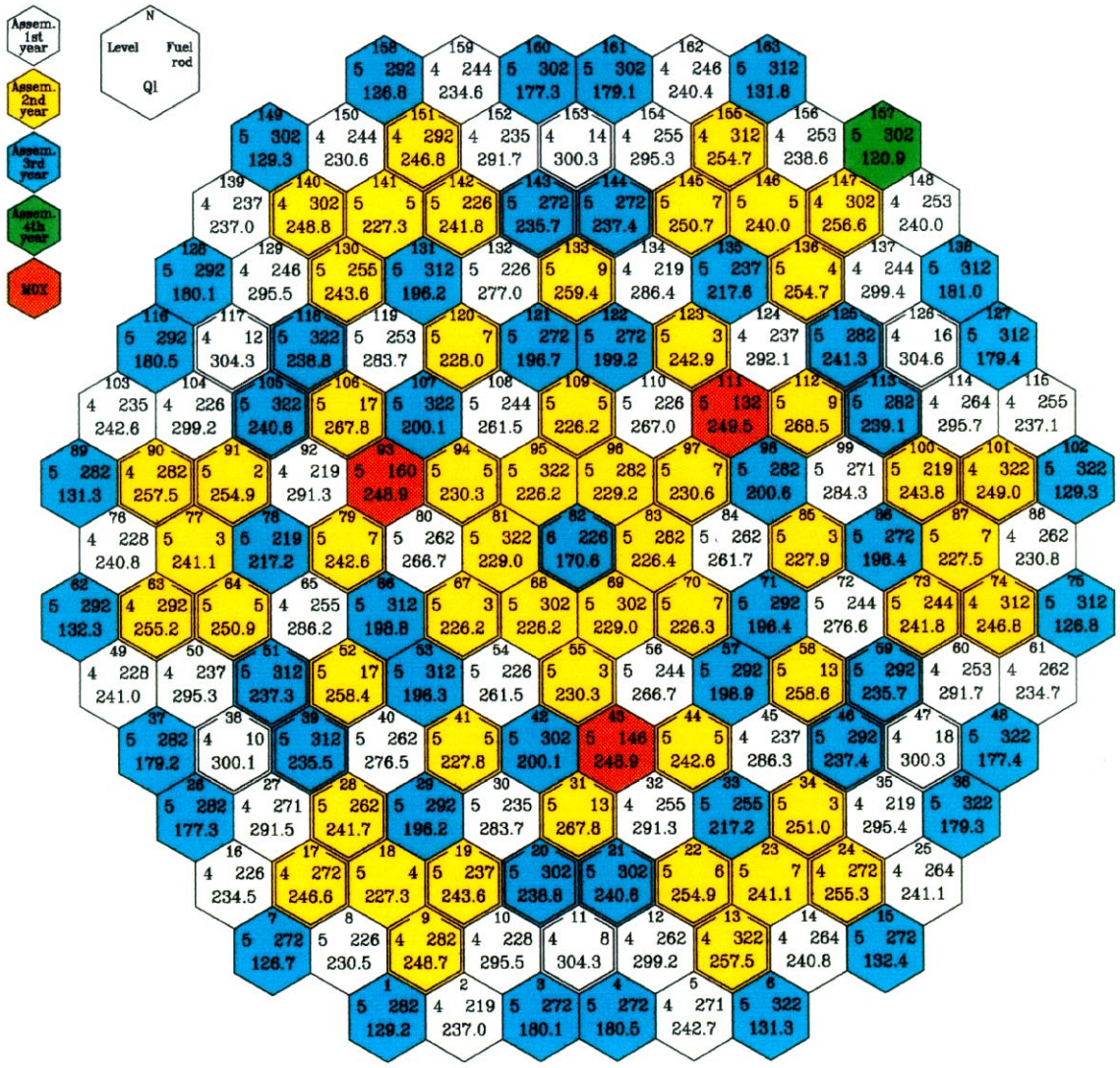

T	=	0.00 EFPD
W	=	3000.0 MW
$C_{H_3BO_3}$	=	5.81 g/kg
Ql_{max}	=	304.6 W/cm
Fuel ass.	=	126
Level	=	4
Fuel rod	=	16

Fig.4.32. Assembly-by-Assembly Maximum Linear Power Distribution in EOC. Third Cycle with 3 "100%Pu" MOX LTAs

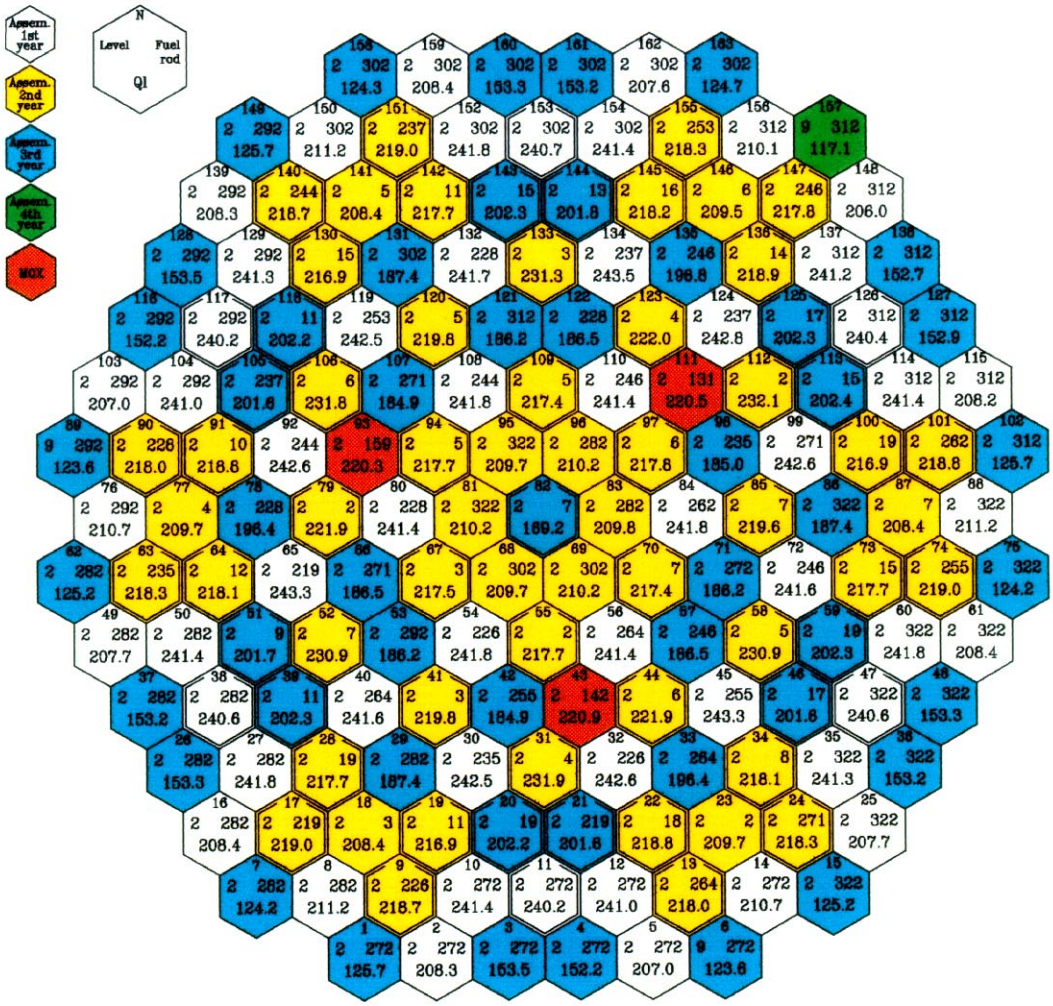

T	= 291.03	EFPD
W	= 3000.0	MW
$C_{H_3BO_3}$	= 0.00	g/kg
Ql_{max}	= 243.5	W/cm
Fuel ass.	= 134	
Level	= 2	
Fuel rod	= 237	

Fig.4.33. Pin-by-Pin Power Distribution in the Most Powered Assembly in BOC. Third Cycle with 3 MOX LTAs

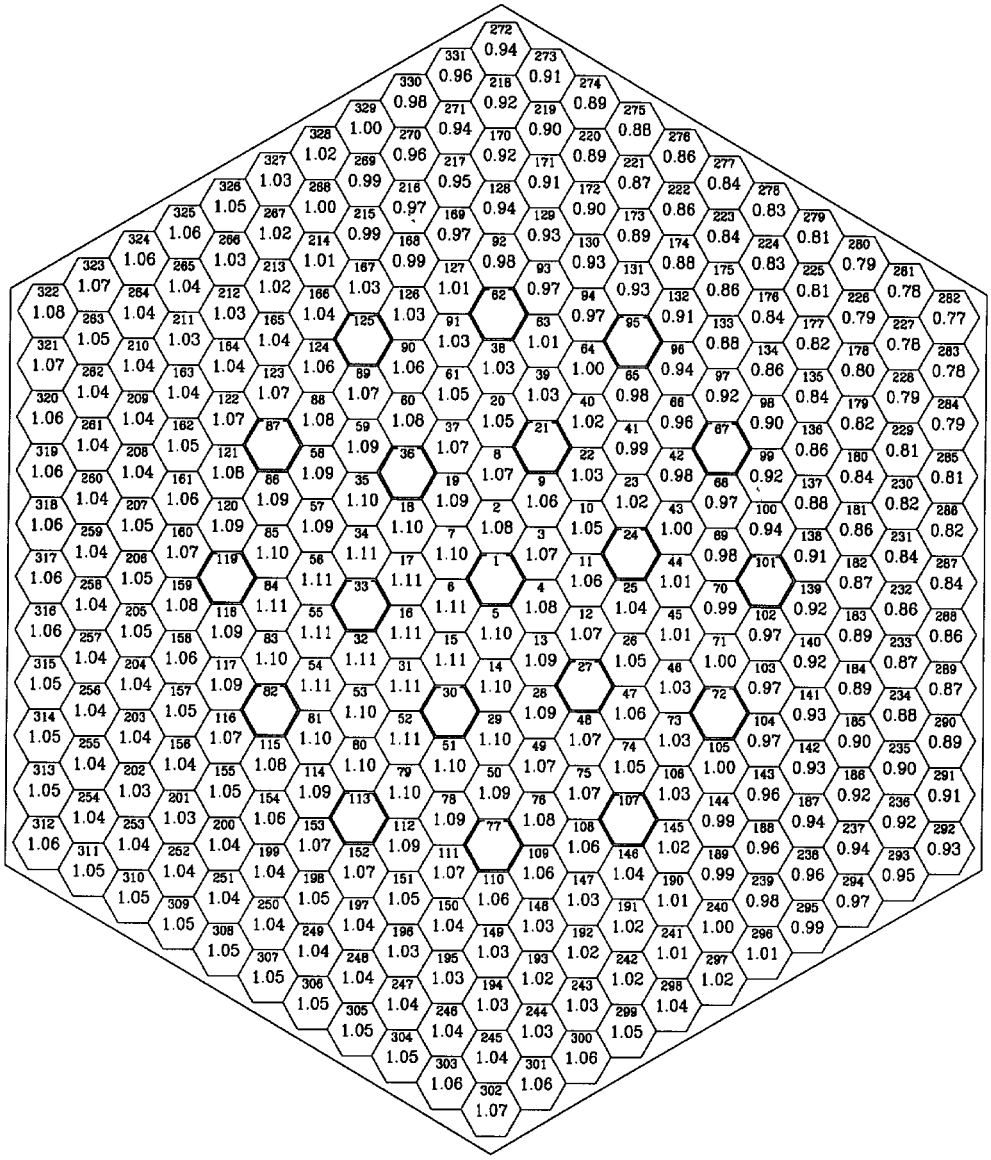

T	0.00	EFPD
W	3000.0	MW
$C_{H_3BO_3}$	5.81	g/kg
Ql	304.6	W/cm
Fuel assembly	126	
Level	4	
Fuel rod	16	
Kk_{max}	1.11	

Fig.4.34. Pin-by-Pin Power Distribution in the Most Powered Assembly in EOC. Third Cycle with 3 "100%Pu" MOX LTAs

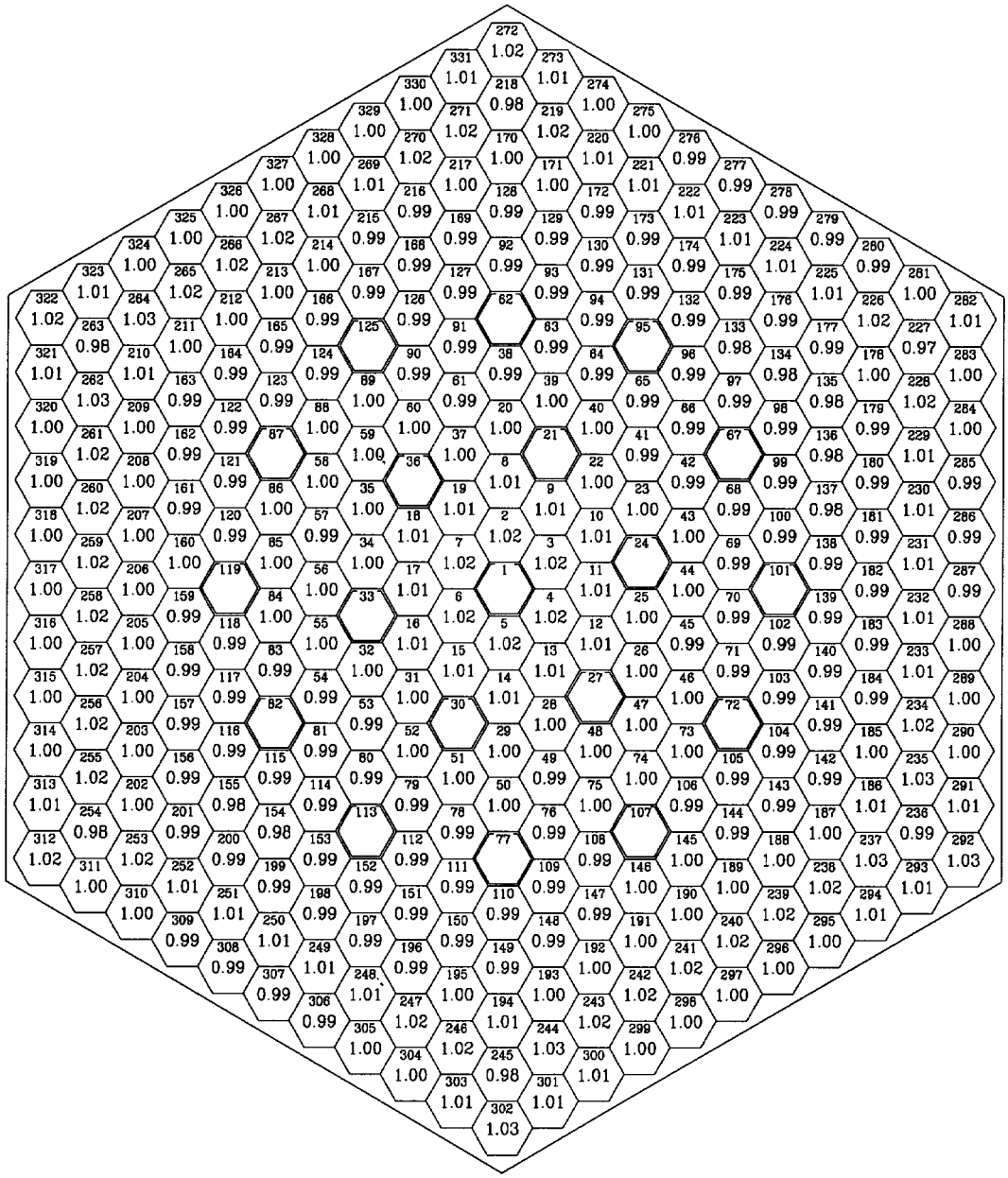

T	291.03	EFPD
W	3000.0	MW
$C_{H_3BO_3}$	0.00	g/kg
Ql	230.0	W/cm
Fuel assembly	134	
Level	4	
Fuel rod	237	
Kk_{max}	1.03	

Fig.4.35. Pin-by-Pin Power Distribution in MOX LTA in BOC. Third Cycle with 3"100%Pu" MOX LTAs

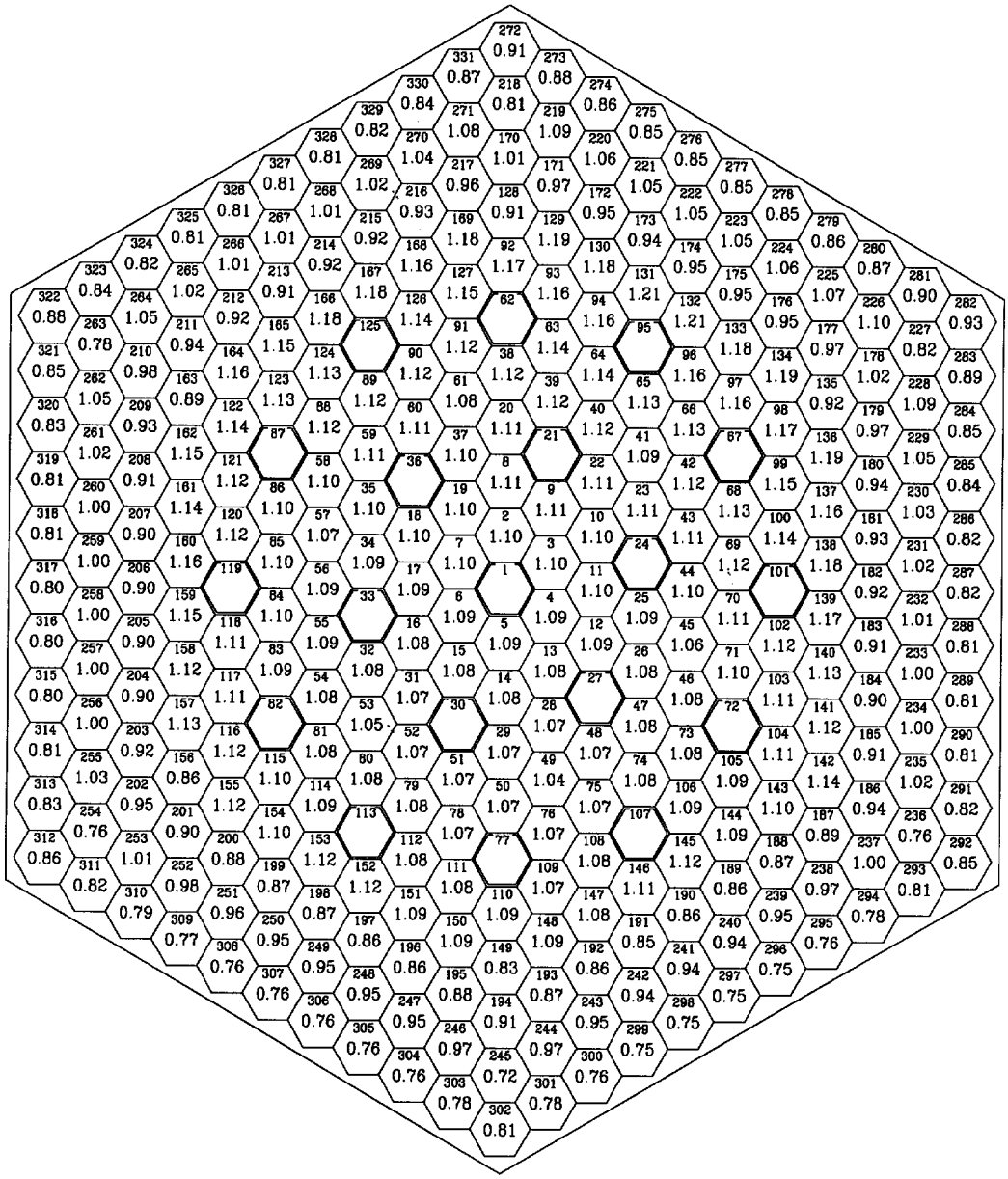

T	0.00	EFPD
W	3000.0	MW
$C_{H_3BO_3}$	5.81	g/kg
Ql	246.7	W/cm
Fuel assembly	111	
Level	4	
Fuel rod	132	
Kk_{max}	1.21	

Fig.4.36. Pin-by-Pin Power Distribution in MOX LTA in EOC. Third Cycle with 3 MOX LTAs of «Island-2» Type (Pu3.8-2.8-U3.7)

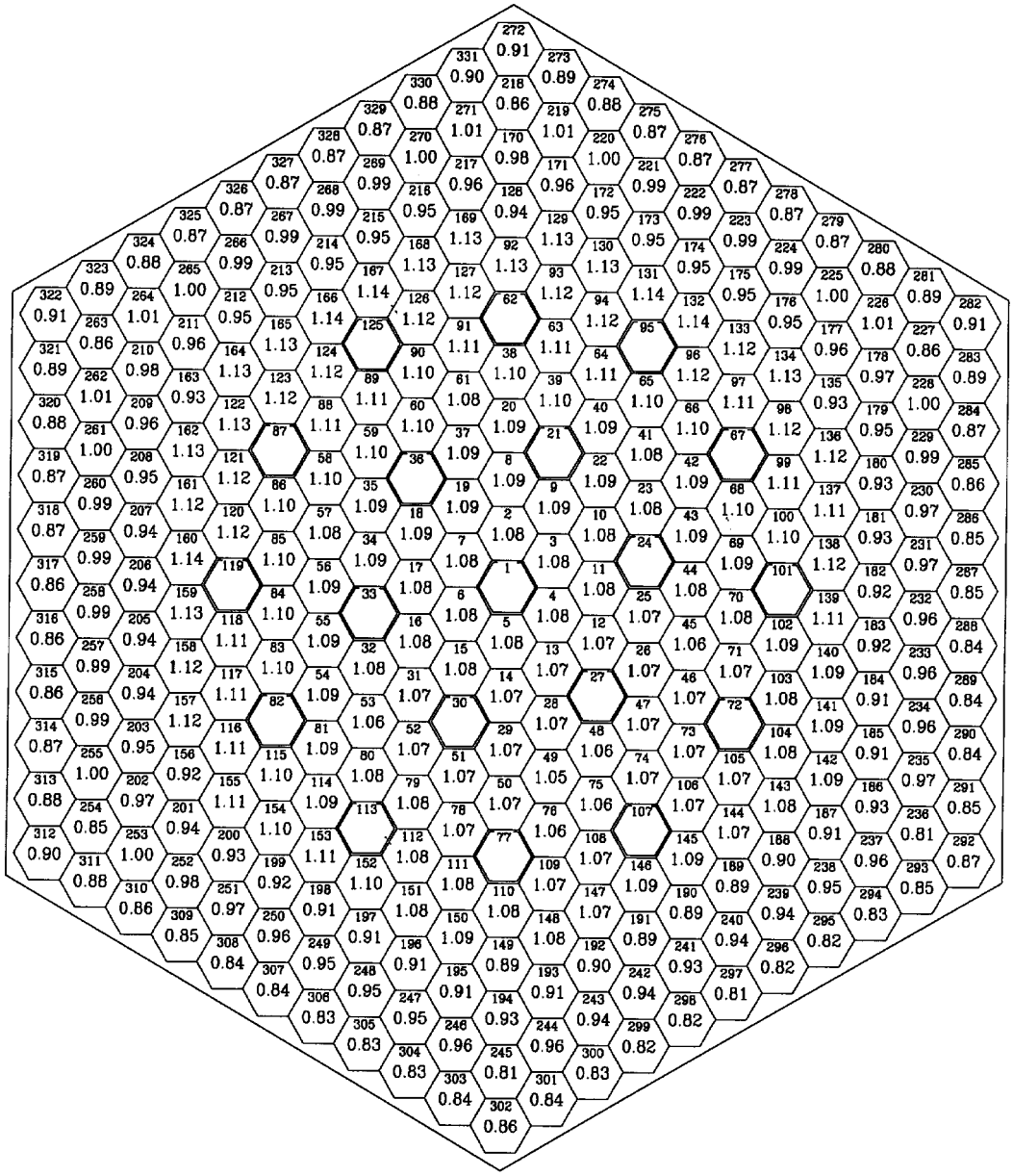

T	291.03	EFPD
W	3000.0	MW
$C_{H_3BO_3}$	0.00	g/kg
Ql	207.5	W/cm
Fuel assembly	111	
Level	4	
Fuel rod	131	
Kk_{max}	1.14	

ANNEX

A.1. Cell Code TVS-M

Nuclear data libraries

The nuclear data library is based on the same files of estimated nuclear data as precision code MCU-RFFI [1*], which uses the Monte Carlo method.

In the epithermal energy region (E>0.625 eV) the calculation is based on slightly modified microcross section library BNAB (see, e.g., [2]) with 24 energy groups. The nuclide libraries can contain both the group and subgroup constants and for some nuclides with temperature dependence.

For the calculation of neutron spectrum in the energy region of resolved resonances E_n<1 keV (15 and higher BNAB group) the library includes files of resonance parameters of individual nuclides obtained on the base of the LIPAR library. For all fissile nuclei the library contains prompt and delayed neutron spectra, group β values and decay constants for six groups of delayed neutrons.

The thermal energy region is divided into 24 groups. For the nuclides with the "1/v" cross-section behavior the absorption cross sections at 2200 m/s are used, for the rest ones the group values of the absorption, scattering and fission cross sections are specified. In addition, for oxygen and carbon the scattering matrices obtained in terms of gas model at 300, 373, 473, 558, 623K are given. For hydrogen bonded in water molecule the scattering matrix is obtained from the ENDF/B recommended data in terms of the Koppel model [3] at the same temperatures.

The library contains the files of cross sections and yields of 98 fission products including ^{135}Xe and ^{149}Sm. The files of fission product yields are based on the ENDF/B-VI data [4].

Uniform lattice

In the energy region of epithermal neutrons (10.5MeV<E_n<0.625 eV, BNAB groups 1-24) a detailed calculation of group spatial-energy distribution of neutron flux is performed. Each group is divided into an arbitrary number of intervals equal in lethargy, and then the calculation is performed at each point of group division. The of elastic scattering process is calculated without use of any approximations when the scattering is isotropic in the inertia center system (i.e.s), otherwise the scattering anisotropy is taken into account by the term not higher than linear in cosine of scattering angle. The slowing down due to inelastic scattering is taken into account via the matrix of inelastic transitions under the assumption of uniform energy distribution of neutrons scattering into the given group.

For nuclides with the subgroup description of cross sections the heterogeneous subgroup calculation of their micro cross sections is performed.

In the energy region of resolved resonances (groups 13-24 BNAB) for resonance nuclides the calculation of all types of cross sections is performed with the use of nuclide

* References in p.A.1 are placed in the end of A.1

resonance parameters. In so doing it is possible to take into account temperature dependence of resonance cross sections.

In the thermal energy region the standard calculation technique is used. It suggests solving the multigroup equation of thermalization with the neutron sources from the epithermal energy region formed when calculation for this energy range was performed.

Calculation of neutron spatial distribution is carried out by dividing the cells into an arbitrary number of annular material zones and by the use of the passing through probability (PTP) method [5]. In the calculation the actual form of the cell boundary is taken into account.

The calculation of the point kinetics parameters $\beta_{eff.}$, ℓ is made by the standard formulas using the value function ψ with respect to K_{eff} and with six groups of delayed neutrons.

The calculation of the fuel nuclide composition during fuel burnup is performed for heavy nuclides from ^{232}Th to ^{244}Cm and for 98 fission products from ^{82}Kr to ^{163}Dy. The burnup equations can be solved both by the Runge-Kutt method and by a faster analytical method described in [6].

Calculation of supercells and fuel assemblies

For the determination of FA neutronic characteristics the code uses the diffusion fine-mesh calculation with an arbitrary number of groups from 4 to 48 and with the mesh width equal to the pitch between fuel rods in the FA. For the boundary mesh cells the compression coefficient is used. Along with the standard six-point scheme the refined scheme whose principles of construction are described in [7] can be used. The mesh equation has a common form however the quantities in this formula have another sense, namely:

$$\frac{4}{3a^2}\sum_{i=1}^{6}\frac{d_0 d_i}{d_0+d_i}(F_0-F_i)+(\Lambda_0^a+\Lambda_0^r+G_0^Z B_z^2)F_0=S_0 \qquad (1)$$

$$F=\varepsilon\Phi \qquad \Lambda=\Sigma/\varepsilon$$

$$G^Z=D^Z/\varepsilon \qquad d=D^R\xi \qquad (2)$$

$$\varepsilon=\psi(1-\gamma/\delta) \qquad \delta=2d/a$$

In formulas (2-7) Φ is the cell neutron flux; the sense of quantities Σ, D^R, D^Z is obvious. Then

$$\psi=\frac{\Phi_b^s}{\bar{\Phi}^s} \qquad \xi=\frac{j_b^a}{\bar{j}^a} \qquad (8)$$

Here Φ is the neutron flux in the given mesh cell; j is the neutron current in the cell; index "*b*" means the value of corresponding quantity at the cell boundary; index "*s*" indicates the solution of transport equation in the cell with symmetric boundary conditions (symmetric inflowing and outflowing neutron current); index "*a*" is the solution with asymmetric boundary conditions (neutron current flowing through the cell); the bar shows the quantity value averaged over the cell.

The use of these quantities permits joining of *accurate* (i.e. obtained from solving of transport equation for the cell) neutron flux and current at the cell boundary and

keeping of the *accurate* connection between the solution of equation (1) and the reaction rates in the cell. In this way it becomes possible to avoid errors peculiar to the standard calculation scheme associated with the finite size and heterogeneous structure of mesh points. For solving the set of equations any modules of diffusion equation solutions can be used.

As usual the process of solving the diffusion equations is divided into the solving of the equation for each group and the determination of fission source by means of external iterations. If the state of FA at power is considered then upon their completion the external iterations are added with the calculation of ^{135}Xe and ^{149}Sm concentrations and a new iteration cycle.

Each mesh point pertains to a definite type: fuel rod, cell with absorber rod, cell corresponding the gap between FAs, etc. The constants for the background type are always calculated in the asymptotic mode, i.e. as for the uniform fuel cell. The constants for non-fuel cells are calculated in the mode of supercell. For the non-background fuel cells including those with integrated burnable poison (named tvegs) the calculation can be performed both in the asymptotic and supercell modes. The homogenized background cell is always considered as the external zone of supercell.

References

1. Gomin E.A., Majorov L.V. The MCU-RFFI Monte Carlo Code for Reactor Design Applications. Proc. of Int. Conf. on Math. and Comp., Reac. Phys. and Envir. Analyses, April 30 -4 May 1995, Portlend, Oregon, USA
2. L.P.Abagyan et al. Group constants for calculation of the reactors and shields. M., Energoizdat, 1981.
3. Koppel J.U., Houston S.H. Reference for ENDF Thermal Neutron Scattering Data, GA-8774, 1978
4. ENDF-102. Data Formats and Procedures for the Evaluated Nuclear Data Files ENDF-6, July 1990, National Nuclear Data Center, Brookhaven National Laboratory, Upton, NewYork, 11973
5. I.E.Rubin. Method of probabilities of transmission in the one-dimensional cylindrical geometry. Izvestiya AN BSSR, ser. fiz-energ. nauk, № 2, p. 25-31, 1983.
6. V.M.Kolobashkin et al. Radiation characteristics of irradiated nuclear fuel M., Energoatomizdat, 1983.
7. V.D.Sidorenko. Homogenization of effective cross sections in the periodic lattice. Preprint IAE-2793, 1977.

A.2. Coarse-Mesh Code BIPR-7A

BIPR-7A is a 3-dimensional hexagonal coarse-mesh code intended to calculate neutronics characteristics of VVER-type reactor core.

Calculational cell represents assembly transversal section in horizontal plane and usually one-tenth of core height in axial direction i.e. there are 1630 cells in VVER-1000 core. Neutronics parameters are homogeneous within a cell.

Radial, upper and lower reflectors are described by border conditions.

Calculation is performed in two energetic groups using the so-called modal presentation of group fluxes [8].

Cell constants, prepared by the code TBC-M [4], form a library and represent a number of polynomials that reflect the two-group neutronics cross sections dependence on moderator density, moderator temperature, fuel temperature, FP concentrations in fuel, boron acid concentration in coolant, Xe and Sm concentration in fuel.

BIPR-7A is a part of industrial super-code KASKAD that allows obtaining in convenient formats all the parameters necessary for reactor safety estimations and licensing.

As a result BIPR-7A calculate the following parameters:

- q_i,
- Kq,
- q_{ij},
- Kv,
- BUi,
- BUij,
- MTC,
- MDC,
- DTC,
- DRO/DCB,
- βeff,
- λm,
- Cb_{CRIT} ,
- RO_{STOP},
- $(RO)_{AP}$.

A.3. Fine-Mesh Code PERMAK-A

PERMAK-A is a 2-dimensional fine-mesh code intended to calculate neutronics characteristics of VVER-type reactor core.

Calculational cell represents fuel pin-type hexagonal cell with homogeneous neutronics parameters within it.

Diffusion finite-differencies neutron balance equation in few energetic groups are resolved.

Radial reflector is described by the same manner as a core.

Neutron flux axial gradients, obtained by BIPR-7A, are used while calculating one (as usual) the most powered core axial level.

Cell (fuel and non-fuel) constants, prepared by the code TBC-M [4], form a special library and represent a number of polynomials that reflect the group neutronics cross sections dependence on moderator density, moderator temperature, fuel temperature, FP concentrations in fuel, boron acid concentration in coolant, Xe and Sm concentration in fuel.

PERMAK-A is a part of industrial super-code KASKAD that allows obtaining in convenient formats all the parameters necessary for reactor safety estimations and licensing.

As a result PERMAK-A calculates the following parameters:

- q_k,
- Kk,
- Kr;
- BUk,
- Q_l,
- $K_{o\text{-}total}$.

A.4. Reflector Description

The simplified structure of VVER-1000 radial reflector is presented in Fig. A.2.. In KI fine-mesh calculations by the code PERMAK-A the radial VVER-1000 reflector is modeled by "reflector assemblies" of five types (Figures A.1, A.3-A.7). Zero flux is applied on the outer reflector borders. The corresponding geometric condensation factors are applied to the cell types of reflector if the cells are situated in "reflector assembly" corners or on the borders.

The upper and lower reflectors can be described on the base of reactor core design presented in [1].

Figure A.1. Equilibrium Loading Pattern for Base Uranium Core with Boron BPRs, Core 60 ° Sector

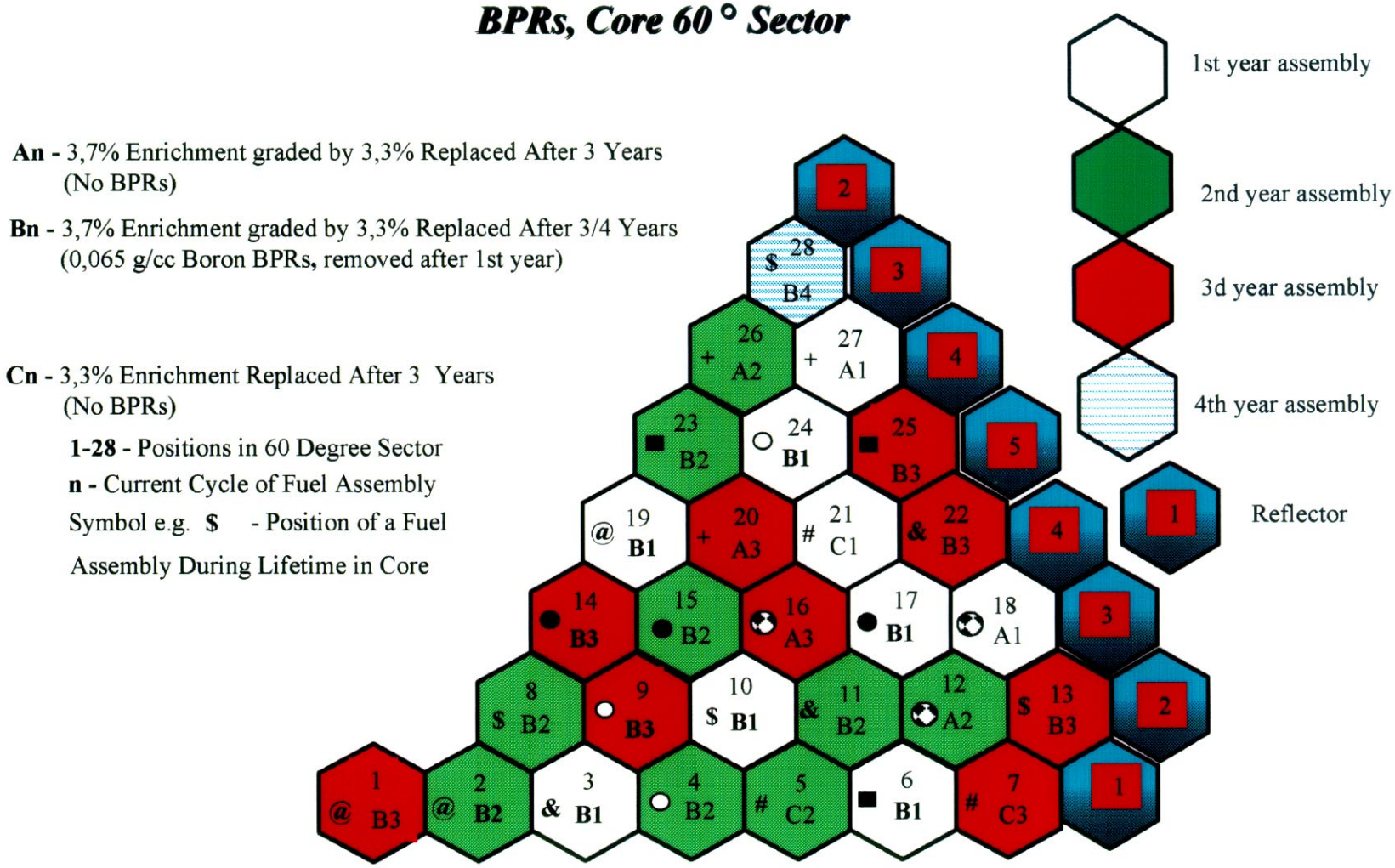

Figure A.2. Model of VVER-1000 Radial Reflector

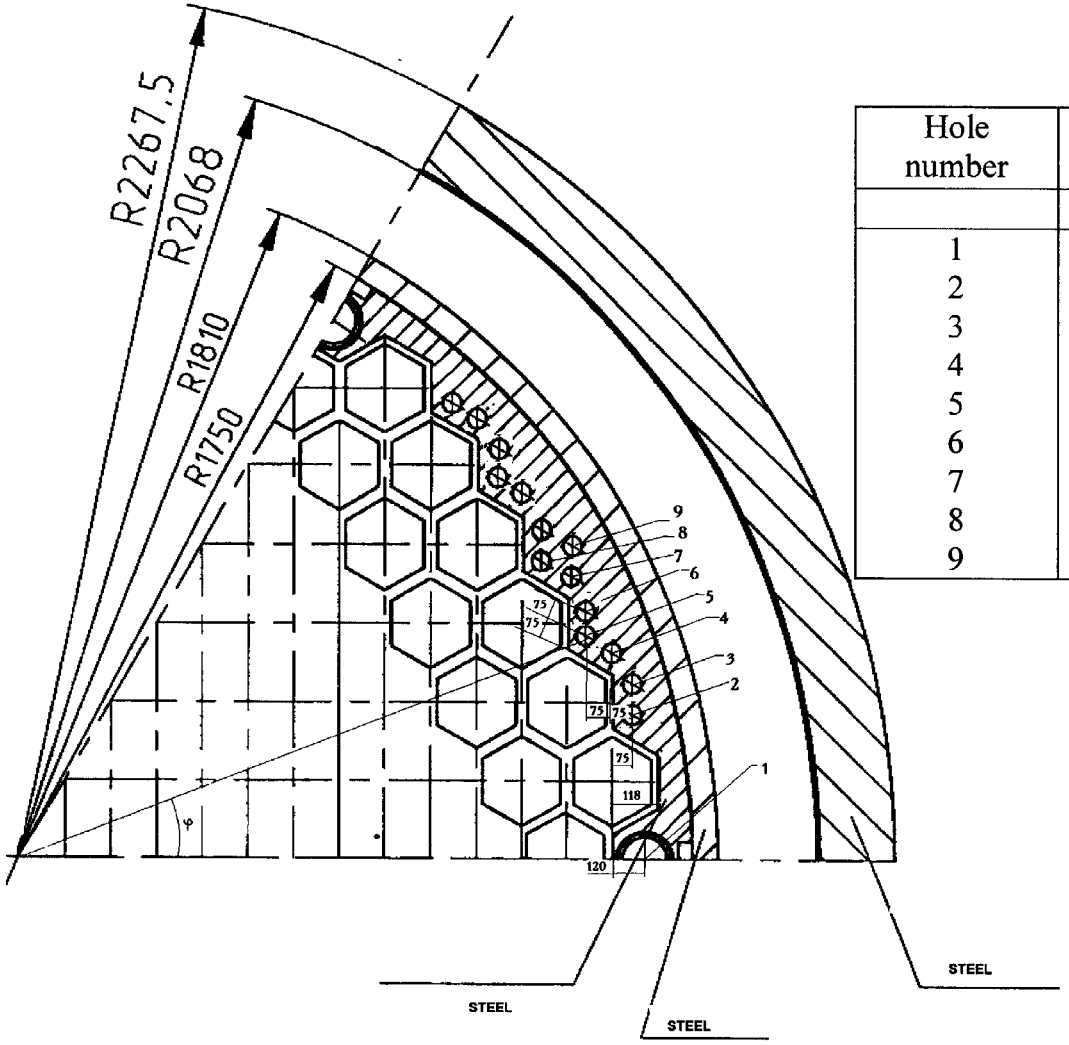

Hole number	Distance from core center (R)	Angle (φ°)	Hole diameter
	mm		mm
1	1655	0	98
2	1655	13	70
3	1675	16	70
4	1655	19	70
5	1600	21	70
6	1635	24	70
7	1625	27	70
8	1575	30	70
9	1665	30	70

Fig.A.3. Reflector "assembly" of type 1

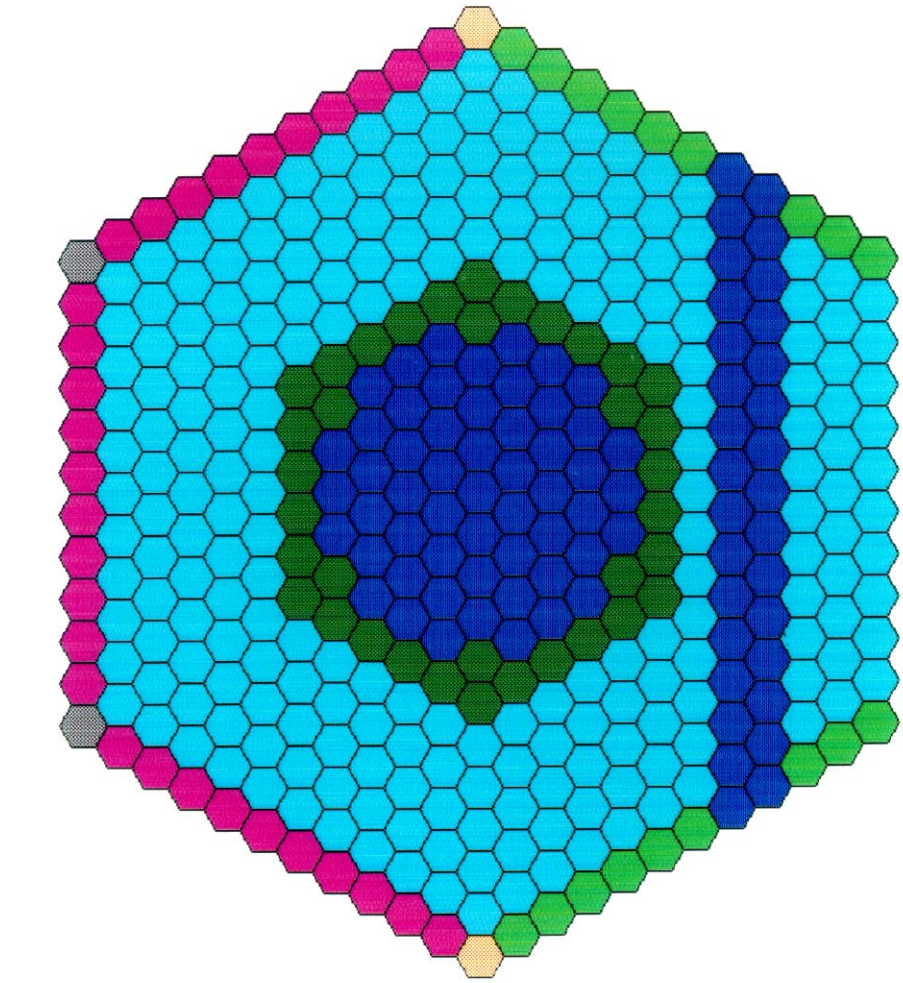

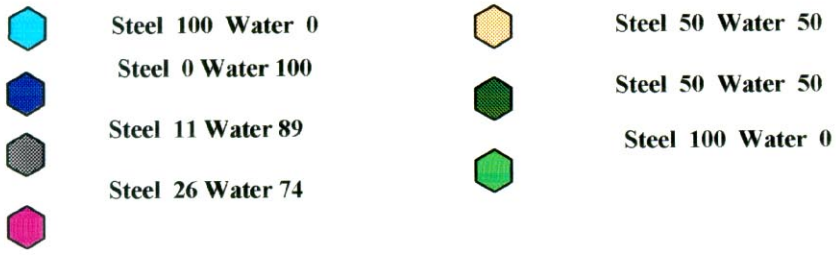

Fig.A.4. Reflector "assembly" of type 2

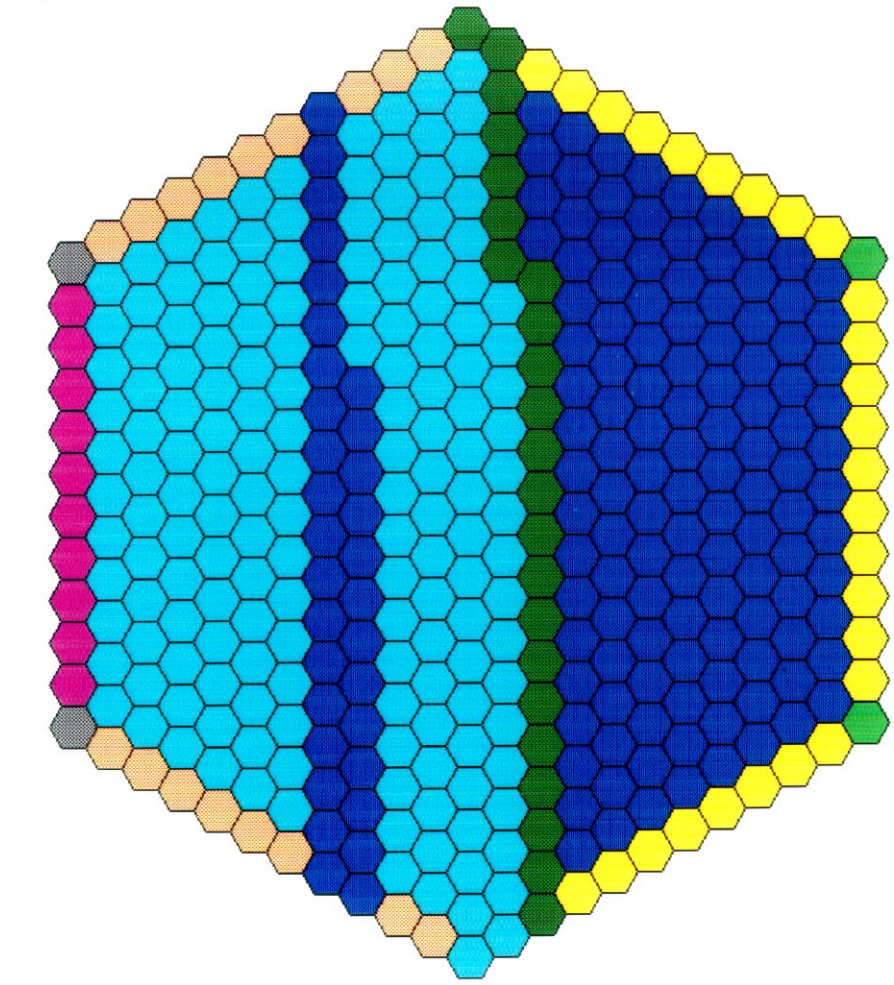

Fig.A.5. Reflector "assembly" of type 3

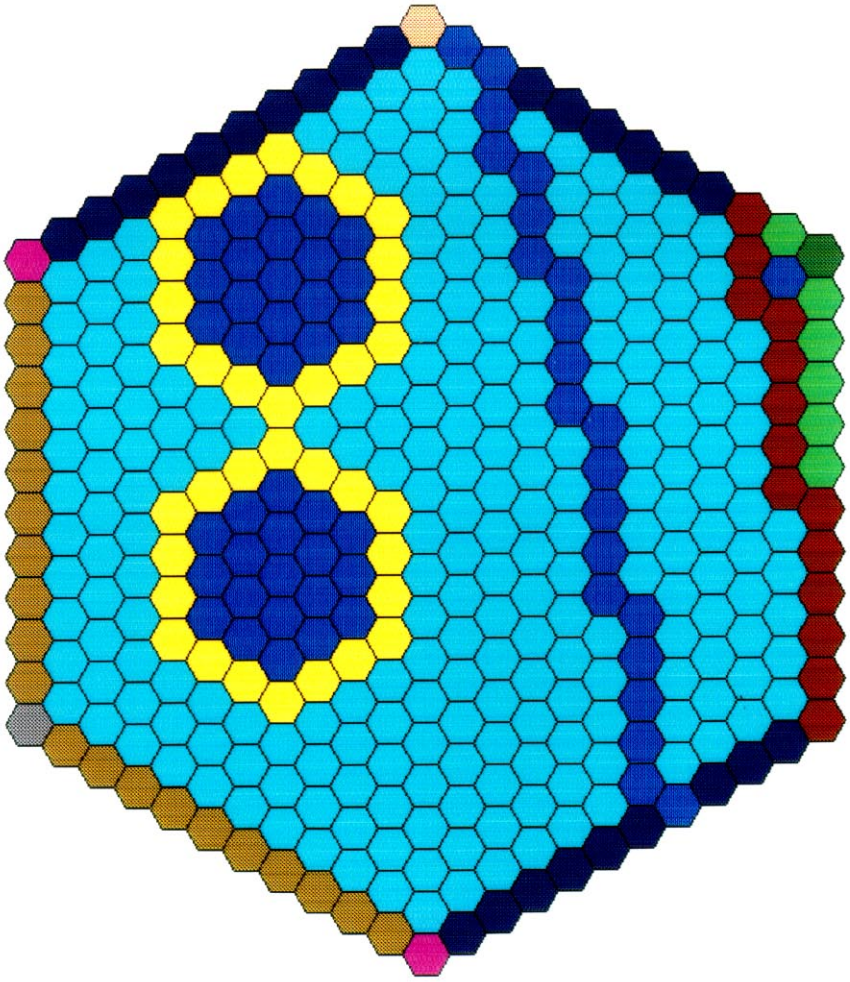

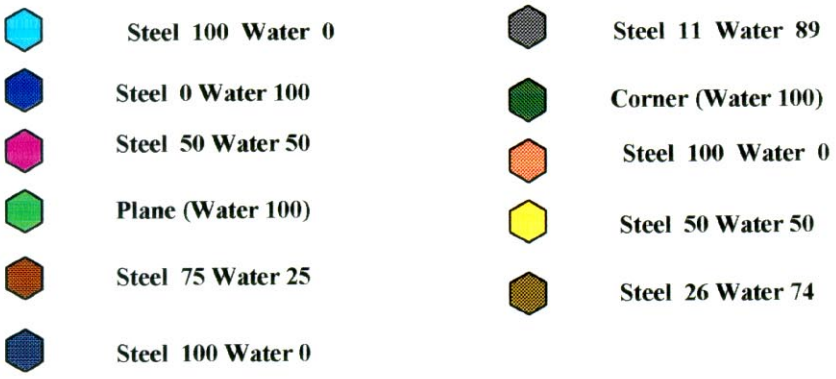

Fig.A.6. Reflector "assembly" of type 4

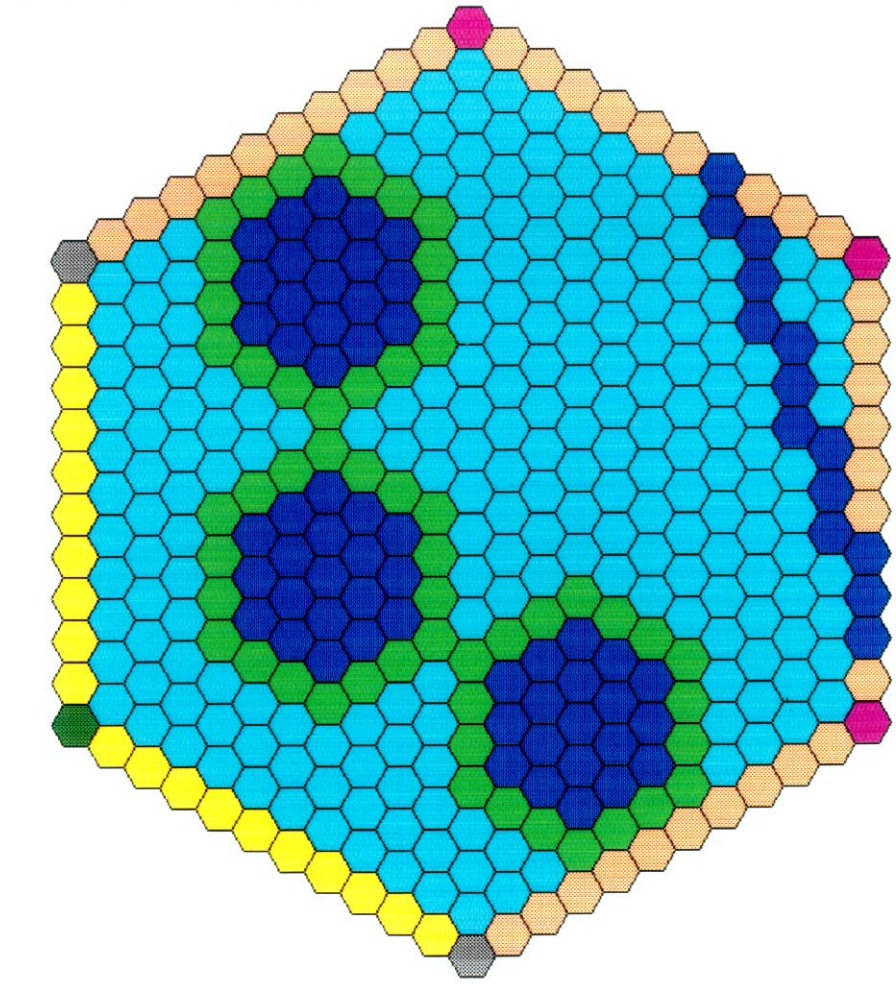

Fig.A.7. Reflector "assembly" of type 5

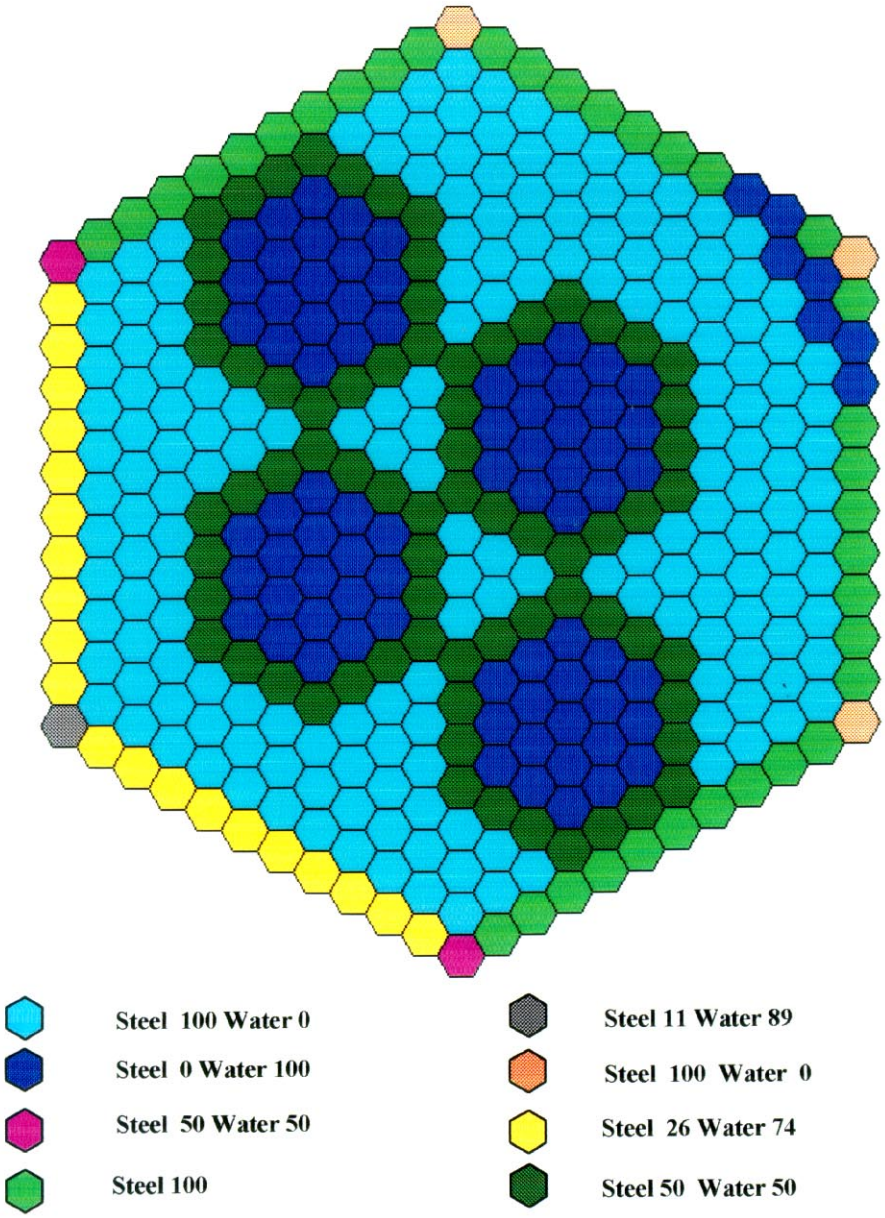

Comments from ORNL staff on the report, *Design Studies of "100% Pu" MOX Lead Test Assembly, ORNL/SUB/99-B99398V-4*

1. On page 11, the reference to "Fig. 2.8" should be changed to "Fig. 2.6".

2. On page 16, bottom line of table, "isotermic" should be changed to "isothermic".

3. On page 17, the units for "Specific reactor thermal power in CS" should be changed from "KW/litre" to "kW/litre". Also the subscript of Beta-effective is lacking one "f", i.e. should be eff.

4. On page 19, the reference to "Tables 2.2-2.6" should be changed to "Tables 2.2–2.6a".

5. On page 19, the units for "Wv" should be changed from "KW/litre" to "kW/litre" and the value of "t_{fuel}" should be changed from "1027 K" to "1027 K".

6. On page 22, the units for "Wv" should be changed from "KWt/l" to "kWt/l".

7. On pages 25–27, the terms "$x_{Pu}{}^{f}$" and "x_5" have not been defined and are not included in the table of definitions listed on pages 13–18.

8. On page 28, the reference to "Tables 2.1–2.6" should be changed to "Tables 2.1–2.6a".

9. On page 29, the Russian word for "and" should be translated to English.

10. On page 38, the term "WWER" should be changed to "VVER" in "Reference 7".

11. On page 40, it is the interpretation of the table that the normal operating position of the regulating rod bank is for the bank to be 80% inserted in the core.

12. On page 41, the units for "Spacer Grid Weight" should be changed from "Kg" to "kg".

13. On page 106, the drawings external to the hexagonal assembly are spurious and should be ignored. Likewise on page 113, a spurious title – Fig. 4.6 … - appears but should be ignored.

14. On page 131, the designation for the equations immediately following equation should be changed from "(2)" to "(2-7)".

15. On page 137, the holes in the reflector region of the reactor are filled with water or detectors during normal operation of the reactor.

16. Throughout the report, the spelling of "zonned" should be "zoned". "Assemblage" should be replaced with "Assembly".

17. The use of the symbols << and >>, as in <<100%>>, should be interpreted as quotes in English, i.e. "100%". (The symbols << and >> are used for quotation in Russian literature.)

18. This report is the deliverable for FY99 Annual Operating Plan Task 10.2.2.1, milestone c. This milestone also had the internal ORNL designation of 99-1b.

INTERNAL DISTRIBUTION

1. R. J. Belles
2–6. B. B. Bevard
7. J. J. Carbajo
8. M. D. DeHart
9. F. C. Difilippo
10. R. J. Ellis
11. S. E. Fisher
12–16. J. C. Gehin
17. S. R. Greene
18. R. Holdaway
19. D. T. Ingersoll
20. M. A. Kuliasha
21. S. B. Ludwig
22. G. E. Michaels
23. D. L. Moses
24. W. P. Poore
25–29. R. T. Primm III
30. C. C. Southmayd
31. G. L. Yoder, Jr.
32. Central Research Library
33–34. ORNL Laboratory Records (OSTI)
35. ORNL Laboratory Records-RC

EXTERNAL DISTRIBUTION

37. M. L. Adams, Department of Nuclear Engineering, Texas A&M University, Zachry 129, College Station, TX 77843
38. D. Alberstein, Los Alamos National Laboratory, MS-K551, P.O. Box 1663, Los Alamos, NM 87545
39. Dr. K. Aratani, Surplus Weapons Plutonium Disposition Group, International Cooperation and Nuclear Material Control Division, Japan Nuclear Cycle Development Institute, 4-49 Muramatsu, Tokai-mura, Naka-gun, Ibaraki-ken, Japan
40. J. Baker, Office of Fissile Materials Disposition, U.S. Department of Energy, MD-3, 1000 Independence Avenue SW, Washington, DC 20585
41. M. S. Chatterton, Office of Nuclear Reactor Regulation, MS O10B3, United States Nuclear Regulatory Commission, Washington, DC 20555-0001
42. K. Chidester, Los Alamos National Laboratory, MS-E502, P.O. Box 1663, Los Alamos, NM 87545
43. Mr. R. H. Clark, Duke/Cogema/Stone & Webster, 400 South Tryon Street, WC-32G, P.O. Box 1004, Charlotte, NC 28202
44. W. Danker, U.S. Department of Energy, MD-3, 1000 Independence Avenue SW, Washington DC 20585
45. N. Fletcher, Office of Fissile Materials Disposition, U.S. Department of Energy, MD-3, 1000 Independence Avenue SW, Washington DC 20585
46. T. Gould, Lawrence Livermore National Laboratory, P.O. Box 808, MS-L186, Livermore, CA 94551
47. L. Holgate, Office of Fissile Materials Disposition, U.S. Department of Energy, MD-1/2, 1000 Independence Avenue SW, Washington DC 20585
48. L. Jardine, Lawrence Livermore National Laboratory, P.O. Box 808, MS-L166, Livermore, CA 94551

49. Dr. A. Kalashnikov, Institute of Physics and Power Engineering, 1 Bondarenko Square, Obninsk, Kaluga Region, Russia 249020

50–54. D. E. Klein, Associate Vice Chancellor for Special Engineering Programs, The University of Texas System, 210 West Sixth Street, Austin, TX 78701

55. R. W. Lee, Office of Nuclear Reactor Regulation, MS O10B3, United States Nuclear Regulatory Commission, Washington, DC 20555-0001

56. S. Nesbit, Duke/Cogema/Stone & Webster, 400 South Tryon Street, WC-32G, P.O. Box 1004, Charlotte, NC 28202

57. J. O. Nulton, Office of Fissile Materials Disposition, U.S. Department of Energy, MD-3, 1000 Independence Avenue SW, Washington, DC 20585

58. N. Ogawa, Director and General Manager, Plant Engineering Department, Nuclear Power Engineering Corporation, Shuwa-Kamiyacho Building, 2F; 3-13, 4-Chome Toranomon; Minato-Ku, Tokyo 105-0001, Japan

59. Dr. S. L. Passman, Booz-Allen & Hamilton, 555 13th Street, NW, No. 480E, Washington, DC 20004

60–64. Dr. Alexander Pavlovitchev, Russian Research Center Kurchatov Institute, Institute of Nuclear Reactors, VVER Division, VVER Physics Department, 123182, Kurchatov Square, 1, Moscow, Russia

65. K. L. Peddicord, Associate Vice Chancellor, Texas A&M University, 120 Zachry, College Station, TX 77843-3133

66. W. D. Reece, Texas A&M University, Department of Nuclear Engineering, Zachry 129, College Station, TX 77843-3133

67. P. T. Rhoads, Office of Fissile Materials Disposition, U.S. Department of Energy, MD-4, 1000 Independence Avenue SW, Washington, DC 20585

68. U. Shoop, Office of Nuclear Reactor Regulation, MS O10B3, United States Nuclear Regulatory Commission, Washington, DC 20555-0001

69. J. Thompson, Office of Fissile Materials Disposition, U.S. Department of Energy, MD-4, 1000 Independence Avenue SW, Washington, DC 20585

70. F. Trumble, Westinghouse Savannah River Company, Building 730R, Room 3402, Aiken, SC 29808